

Article

Tensile Strength and Microstructure of Rotary-Friction-Welded Carbon-Steel and Stainless-Steel Joints

Hudiyo Firmanto ^{1,*}, Susila Candra ¹, Mochammad Arbi Hadiyah ² , Yesa Priscilla Triastomo ¹ and Ivan Wirawan ¹¹ Department of Mechanical and Manufacturing Engineering, University of Surabaya, Surabaya 60293, Indonesia² Department of Industrial Engineering, University of Surabaya, Surabaya 60293, Indonesia

* Correspondence: hudiyo@staff.ubaya.ac.id

Abstract: Due to the different properties of the materials, the fusion welding of dissimilar metals may be difficult. Structural irregularities may form as a result of various phase transformations during welding. Solid-state welding, as opposed to fusion welding, occurs below the melting temperature. As a result of the melting and solidification phenomena that happen in fusion welding, solid-state welding is expected to reduce the potential for phase transformation. This paper describes the use of a rotary friction welding technique to join carbon steel and 304 stainless steel. The purpose of this work is to investigate the characteristics of rotary friction welding (RFW) when joining 304 stainless steel to carbon steels with different carbon contents. Experiments were carried out on the RFW of low- and medium-carbon steels with 304 stainless steel. The investigation was carried out using the Taguchi method of experimental design. The joints' tensile strengths and microstructures were evaluated. The parameters that had the greatest influence on the tensile strengths of the welding results were identified. The combination of parameters resulting in the greatest tensile strength is also suggested. A microstructural examination of the weldment revealed mechanical mixing and interlocking.

Keywords: rotary friction welding; carbon steel; 304 SS; tensile strength; microstructure; Taguchi



Citation: Firmanto, H.; Candra, S.; Hadiyah, M.A.; Triastomo, Y.P.; Wirawan, I. Tensile Strength and Microstructure of Rotary-Friction-Welded Carbon-Steel and Stainless-Steel Joints. *J. Manuf. Mater. Process.* **2023**, *7*, 7. <https://doi.org/10.3390/jmmp7010007>

Academic Editor: Dulce Maria Rodrigues

Received: 15 November 2022

Revised: 14 December 2022

Accepted: 22 December 2022

Published: 28 December 2022



Copyright: © 2022 by the authors. Licensee MDPI, Basel, Switzerland. This article is an open access article distributed under the terms and conditions of the Creative Commons Attribution (CC BY) license (<https://creativecommons.org/licenses/by/4.0/>).

1. Introduction

The rotary friction welding (RFW) process has been used to join dissimilar metals on numerous occasions. This method can be used instead of fusion welding. When welding dissimilar metals, the latter process frequently encounters difficulties. Brittle intermetallic compound formation was found to be sensitive in nonferrous dissimilar gas metal arc welding [1]. Excessive heat-affected zones were also produced by fusion welding techniques such as electric arc welding [2]. Another significant issue in this process is the formation of residual stresses due to compositional differences in joining metals [3]. The differences in the physical properties of the joined metals influence the formation of the joint. As a result, the heat input must be properly controlled in order to improve the joint [4]. Methods involving the least amount of melting were suggested to avoid fusion problems when welding dissimilar metals [5].

RFW has also been used to join stainless steel to other materials. RFW was used to join this material to nonferrous metals such as copper [6–10], Inconel [11,12], titanium [13–15], and aluminum [16–19].

The joining of carbon steel to stainless steel is used in various industries. It has been applied in the petrochemical and power generation industries [20]. For medical applications, the materials have been combined to produce semi-biodegradable bone screws [21]. In the construction sector, a combination of carbon steel and stainless steel was used in the construction of concrete structures in a marine environment [22]. Other applications were piping system components [23] and aerospace industry components [24].

The work on the RFW of stainless steel with carbon steel or cast iron focused on the influence of RFW parameters on joint strength and microstructure. Forging pressure was

said to improve the joint strength of 1045 steel and 316 L stainless steel [20]. The peak temperature of the joint increased as the friction increased. Nonetheless, increased friction pressure improved heat generation and the efficiency of converting mechanical work into heat [25]. While keeping the upset pressure constant, the most influential parameters of friction pressure and friction time were suggested in the RFW of AISI 1018–AISI 2205 steel [26]. In the RFW of low-carbon steel with nodular iron, however, the friction time is the most important determinant of tensile strength improvement, followed by the upset force and friction force [27]. The heating stage parameters (i.e., the friction time and friction pressure) were discovered to have a greater influence on the RFW of 304 stainless steel (SS) with carbon steel than the upset parameters (the forging pressure and forging time) [28]. A certain combination of heating pressure, upset pressure, and heating time was suggested to achieve the best tensile strength in RFW 304 SS with 316 stainless steel [29]. The parameter combinations of the rotating speed, friction pressure, forging pressure, and friction time for achieving the maximum tensile strength were found in the RFW of low-carbon steel and 202 stainless steel, which were used for semi-biodegradable bone screws [21].

Numerical and computational modeling were also used to study RFW process optimization. The method was used to simulate the thermomechanical phenomenon in relation to the process parameters. Using this technique, increasing the frictional pressure was expected to lower the peak temperature, while increasing the rotational speed would increase the RFW temperature of 1045 carbon steel and 304 SS [25]. The application of numerical analysis found the same effect of these parameters on heat generation in mild steel RFW [30]. Increasing any of three parameters (e.g., the workpiece radius, rotational speed, or frictional pressure) has been found to increase the maximum temperature range in the RFW of Cu [31]. For aluminum–steel RFW, this method showed that individually increasing the velocity, friction pressure, and friction time increased the maximum temperature [32].

The RFW of carbon steel and stainless steel has been reviewed and has produced a variety of results in terms of the factors that affected the tensile strength of the joint for different materials. This demonstrated that the welded materials' combination also affects the mechanical properties of the RFW joint. However, not much research has been conducted to link the study to the type of material being welded. Many studies on the RFW of carbon steels and stainless steels have focused on the influences of process parameters on the mechanical properties of the joints. However, they did not link the research to the material type, such as the effect of the carbon content in carbon steel. In a thermomechanically controlled process, the mechanical properties and process stability during the process were influenced by the chemical composition, process parameter control, and optimization as well as post-forming cooling strategies and thermal treatments [33]. Therefore, the carbon content in carbon steel may influence the tensile properties of the RFW joint, as it involves the thermomechanical process. Hence, the different carbon contents in carbon steels can affect the strength of the connection to stainless steel. The current study investigated the RFW of 304 SS and carbon steels with varying carbon concentrations. The purpose of this work was to assess the characteristics of joining 304 SS and carbon steel using the RFW technique and to figure out how the carbon content of carbon steel affects the mechanical properties and microstructure of the joint. To achieve this goal, experiments on the RFW of 304 SS with low-carbon steel and medium-carbon steel were carried out. The studies were conducted to determine the RFW combination parameters that would provide the greatest tensile strength. The microstructure of the joint was evaluated in comparison with those of low-carbon steel and medium-carbon steel when they were welded with 304 stainless steel.

2. Materials and Methods

2.1. Materials

The materials used in the experiments were 16 mm diameter rods of low-carbon steel, medium-carbon steel, and 304 SS. Tables 1–3 show the chemical compositions of

the materials, respectively. The materials were cut into 20 mm lengths prior to the RFW experiment. To perform an RFW process, a flat surface is necessary to create a perfect mating between the surfaces of the welded materials. To obtain the flat surface, a facing process using a lathe machine was carried out on the surfaces of the two materials. The end of the bar was machined perpendicular to the axis of the bar. Shallow depth-of-cut machining was performed, creating a flat, smooth surface at the rod's end.

Table 1. Chemical composition of low-carbon steel.

C	Si	Mn	P	S	Fe
0.09	0.08	0.55	0.009	0.010	Balance

Table 2. Chemical composition of medium-carbon steel.

C	Si	Mn	P	S	Ni	Cr	Cu	Fe
0.45	0.25	0.70	0.014	0.003	0.01	0.36	0.01	Balance

Table 3. Chemical composition of SS 304.

C	Si	Mn	P	S	Ni	Cr	Cu	Fe
0.019	0.28	1.60	0.038	0.024	8.07	18.22	0.01	Balance

2.2. Experiment Setting and Procedure

The friction welding was performed with a lathe machine with a hydraulic power pack and a rod pusher. Figure 1 shows a representation of the machine. The hydraulic pack and the timer were to control the pressure and timing of its application. The hydraulic mechanism could withstand axial pressures of up to 200 bar.

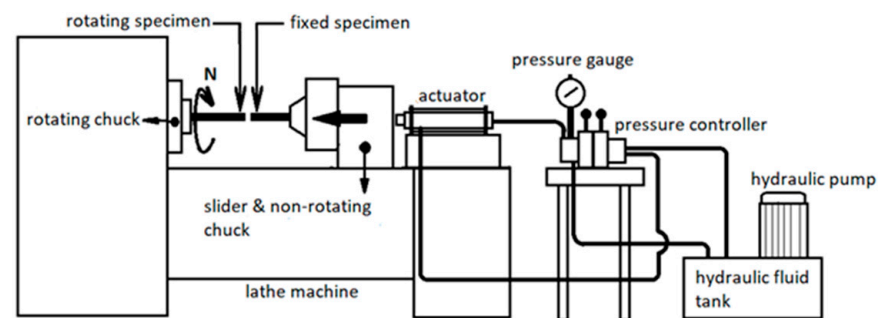


Figure 1. Lathe machine equipped with hydraulic pack for RFW process.

A fixture was installed on a lathe for the welding process. It was located on the machine guideways and could be moved toward the spindle. This equipment was designed so the center of the specimen holder was aligned with the center of the spindle to maintain the axial alignment of the two specimens. The fixed sample holder was installed in a sleeve cylinder so that it could slide and move axially. The position of the device was fixed using a bolted clamp when the required position was reached so that it could resist the force during welding. Additionally, the length of the free end of the specimen was adjusted to avoid excessive vibration and maintain the axially of the force. Prior to welding, the positions of both specimens were adjusted so that their faces were at around a 1–3 mm distance. Then, the axial force was supplied by the hydraulic piston rod of the power pack unit to provide interfacial contact between the specimens. The 304 SS was used as a fixed specimen in the RFW experiments, while the carbon-steel sample was placed on the spindle of the machine and rotated continuously. Based on the implemented experimental design, two welding processes were performed for each experimental condition.

The study used a Taguchi L_8 orthogonal array design with two replications (Table 4), which accommodated the main effect and potential interactions among factors based on its linear graph [34]. In addition to providing a useful interpretation, this Taguchi design supported an ANOVA analysis to statistically evaluate factor influences [35]. Based on the preliminary experimental results, the RFW parameters for low-carbon steel–stainless steel and medium-carbon steel–stainless steel are presented in Tables 5 and 6, respectively.

Table 4. Taguchi L_8 orthogonal array.

Experiment Run Number	P_f	T_f	P_u
1	1	1	1
2	1	1	2
3	1	2	1
4	1	2	2
5	2	1	1
6	2	1	2
7	2	2	1
8	2	2	2

Lower and higher factor levels are represented by 1 and 2, respectively. P_f : pressure during friction. T_f : time spent during friction. P_u : forging pressure after the friction stops (upset).

Table 5. Input parameters for each level in RFW of low-carbon steel–304 SS.

No.	Parameter	Low	High
1	P_f (bar)	16	35
2	T_f (second)	4	9
3	P_u (bar)	40	70

Table 6. Input parameters for each level in RFW of medium-carbon steel–304 SS.

No.	Parameter	Low	High
1	P_f (bar)	10	90
2	T_f (second)	7	11
3	P_u (bar)	95	120

Three variables, namely the friction pressure (P_f), friction time (T_f), and upset pressure (P_u), were the focus of the experimental procedure. The two previous parameters represent the heating parameters, while the most recent parameter represents the joining stage. They were chosen because they could potentially influence the tensile strength as an experimental response. To determine the high and low settings for each factor, an initial one-factor-at-a-time experiment was carried out. Other parameters, such as the spindle speed and upset time, remained constant. The spindle speeds for medium-carbon steel–304 SS and low-carbon steel–304 SS were set at 2000 RPM and 1330 RPM, respectively, while the upset time for both joints was set at three seconds.

The primary goal of the Taguchi analysis was to identify the optimal factor level combinations that maximized the experimental response, i.e., the tensile strength. Taguchi provided a transformation formula for the experimental data based on the signal-to-noise ratio (see Equation (1)). The transformed value was then analyzed using a standard ANOVA and a response table to evaluate significant factors, including their interactions, and optimal factor levels were obtained. The signal-to-noise ratio based optimization process yielded an optimal solution while minimizing the variation within factors [35].

$$\text{Signal – to – noise ratio} = -10 \log \left(\frac{1}{n} \sum_{i=1}^n \frac{1}{y_i^2} \right) \quad (1)$$

2.3. Microstructure Analysis

To prepare metallographic samples, the welded specimen was cut, leaving the welded joint. The joint was then cross-sectioned with an abrasive cutting machine and mounted using epoxy, exposing the surface for polishing. The sample surface was mechanically ground and polished using different grits of emery paper and alumina powder on a rotating disk of a polishing machine. Subsequently, the specimen's surface was etched using nital and aqua regia etching reagents for the carbon steel and stainless steel, respectively. The nital reagent was a mixture of 90% ethanol (100 mL) and HNO_3 (1–10 mL), while the aqua regia reagent consisted of 15 mL of HCl and 5 mL of HNO_3 . The characterization of the microstructure was then carried out on the sample using Amscope ME300TC-14M3 optical microscopy. Finally, the sample was used for elemental analysis using FEI Inspect S50 scanning electron microscopy (SEM) equipped with energy-dispersive spectroscopy (EDS).

2.4. Tensile Test

The welded rods were machined to make tensile test specimens on a Leadwell LTC-20B CNC lathe. During the machining, one end of a rod was fixed to the spindle of the machine, while the other end was supported by the tail stock. This was performed to prevent any defects in the samples during the machining process. The tensile samples were prepared according to ASTM E8 [36], as shown in Figure 2. The welded joint was positioned in the middle of the gauge length. To confirm that the machining process did not affect the joint, a non-destructive inspection using a liquid penetrant was carried out on the machined surfaces of several samples. The inspection revealed that there were no defects or cracks found on the machined surfaces. The tensile test was then performed on a Tarno Grocki UPH 100KN universal testing machine, which was operated in displacement control and had a crosshead speed of 5 mm/min.

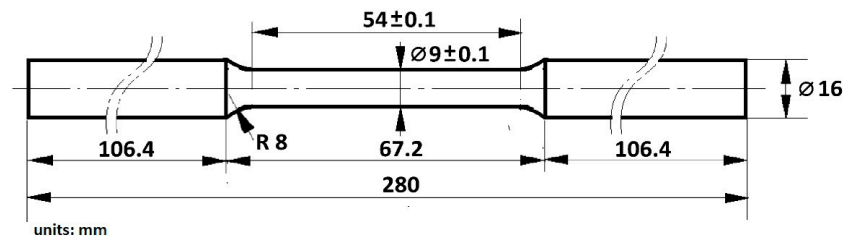


Figure 2. Dimensions of tensile test specimen based on ASTM E8M.

3. Results and Discussion

3.1. Visual Observation

Figure 3a,b show several samples of low-carbon steel and medium-carbon steel welded with 304 stainless steel. The illustrations exhibit sound joints for the two materials. Both the carbon-steel and stainless-steel sides of both pairs produced flash. The samples depict a variety of flash conditions at the joint. The higher the values of the experiment parameters, the more flash that was produced. Higher and longer friction pressures (P_f and T_f) and upset pressure (P_u) caused more heat and deformation. This caused more flash at the joint. Figure 3a shows that the setting parameters of $P_f = 16$, $T_f = 4$, and $P_u = 40$ (sample 4) produced the highest flash at the joint of low-carbon steel–304 SS. Conversely, the parameters of $P_f = 16$, $T_f = 4$, and $P_u = 40$ led to the smallest flash at the joint (sample 1). Similarly, Figure 3b illustrates that sample number 4, which had high values for the RFW parameters (i.e., $P_f = 90$, $T_f = 11$, and $P_u = 120$) yielded the highest flash compared to sample 1 ($P_f = 10$, $T_f = 7$, and $P_u = 95$), which gave the smallest flash at the joint of medium-carbon steel–304 SS.

A higher flash was produced at the carbon steel part in both the low-carbon steel–stainless steel and medium-carbon steel–stainless steel joints. The higher heat conductivity of the carbon steel compared to the stainless steel allowed the material to soften and deform more severely. Because of its lower deformation resistance, more materials on the side of

the carbon steel workpiece were forced radially outward from the flash [25]. As a result, more flash was formed on the carbon steel parts.



Figure 3. Samples of welded specimens of (a) low-carbon steel–304 SS: 1. $P_f = 16$, $T_f = 4$, and $P_u = 40$; 2. $P_f = 16$, $T_f = 4$, and $P_u = 70$; 3. $P_f = 35$, $T_f = 4$, and $P_u = 40$; and 4. $P_f = 35$, $T_f = 9$, and $P_u = 70$ and (b) medium-carbon steel–304 SS: 1. $P_f = 10$, $T_f = 7$, and $P_u = 95$; 2. $P_f = 10$, $T_f = 11$, and $P_u = 95$; 3. $P_f = 90$, $T_f = 7$, and $P_u = 95$; and 4. $P_f = 90$, $T_f = 11$, and $P_u = 120$ (units: P = bar, T = second).

3.2. Microstructure of the Joint

The macrostructures of the low-carbon steel–304 SS and medium-carbon steel–304 SS joints are presented in Figure 4a,b, respectively. Both figures identify three parts of the structures at the joints. They are the interface (IF) layer, the thermomechanically affected (TMA) zone, and the heat-affected zone (HAZ). As shown in Figure 2b, the TMA and HAZ at the joint of medium-carbon steel and 304 SS are thicker than those of low-carbon steel and medium-carbon steel. The higher hardness of medium-carbon steel generated more heat around the joint when it was in friction with the 304 SS; thus, it resulted in thicker TMA and HAZ at the medium-carbon steel–304 SS joint.

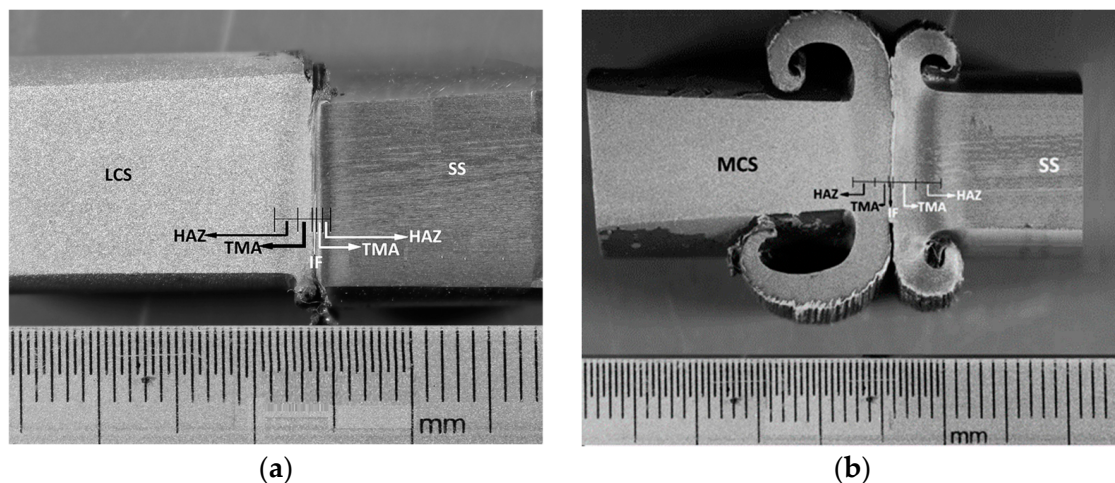


Figure 4. Macrostructures at the joints of (a) low-carbon steel–304 SS ($P_f = 16$, $T_f = 4$, and $P_u = 40$) and (b) medium-carbon steel–304 SS ($P_f = 90$, $T_f = 7$, and $P_u = 95$).

Heat was generated during the application of friction pressure due to the friction of the mating surfaces. The applied pressure caused heavy deformation in both metals at the same time. The microstructural change was caused by a temperature increase and heavy deformation. Deformation, dynamic recovery, and recrystallization occurred, stimulating microstructural change around the joint. Aside from structural changes, the different element concentrations in the metals may cause element diffusion. As a result, elemental irregularities and the formation of new phases around the joint were also possible.

Figure 5 presents the microstructure of the low-carbon steel–stainless steel joint (a). It illustrates three parts, namely the base metal of carbon steel, the interface zone, and the base metal of stainless steel. However, in low-carbon steel and 304 SS, two parts of the microstructure zone were indicated in the macrostructure of the joint, as shown in Figure 4, i.e., the TMA and HAZ. The structure of the carbon steel consisted of ferrite and pearlite (Figure 5a). At the 304 SS part, austenite grain was observed as a typical structure of the austenitic stainless steel. Near the interface zone, some areas with different microstructures were observed on both the carbon-steel and stainless-steel sides. The figure depicts finer ferrite and pearlite grains on the carbon-steel side closest to the interface. This part was the structure of the TMA in low-carbon steel. An enlarged view of the 304 SS is given in Figure 5c. The figure shows that the TMA structure, which was closed to the interface, contained a very fine deformed grain. The coarser elongated grain appeared beyond this area. The structure at the TMA indicated the process of deformation, which was followed by recovery and recrystallization. The product of this process was a very fine grain. As the process continued, the grain grew into the larger size that appeared at the HAZ.

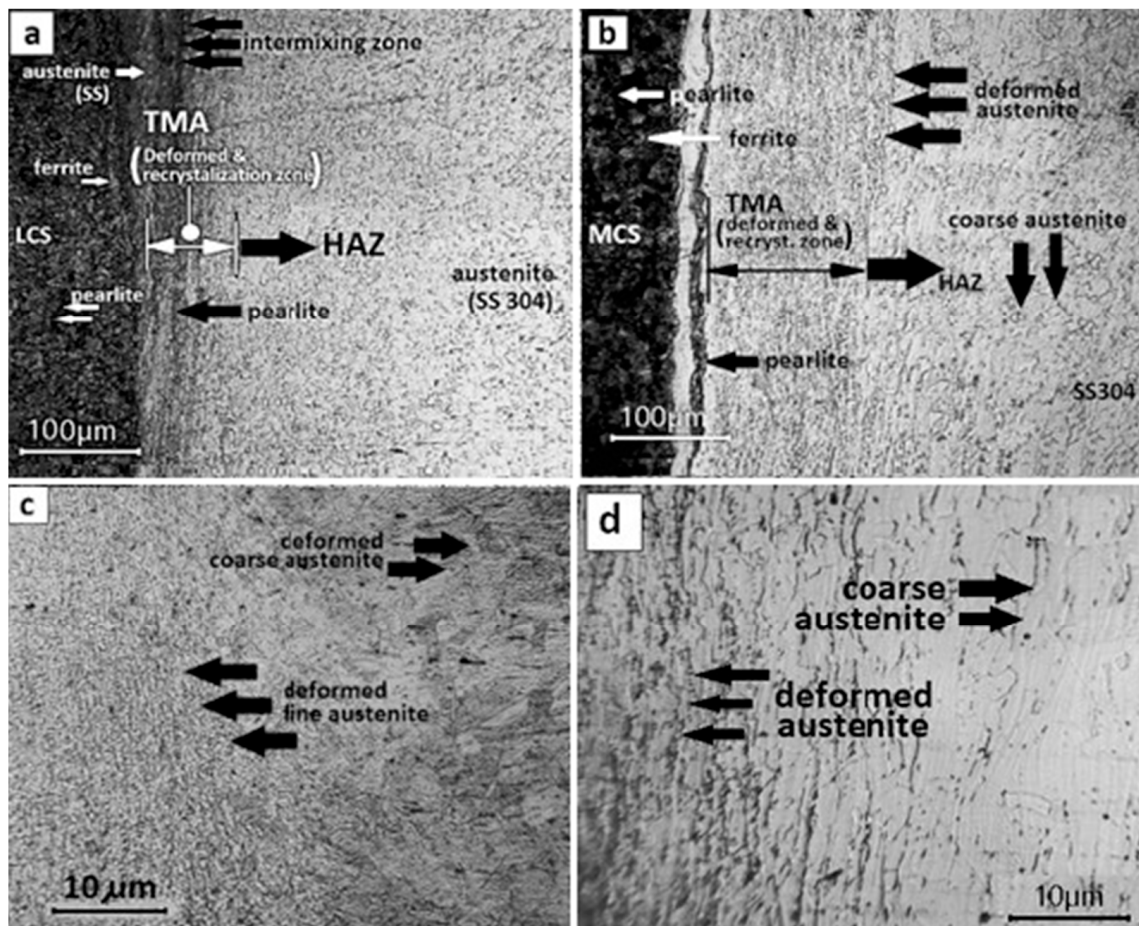


Figure 5. Microstructure of the interface at the joint of carbon steel–304 SS: (a) low-carbon steel–304 SS joint; (b) medium-carbon steel–304 SS joint; (c) enlarged view of deformed structure at TMA and coarse austenite in HAZ in low-carbon steel–304 SS joint; (d) enlarged view of deformed structure and coarse grain of austenite in HAZ in medium-carbon steel–304 SS joint.

The interface of the low-carbon steel–304 SS joint illustrated a mixing zone of the low-carbon steel and stainless steel (see Figure 6). The severe deformation of both materials had built this mixing area, which produced an interlock between the materials. A darker zone at the joint was part of the carbon steel, which moved and mixed with the 304 SS. This was observed in a previous work in the RFW of mild steel with 304 SS [37]. This

could happen due to a combination of heating and deformation. The axial force exerted by the upset pressure caused excessive deformation, which pushed the materials. Previous research suggested that angular velocity during the friction [38] led the softened metals to move away from the center. However, some materials remained at the center and mixed with the other metal. This resulted in an intermixing zone at the joint, as also seen in the current work. It seems that this mixing phenomenon occurs especially in the joining of carbon steel with 304 SS. Previous studies in the RFW of mild steel [37] and 1045 carbon steel with 304 SS [38] discovered this. As a result, they proposed that it was also dependent on the type of welded metal.

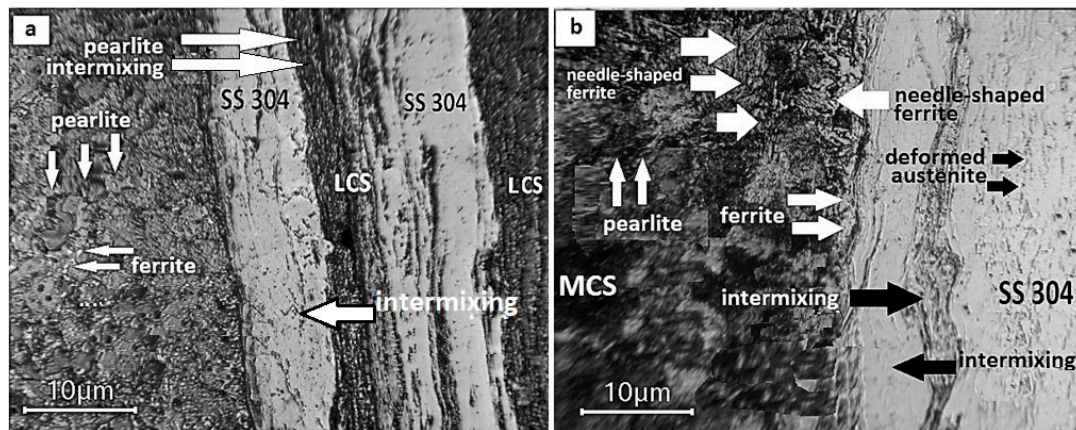


Figure 6. Microstructure of the interface at the joint of low-carbon steel–304 SS (a) and medium-carbon steel–304 SS (b).

The EDS mapping of the elements at the joint, as given in Figure 7, shows the distribution of Cr (dominant elements of SS) and Fe elements. The figure exhibits less Cr at the island on the SS side, indicating that the island was a part of the carbon steel. This phenomenon was observed previously in the RFW of 304 SS with mild steel [37]. A higher portion of carbon steel that moved and mixed with stainless steel was found at the periphery of the joint. This part also increased with an increasing friction time [38]. The two conditions indicated that the mixing of carbon steel and stainless steel at the joint was caused by the deformation of both metals. In the present work, the mixing zone at the joint of low-carbon steel and stainless steel was higher than at the joint of medium-carbon steel and stainless steel. Since low-carbon steel is more ductile than medium-carbon steel, the low-carbon steel experienced more deformation at the joint and produced a larger mixing zone.

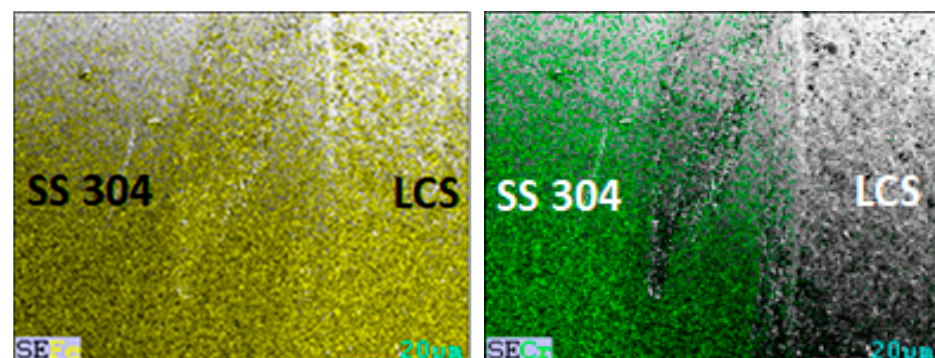


Figure 7. EDS element (Fe and Cr) mapping at the joint of low-carbon steel–304 SS.

The general microstructure of medium-carbon steel–stainless steel is depicted in Figure 5b. The figure shows a dark, thin layer closed to the interface on the stainless-steel

side. This is the carbon steel that was pushed to the stainless-steel side and created a mixing zone. This intermixing was possible due to hot deformation during the RFW process.

The formation of thicker TMA and HAZ at the medium-carbon steel–stainless steel joint can be seen in the figure. This suggested that friction generated more heat during the RFW process and allowed for more deformation. The higher temperature at the medium-carbon steel–stainless steel joint was also confirmed by temperature measurements taken during the RFW process experiment. Furthermore, the higher thermal conductivity of medium-carbon steel enabled longer heat transmission, resulting in a larger TMA and HAZ.

A fine grain of ferrite and pearlite could be seen at the interface between low-carbon steel–304 SS and medium-carbon steel–304 SS. Figure 6 illustrates this. A ferrite structure appeared at the interface and border of the medium-carbon steel. This was identified as proeutectoid ferrite [39], which was formed earlier during the hypoeutectoid steel phase transformation of austenite to pearlite. As claimed in the friction welding of 1045 steel, martensite could also form in this area [40,41]. In the current work, a needle-shaped structure was observed at the TMA of medium-carbon steel. This can be seen in Figure 6b. The needle-plate structure resembles acicular ferrite, which is commonly formed in weld metal/HAZ [42] and thermomechanically treated steel [43]. It was discovered in medium-carbon steel–316L stainless steel RFW [20]. The authors hypothesized that it was formed as a result of the TMA zone overheating. The isothermal or continuous cooling transformation of medium-carbon microalloyed forging steel produced this [44]. The acicular ferrite was most efficiently produced when the steel had a medium carbon content [45]. It was identified as a microstructure that could potentially improve a combination of weld metal and HAZ strength, toughness, and fatigue properties in high-strength low-alloy (HSLA) steels [44]. The welding efficiency of medium-carbon steel and stainless steel joined by RFW in this work was 109.5% compared to stainless steel, the weaker material, and 98.7% compared to medium-carbon steel. This was much better than the strength of a low-carbon steel–304 SS joint. The possible reason for this strength improvement is discussed in the next section.

The interface of the medium-carbon steel–304 SS joint was like that of the previously discussed low-carbon steel–304 SS joint. At the joint, a medium-carbon steel–304 SS mixing zone was observed. Figures 5b and 6b demonstrate this. The medium-carbon steel is the thin, dark island in the stainless steel that transferred and mixed with the stainless steel because of heating and deformation. The EDS mapping of the elements at the joint, as shown in Figure 8, confirmed this. A lower Cr concentration in the thin layer at the stainless steel revealed that it was medium-carbon steel that mixed with the stainless steel. The intermixing zone in medium-carbon steel–stainless steel was thinner than the mixing zone in low-carbon steel–stainless steel. This could be due to the lower yield strength and greater ductility of low-carbon steel, which allow for greater deformation. Figure 8 depicts the distribution of elements at the joint but does not depict the colony of a compound or a specific phase. As a result, no intermetallic compound was detected at the joint in this study.

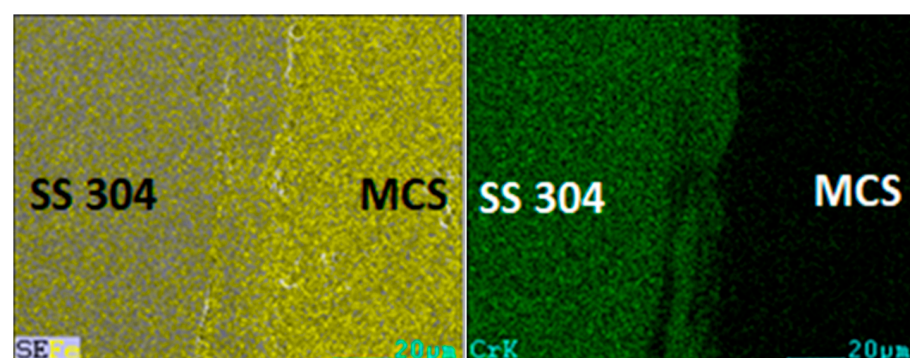


Figure 8. EDS element (Fe and Cr) mapping at the joint of medium-carbon steel–304 SS.

A flow of transversal deformation appeared near the medium-carbon steel–304 SS joint. This part was the TMA zone, which indicated the deformation, recovery, and recrystallization areas during the RFW process of medium-carbon steel–304 SS. The clearer, elongated grain, indicating the deformed structure and its boundary with the coarse structure of the HAZ, can be seen in its enlarged picture in Figure 5d. Beyond this area, the microstructure of the stainless steel consisted of larger equiaxed-grain austenite. Comparing the joints of low-carbon steel–304 SS with those of medium-carbon steel–304 SS, Figure 5a,b) showed that a thicker TMAZ and HAZ were indicated at the joint of medium-carbon steel–304 SS. This could indicate that more heat was generated and transmitted further in medium-carbon steel–304 SS than in low-carbon steel–304 SS. The deformation zone terminated at the HAZ, where the microstructure was a small, equiaxed, austenite grain (Figure 5b). Beyond the HAZ, the structure was austenite with a larger grain because it was owned by the base metal structure of the stainless steel.

The preceding discussion described similar microstructural joint conditions in the RFW of low-carbon steel–304 SS and medium-carbon steel–304 SS. The TMA zone was observed in the carbon steel and 304 SS as a deformation, dynamic recovery, and recrystallization zone. The microstructure of this part was composed of fine ferrite and pearlite at the low-carbon steel–304 SS joint. At the HAZ, a larger regular structure was formed until it reached the base metal, which had the typical low-carbon-steel structure of ferrite and pearlite. A fine structure was also observed at the medium-carbon-steel portion of the medium-carbon steel–304 SS joint. However, a needle-plate structure was discovered near the joint interface. This structure may have been acicular ferrite formed during the deformation and thermomechanical treatment [43,45]. The higher carbon content in medium-carbon steel may promote the formation of acicular ferrite during the thermomechanical treatment's continuous cooling transformation [45]. As previously stated, the structure was acknowledged to improve the material's strength.

The metallographic analysis of the joint revealed a zone of carbon steel and 304 SS intermixing at both the low-carbon steel–304 SS and medium-carbon steel–304 SS joints. It was observed that carbon steel was transferred to stainless steel and vice versa. The element distribution obtained from the EDS analysis confirmed the presence of carbon steel both on the 304 SS side and the carbon-steel side. The mechanical interlocking of the materials was caused by heating and severe deformation during the RFW process. It was discovered that friction time influenced the width of the intermixing zone [38]. However, the current study found that the low-carbon steel–304 SS joint experienced more material mixing than the medium-carbon steel–304 SS joint. This was due to the low-carbon steel having a lower yield strength and greater ductility than the medium-carbon steel. This allowed for more deformation and material mixing at the joint. As a result, in addition to the friction time, the types of materials influenced the width of the intermixing zone.

According to the EDS analysis, elements transferred at the joint. The diffusion of these elements has been widely recognized in the RFW of dissimilar materials [26,37]. However, in the current work, the element distribution did not preclude the occurrence of intermetallic compounds.

3.3. Tensile Strength

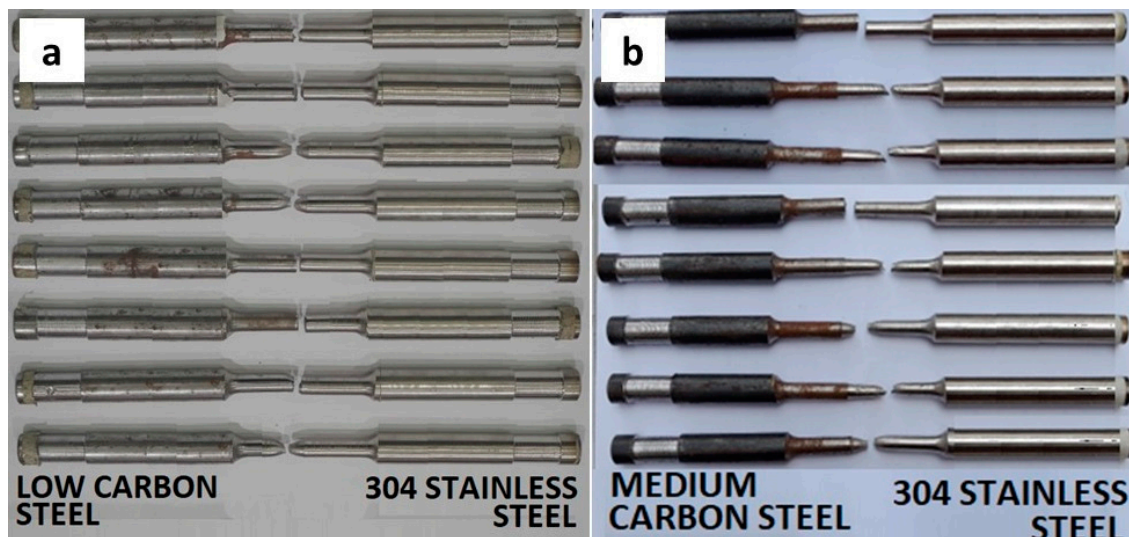
The tensile strength data from the RFW experiments on low-carbon steel–304 SS and medium-carbon steel–304 SS are shown in Tables 7 and 8, respectively. During the tensile test of low-carbon steel–304 SS, most fractures occurred at the joints; however, fractures at the carbon-steel base metal were also found in some conditions. Meanwhile, some medium-carbon steel–304 SS specimens showed fractures in the 304 SS material, indicating that the strength of joined parts was greater than those of the weaker base materials (Figure 9). The tensile strengths of the low-carbon steel and 304 SS were found to be in the range of 296.01–492.40 MPa, while the tensile strengths of the medium-carbon steel and 304 SS were found to be in the range of 246.27–745.49 MPa.

Table 7. Tensile strength of RFW low-carbon steel–304 SS.

Parameters					Tensile Strength (MPa)	
P_f (sec)	T_f (sec)	P_u (bar)	T_u (sec)	R Speed (RPM)	Replication 1	Replication 2
16	4	40			443.82	492.40
16	4	70			437.47	420.33
35	9	40			319.65	302.89
35	9	70			334.23	353.87
16	9	40	3	1330	451.95	484.10
16	9	70			487.03	473.96
35	4	40			356.58	296.01
35	4	70			356.21	403.59

Table 8. Tensile strength of RFW medium-carbon steel–304 SS.

Parameters					Tensile Strength (MPa)	
P_f (sec)	T_f (sec)	P_u (bar)	T_u (sec)	R Speed (RPM)	Replication 1	Replication 2
10	7	95			333.06	314.67
10	7	120			444.15	246.26
90	11	95			692.02	751.23
90	11	120			704.82	714.66
10	11	95	3	2000	417.05	466.64
10	11	120			386.72	462.23
90	7	95			745.49	744.44
90	7	120			701.40	752.93

**Figure 9.** Broken specimens of low-carbon steel–304 SS (a) and medium-carbon steel–304 SS (b) after tensile testing.

The welding efficiency is the percentage of the joint strength relative to the strength of the base metal. Thus, it was calculated as (tensile strength of the welding joint/tensile strength of the base metal) \times 100%. The maximum RFW efficiencies of low-carbon steel and 304 SS were 103.3% and 72.4%, respectively, when compared to the tensile strengths of the two materials. When compared to 304 SS, as the weaker material, the RFW of medium-carbon steel–304 SS had the highest welding efficiency of 109.5%. The RFW efficiency for these materials was 98.7% when compared to medium-carbon steel. As a result, the joint strength of medium-carbon steel and SS 304 was nearly equal to that of the

stronger material. Assuming that the welding process remained highly efficient, all of the experiment data (tensile strength) could be statistically analyzed.

The joint tensile strength data revealed that welding 304 SS to medium-carbon steel produced a higher welding efficiency than welding 304 SS to low-carbon steel. This could relate to the microstructure of the joint. The microstructure of the joint consisted of three parts: the interface layers, TMA, and HAZ. The deformed microstructure at the TMA was indicated by the elongated grain. This can be seen in Figure 5. The TMA zone ended with fine grain as a result of recovery and recrystallization. This was found at the joint of low-carbon steel and 304 SS as well as in medium-carbon steel and 304 SS joints. Nevertheless, the TMA zone at the joint of medium-carbon steel–304 SS was thicker than at the joint of low-carbon steel–304 SS. Several studies have claimed the existence of intermetallic compounds or carbide precipitations in the carbon steel–stainless steel joint [20,39,46]. The intermetallic compound is normally brittle, which decreases the joint's strength. In this work, however, intermetallic compounds or precipitations were not observed. Although the distribution of elements was detected in both welded materials, no precipitate could be detected.

The better strength of the medium-carbon steel–304 SS joint compared to the low-carbon steel–304 SS joint could be due to the thicker TMA produced at the joint. It consisted of a deformed and fine-grained structure. It was well known in the literature that the deformed structure was related to the dislocation density and improved the material's strength. The deformation due to the compressive force created an accumulation of dislocation density in the microstructure of the high-carbon steel. The dislocation increased as the deformation lengthened. The dislocation motion became constrained as the dislocation density increased. This increased the hardness of the structure [47]. In low-alloy carbon steel, both deformation and phase transformation resulted in a high dislocation density [48]. Hot forming combined with quenching, partitioning, and tempering in medium-carbon steel increased the dislocation density and improved the tensile strength [49]. Based on the relations between deformation, dislocation, and strength improvement suggested by the reviewed studies, it could be expected that the presence of the deformed and fine-grained structure in the joint of medium-carbon steel–304 SS contributed to the strength of the joint. Furthermore, a thicker TMA in the joint may also result in a higher joint strength than in a low-carbon steel–304 SS RFW joint.

Besides the deformed structure, the influence of fine grain on the material's strength has also been revealed. Increasing the grain size decreased the yield and the ultimate strength of manganese austenitic steel [50]. Fine grain also improved the mechanical properties of high-carbon steel [51]. A reduction in grain size significantly increased the strength of low-carbon, high-Mn austenitic steel [52]. Thus, the small grain size at the joint of the RFW seems to improve joint strength.

As a summary, a microstructural change in the joint of carbon steel and 304 SS took place during the RFW process. This was caused by the thermomechanical processing. Intermetallic compounds may be formed as the result of the reaction of elements from the welded metals. In this work, however, we were unable to observe any precipitations at the joint. Mechanical interlocking caused by mechanical mixing due to excessive deformation occurred at the joint. Near the interface, the thermomechanical processing produced a deformed structure and fine grain, which resulted from the recovery and recrystallization processes. Beyond the TMA, coarser-equiaxed grain was formed in the HAZ. This zone ended with an unaffected base metal that retained the metal's original coarse structure. The structure of the TMA, which consisted of a deformed and fine-grained structure, may have enhanced the strength of the welded joint.

3.4. Taguchi Analysis and Optimization

The Taguchi design and analysis have the advantage of identifying the best factor combinations to maximize the tensile strength while minimizing variance. The measured value was converted into a signal-to-noise ratio using the larger-is-better formula

(see [27] and [28]). As a result, the signal-to-noise ratio as well as the ANOVA and effect plots were included in the statistical analysis in this paper, which followed the standard Taguchi procedure.

Tables 9 and 10 show the ANOVA for low-carbon steel–304 SS and medium-carbon steel–304 SS welding based on the signal-to-noise ratio. All of the individual main effects were significant when compared to the p -value using a significance level of 5%, indicating that this experiment successfully captured the influencing factors in RFW. Furthermore, except for one interaction in low-carbon steel–304 SS (see Table 6), almost all interactions were significant. These results indicated that these predetermined factors cannot be separated; all factors influence tensile strength simultaneously. The ANOVA and effect plots, on the other hand, revealed some differences between low-carbon steel–304 SS and medium-carbon steel–304 SS welding (Figures 10 and 11).

Table 9. Low-carbon steel–304 SS ANOVA analysis for the signal-to-noise ratio (the larger the better).

Source	DF	Seq SS	Adj SS	Adj MS	F	p	% Contrib.
P_f	1	0.5699	0.5699	0.5699	40.87	0.024	3.42%
T_f	1	14.4654	14.4654	14.4654	1037.27	0.001	86.80%
P_u	1	0.3885	0.3885	0.3885	27.86	0.034	2.33%
P_f*T_f							
P_f*P_u	1	0.2759	0.2759	0.2759	19.78	0.047	1.66%
T_f*P_u	1	0.9385	0.9385	0.9385	67.3	0.015	5.63%
Residual	2	0.0279	0.0279	0.0139			
Total	7	16.666					

Table 10. Medium-carbon steel–304 SS ANOVA analysis for the signal-to-noise ratio (the larger the better).

Source	DF	Seq SS	Adj SS	Adj MS	F	p	% Contrib.
P_f	1	69.8307	69.8307	69.8307	7298282	0.000	90.03%
T_f	1	3.0678	3.0678	3.0678	320626	0.001	3.96%
P_u	1	0.2056	0.2056	0.2056	21491.8	0.004	0.27%
P_f*T_f	1	4.4115	4.4115	4.4115	461065.6	0.001	5.69%
P_f*P_u	1	0.0426	0.0426	0.0426	4454.28	0.010	0.05%
T_f*P_u	1	0.0058	0.0058	0.0058	607.83	0.026	0.01%
Residual	1	0	0	0			
Total	7	77.564					

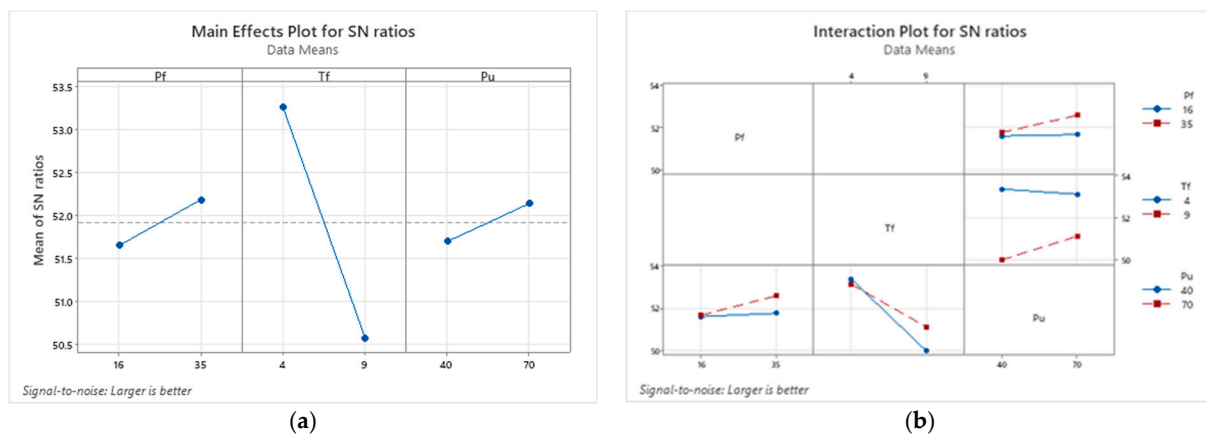


Figure 10. Low-carbon steel–304 SS main effect (a) and interaction (b) plots for SNR.

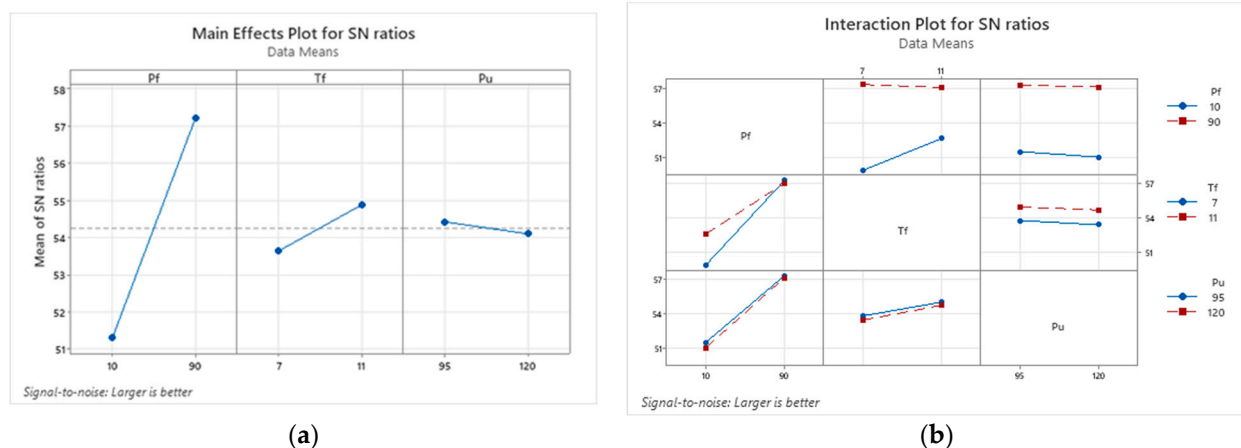


Figure 11. Medium-carbon steel–304 SS main effect (a) and interaction (b) plots for signal-to-noise ratio.

Although all the individual effects were significant, the contribution ratio varied, depending on the welded material. In medium-carbon steel–304 SS, the friction pressure had a high contribution ratio (see Table 10 and Figure 11); in low-carbon steel–304 SS, the friction time had a high contribution ratio (see Table 9 and Figure 10). As a result of these discoveries, special characteristics for welding carbon steel with SS 304 were discovered, namely that the hardest factor influencing joint strength is the material's hardness. When welding a harder material (i.e., medium-carbon steel) with 304 SS, careful control of the friction pressure was required, whereas welding low-carbon steel, as the softer material, required more consideration of the friction time variation. This phenomenon could be explained by the suggestion that the friction time was required to bring the material to its peak temperature [21]. As a result, a sufficient friction time was required to heat up the softer materials. In other words, to obtain a stronger joint, a longer friction time was needed. Hence, increasing the friction time in the RFW of low-carbon steel–304 SS improved the tensile strength more than the other parameters.

For the case of a harder material, e.g., medium-carbon steel as compared to low-carbon steel, sufficient friction pressure was also required to promote deformation. Thus, a higher friction pressure was required when joining the harder material. The increased friction pressure improved the heat generation and enhanced the efficiency of converting mechanical work into heat. A higher pressure was needed to spur the deformation required for the joining of the harder material, such as medium-carbon steel, when compared to low-carbon steel [25]. As a result, a higher friction pressure may result in a higher tensile strength in a medium-carbon steel with a 304 SS joint. Therefore, in the RFW of medium-carbon steel with 304 SS, the friction pressure was a more influential factor in improving the joint strength than the other parameters.

Finally, the goal of the Taguchi analysis was to find the best factor level combination that maximized the tensile strength based on the signal-to-noise ratio. The Taguchi method recommended selecting 50% of the significant factors as the basis for selecting the optimal level [28] and remaining involved in existing interactions. Nevertheless, in this case, with only three factors included in the experiment, all these factors must be involved to find an optimal level. The selection of optimal factor levels referred to the highest signal-to-noise ratio value, as shown in Table 11. Therefore, besides the dominant factor discussed previously, the prediction of these selected optimal levels gave a high tensile strength compared to those in Tables 7 and 8. This optimal condition suggested the combination of RFW parameters (i.e., the friction force, friction time, and upset pressure) that would provide the highest tensile strength.

Table 11. Optimal factor levels based on Taguchi analysis.

Welded Material	Selected Factors for Optimization	Interaction between Factors	Optimal Selected Factor Level	Tensile Strength Prediction (MPa)	
				Mean	SNR
Low-carbon steel–304 SS	P_f, T_f, P_u	Not significant (optimal factors ignore the interaction)	$P_f = 35$ bar $T_f = 4$ s $P_u = 70$ bar (based on Figure 10a)	476.56	53.59
Medium-carbon steel–304 SS	P_f, T_f, P_u	Significant	$P_f = 90$ bar $T_f = 7$ s $P_u = 95$ bar (based on Figure 11a)	739.39	57.44

4. Conclusions

Medium-carbon steel and low-carbon steel were successfully welded with 304 SS using the RFW method. The RFW of medium-carbon steel–304 SS produced a stronger joint and better efficiency than the RFW of low-carbon steel–304 SS. The welding efficiency for medium-carbon steel–304 SS was 109.5% compared to SS 304, as the weaker material, while the welding efficiency for low-carbon steel–304 SS was 103.3% compared with the low-carbon steel.

Three factors, i.e., P_f , T_f , and P_u , had a significant influence on the tensile strength, including their interaction. Among those parameters, P_f was more influential when joining medium-carbon steel (the harder material) with 304 SS, whereas the friction time had a greater effect when joining low-carbon steel with 304 SS. Optimization processes using a Taguchi analysis revealed that the highest tensile strength of low-carbon steel–304 SS, i.e., 476.56 MPa, was produced by the parameter combination of $P_f = 35$ bars, $T_f = 4$ s, and $P_u = 70$ bars. For the medium-carbon steel–304 SS, the highest tensile strength was 739.39 MPa, which resulted from the parameter combination of $P_f = 90$ bars, $T_f = 7$ s, and $P_u = 95$ bars.

At the interface of carbon steel and 304 SS, a metal mixing zone was formed. Because low-carbon steel has a lower yield strength and better ductility than medium-carbon steel, a thicker mixing zone tends to form at the joint of low-carbon steel and 304 SS. Medium-carbon steel produced more heat and transmitted it further during friction due to its higher carbon content and heat conductivity. It resulted in a thicker deformation zone and a larger HAZ. These factors also influenced the formation of an acicular ferrite phase, which increased the strength of the joint.

Author Contributions: Conceptualization, H.F. and S.C.; methodology, M.A.H.; software, M.A.H.; investigation, Y.P.T. and I.W.; writing—original draft preparation, H.F.; writing—review and editing, M.A.H.; All authors have read and agreed to the published version of the manuscript.

Funding: This research was funded by the Directorate of Research, Technology, and Community Services, Ministry of Education, Culture, Research, and Technology, Republic of Indonesia, grant number 073/E5/P6.02.00.PT/2022, dated 16 March 2022, contract number 004/SP2H/PT-L/LL7/2022.

Data Availability Statement: Not applicable.

Conflicts of Interest: The authors declare no conflict of interest. The funders had no role in the design of the study; in the collection, analyses, or interpretation of the data; in the writing of the manuscript; or in the decision to publish the results.

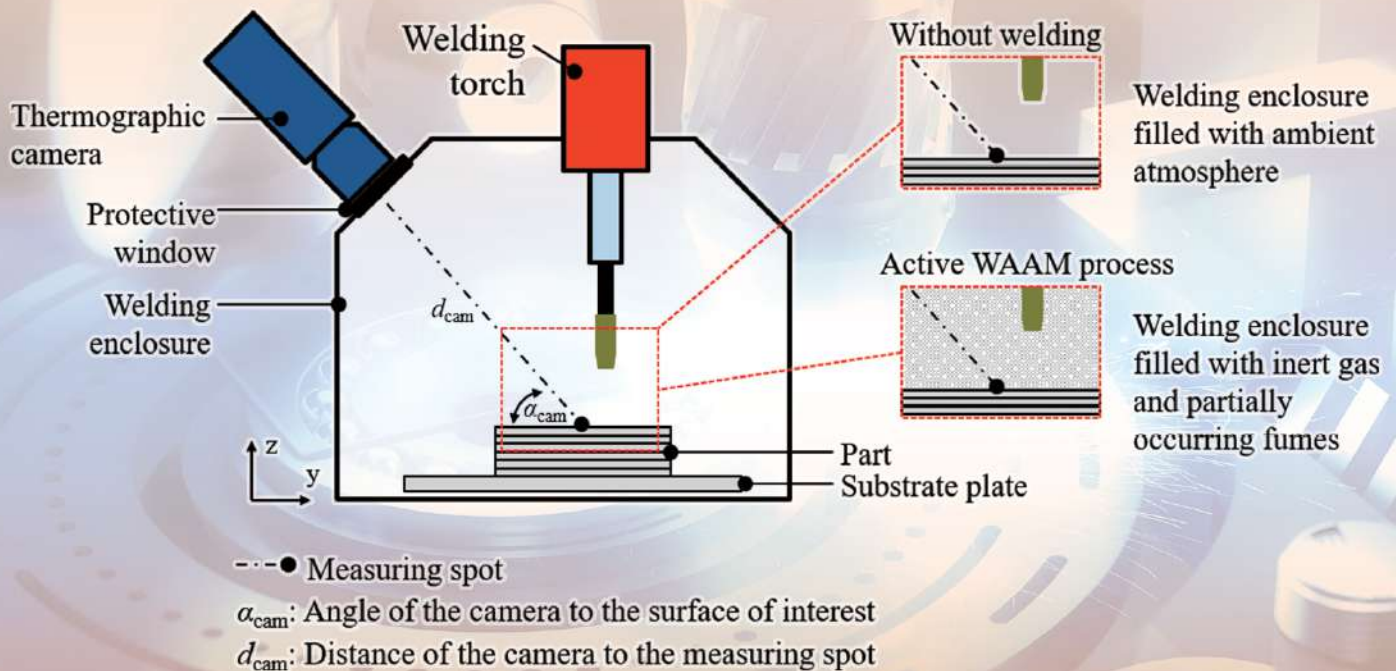
References

1. Mvola, B.; Kah, P.; Martikainen, J. Welding of dissimilar non-ferrous metals by GMAW processes. *Int. J. Mech. Mater. Eng.* **2014**, *9*, 119. [\[CrossRef\]](#)
2. Karim, A.; Park, Y.-D. A Review on Welding of Dissimilar Metals in Car Body Manufacturing. *J. Weld. Join.* **2020**, *38*, 8–23. [\[CrossRef\]](#)
3. Chaudhari, R.; Loharkar, P.K.; Ingle, A. Applications and challenges of arc welding methods in dissimilar metal joining. *IOP Conf. Ser. Mater. Sci. Eng.* **2020**, *810*, 012006. [\[CrossRef\]](#)

4. Zeng, H.; Zhang, Y.; Zhou, J.; Sun, D.; Li, H. Research Progress of Fusion Welding Techniques for Steel to Other Metals. *Am. J. Mech. Mater. Eng.* **2022**, *6*, 6–9. [\[CrossRef\]](#)
5. Kah, P.; Shrestha, M.; Martikainen, J. Trends in Joining Dissimilar Metals by Welding. *Appl. Mech. Mater.* **2014**, *440*, 269–276.
6. Vyas, H.D.; Mehta, K.P.; Badheka, V.; Doshi, B. Friction welding of dissimilar joints copper-stainless steel pipe consist of 0.06 wall thickness to pipe diameter ratio. *J. Manuf. Process.* **2021**, *68*, 1176–1190. [\[CrossRef\]](#)
7. Shanjeevi, C.; Satish Kumar, S.; Sathiya, P. Evaluation of Mechanical and Metallurgical Properties of Dissimilar Materials by Friction Welding. *Procedia Eng.* **2013**, *64*, 1514–1523. [\[CrossRef\]](#)
8. Zhao, S.; Wang, M.; Kou, S.; Jia, Z.; Wang, W.; Li, Q.; Luo, G.N. Realization of ODS-Cu/T91 Tube-to-tube Joining with Rotary Friction Welding. *Fusion Eng. Des.* **2020**, *158*, 111699. [\[CrossRef\]](#)
9. Wang, M.; Zhao, S.; Wang, W.; Li, Q.; Luo, G.-N. Preliminary results of CuCrZr/316L tube-to-tube junctions fabricated with rotary friction welding. *Fusion Eng. Des.* **2019**, *148*, 111275. [\[CrossRef\]](#)
10. Shanjeevi, C.; Arputhabalan, J.; Dutta, R. Pradeep Investigation on the Effect of Friction Welding Parameters on Impact Strength in Dissimilar Joints. *IOP Conf. Ser. Mater. Sci. Eng.* **2017**, *197*, 012069. [\[CrossRef\]](#)
11. Karabey, Ö.; Akkuş, A. Effect of Welding Parameters on Axial Shortening in Continuous Friction Welded Inconel 718 Superalloy and AISI 316L Stainless Steel. *Eur. J. Sci. Technol.* **2022**, *34*, 311–316. [\[CrossRef\]](#)
12. Anitha, P.; Majumder, M.C.; Saravanan, V.; Rajakumar, S. Effect of Burn-Off Length for Friction Welded Dissimilar Joints of Inconel 718 and SS410. *J. Adv. Mech. Eng. Sci.* **2018**, *4*, 30–37. [\[CrossRef\]](#)
13. Kumar, R.; Balasubramanian, M. Application of response surface methodology to optimize process parameters in friction welding of Ti-6Al-4V and SS304L rods. *Trans. Nonferrous Met. Soc. China* **2015**, *25*, 3625–3633. [\[CrossRef\]](#)
14. Muralimohan, C.H.; Muthupandi, V.; Sivaprasad, K. Properties of Friction Welding Titanium-Stainless Steel Joints with a Nickel Interlayer. *Procedia Mater. Sci.* **2014**, *5*, 1120–1129. [\[CrossRef\]](#)
15. Cheepu, M.; Che, W.S. Friction Welding of Titanium to Stainless Steel Using Al Interlayer. *Trans. Indian Inst. Met.* **2019**, *72*, 1563–1568. [\[CrossRef\]](#)
16. Alves, E.P.; Toledo, R.C.; Botter, F.G.; An, C.Y. Experimental Thermal Analysis in Rotary Friction Welding of Dissimilar Materials. *J. Aerosp. Technol. Manag.* **2019**, *11*, 1068. [\[CrossRef\]](#)
17. Vishnoi, M.; Kumar, V.A.N.; Murugan, S.S. Friction welding of stainless steel-aluminum alloy and optimization of different parameters using Taguchi-L8 array method. *J. Mech. Mech. Eng.* **2017**, *4*, 1–10.
18. Dong, H.; Yang, J.; Li, Y.; Xia, Y.; Hao, X.; Li, P.; Sun, D.; Hu, J.; Zhou, W.; Lei, M. Evolution of interface and tensile properties in 5052 aluminum alloy/304 stainless steel rotary friction welded joint after post-weld heat treatment. *J. Manuf. Process.* **2020**, *51*, 142–150. [\[CrossRef\]](#)
19. Allali, A.; Aissani, M.; Mesrati, N.; Othmani, B.; Medkour, M.; Boukhadouni, I.; Khiali, A. Experimental, mechanical characterizations of friction welding of steel and aluminum joints. *J. Adv. Manuf. Eng.* **2020**, *1*, 9–15.
20. Khidhir, G.I.; Baban, S.A. Efficiency of dissimilar friction welded 1045 medium carbon steel and 316L austenitic stainless-steel joints. *J. Mater. Res. Technol.* **2019**, *8*, 1926–1932. [\[CrossRef\]](#)
21. Nasution, A.K.; Gustami, H.; Suprastio, S.; Fadillah, M.A.; Octavia, J.; Saidin, S. Potential use of Friction Welding for Fabricating Semi-Biodegradable Bone Screws. *Int. J. Autom. Mech. Eng.* **2022**, *19*, 9660–9667. [\[CrossRef\]](#)
22. Hernández-Leos, R.; Pérez-Quiroz, J.T.; Martínez, M.; Torres, J.; Castañeda, F.; Morales, J.; Antaño, R. Corrosion Evaluation of the Welded Zone between Carbon Steel and Stainless Steel Embedded in Concrete and Exposed to a Marine-Like Environment. *Int. J. Electrochem. Sci.* **2019**, *14*, 5690–5706. [\[CrossRef\]](#)
23. Lee, S.H. A Hot Cracking on Dissimilar Metal Weld between A106Gr.B and A312 TP316L with Buttering ERNiCr-3. *Metals* **2019**, *9*, 533. [\[CrossRef\]](#)
24. Khdir, Y.K.; Kako, S.A.; Gardi, R.H. Study of Welding Dissimilar Metals—Low-carbon Steel AISI 1018 and Austenitic Stainless Steel AISI 304. *Polytech. J.* **2020**, *10*, 1–5. [\[CrossRef\]](#)
25. Geng, P.; Qin, G.; Zhou, J. Numerical and experimental investigation on friction welding of austenite stainless steel and middle carbon steel. *J. Manuf. Process.* **2019**, *47*, 83–97. [\[CrossRef\]](#)
26. Alza, V.A. Rotational friction welding in dissimilar steels AISI 1018-AISI 2225: Effects on hardness, fatigue and microstructure. *IOSR J. Mech. Civ. Eng.* **2022**, *19*, 37–39.
27. Winiczenko, R. Effect of friction welding parameters on the tensile strength and microstructural properties of dissimilar AISI 1020-ASTM A536 joints. *Int. J. Adv. Manuf. Technol.* **2016**, *84*, 941–955. [\[CrossRef\]](#)
28. Paventhan, R.; Lakshminarayanan, P.R.; Balasubramanian, V. Optimization of Friction Welding Process Parameters for Joining Carbon Steel and Stainless Steel. *J. Iron Steel Res. Int.* **2012**, *19*, 66–71. [\[CrossRef\]](#)
29. Akhil, V.; Charles, M.M. An investigation of mechanical and metallurgical properties of friction welded steel joint. *Int. J. Innov. Sci. Res. Technol.* **2017**, *2*, 265–271.
30. Yohanes, Y.; Abdurrahman, R.; Ridwan, A. Finite element study on rotary friction welding process for mild steel. *IOP Conf. Ser. Mater. Sci. Eng.* **2019**, *620*, 012111. [\[CrossRef\]](#)
31. Dawood, A.B.; Butt, S.I.; Hussain, G.; Siddiqui, M.A.; Maqsood, A.; Zhang, F. Thermal Model of Rotary Friction Welding for Similar and Dissimilar Metals. *Metals* **2017**, *7*, 224. [\[CrossRef\]](#)
32. Salih, F.I.; Dawood, A.S.; Hamid, A.A. Effects of Key Processing Parameters of Continuous Drive Rotary Friction Welding on Thermal Characteristics of Similar and Dissimilar Joints. *Al-Rafidain Eng. J.* **2022**, *27*, 116–126. [\[CrossRef\]](#)

33. Uranga, P.; Rodríguez-Ibabe, J.M. Thermomechanical Processing of Steels. *Metals* **2020**, *10*, 641. [\[CrossRef\]](#)
34. Roy, R.K. *A Primer on The Taguchi Method*; Society of Manufacturing Engineers (SME): Southfield, MI, USA, 2010.
35. Belavendram, N. *Quality by Design: Taguchi Techniques for Industrial Experimentation*; Prentice Hall: New York, NY, USA, 1995.
36. ASTM E8/E8M-22; Standard Test Methods for Tension Testing of Metallic Materials. ASTM International: West Conshohocken, PA, USA, 2016.
37. Purwanto, H. Interface Structure in Friction Welded Joints between Stainless Steel 304 and Mild Carbon Steel. *J. Chem. Process Mater. Technol.* **2022**, *1*, 8–14. [\[CrossRef\]](#)
38. Kantumuchu, V.C.; Cheepu, M.M. The Influence of Friction Time on the Joint Interface and Mechanical Properties in Dissimilar Friction Welds. *J. Met. Mater. Res.* **2022**, *5*, 4209. [\[CrossRef\]](#)
39. Ma, H.; Qin, G.; Geng, P.; Li, F.; Fu, B.; Meng, X. Microstructure characterization and properties of carbon steel to stainless steel dissimilar metal joint made by friction welding. *Mater. Des.* **2015**, *86*, 587–597. [\[CrossRef\]](#)
40. Li, W.-Y.; Ma, T.J.; Yang, S.Q.; Xu, Q.Z.; Zhang, Y.; Li, J.L.; Liao, H.L. Effect of friction time on flash shape and axial shortening of linear friction welded 45 steel. *Mater. Lett.* **2008**, *62*, 293–296. [\[CrossRef\]](#)
41. Taysom, B.S.; Sorens, C.D. Controlling martensite and pearlite formation with cooling rate and temperature control in rotary friction welding. *Int. J. Mach. Tools Manuf.* **2020**, *150*, 103512. [\[CrossRef\]](#)
42. Cho, L.; Tselikova, A.; Holtgrewe, K.; De Moor, E.; Schmidt, R.; Findley, K.O. Critical assessment 42: Acicular ferrite formation and its influence on weld metal and heat-affected zone properties of steels. *Mater. Sci. Technol.* **2022**, *38*, 1425–1433. [\[CrossRef\]](#)
43. Wang, C.; Wang, X.; Kang, J.; Yuan, G.; Wang, G. Effect of Thermomechanical Treatment on Acicular Ferrite Formation in Ti–Ca Deoxidized Low Carbon Steel. *Metals* **2019**, *9*, 296. [\[CrossRef\]](#)
44. Madariaga, I.; Gutiérrez, I.; García-De-Andrés, C.; Capdevila, C. Acicular ferrite formation in a medium carbon steel with a two stage continuous cooling. *Scr. Mater.* **1999**, *41*, 229–235. [\[CrossRef\]](#)
45. Loder, D.; Mayerhofer, A.; Michelic, S.K. On the formation potential of acicular ferrite microstructure in different steel grades focusing on the influence of carbon content. In Proceedings of the AISTech 2016, Pittsburgh, PA, USA, 16–19 May 2016; pp. 2465–2474.
46. Ananthapadmanaban, D.; Seshagiri Rao, V.; Abraham, N.; Prasad Rao, K. A study of mechanical properties of friction welded mild steel to stainless steel joints. *Mater. Des.* **2009**, *30*, 2642–2646. [\[CrossRef\]](#)
47. Hossain, R.; Pahlevani, F.; Sahajwalla, V. Evolution of Microstructure and Hardness of High Carbon Steel under Different Compressive Strain Rates. *Metals* **2018**, *8*, 580. [\[CrossRef\]](#)
48. Hossain, R.; Pahlevani, F.; Sahajwalla, V. Revealing the mechanism of extraordinary hardness without compensating the toughness in a low alloyed high carbon steel. *Sci. Rep.* **2020**, *10*, 181. [\[CrossRef\]](#)
49. Peng, Y.; Liu, C.; Wang, N. Effect of Deformation on Microstructure and Mechanical Properties of Medium Carbon Steel During Heat Treatment Process. *Chin. J. Mech. Eng.* **2021**, *34*, 113. [\[CrossRef\]](#)
50. Yuan, X.; Chen, L.; Zhao, Y.; Di, H.; Zhu, F. Dependence of Grain Size on Mechanical Properties and Microstructures of High Manganese Austenitic Steel. *Procedia Eng.* **2014**, *81*, 143–148. [\[CrossRef\]](#)
51. Torganchuk, V.; Belyakov, A.; Kaibyshev, R. Improving Mechanical Properties of 18%Mn TWIP Steels by Cold Rolling and Annealing. *Metals* **2019**, *9*, 776. [\[CrossRef\]](#)
52. Opiela, M.; Fojt-Dymara, G.; Grajcar, A.; Borek, W. Effect of Grain Size on the Microstructure and Strain Hardening Behavior of Solution Heat-Treated Low-C High-Mn Steel. *Materials* **2020**, *13*, 1489. [\[CrossRef\]](#)

Disclaimer/Publisher’s Note: The statements, opinions and data contained in all publications are solely those of the individual author(s) and contributor(s) and not of MDPI and/or the editor(s). MDPI and/or the editor(s) disclaim responsibility for any injury to people or property resulting from any ideas, methods, instructions or products referred to in the content.



Thermal Process Monitoring for Wire and Arc Additive Manufacturing – Methodology

Volume 7 • Issue 1 | February 2023



[Journals \(/about/journals\)](#)

[Topics \(/topics\)](#)

[Information \(/authors\)](#)

[Author Services \(/authors/english\)](#)

[Initiatives \(/about/initiatives\)](#)

[About \(/about\)](#)

[Toggle desktop layout](#) [cookies](#)

[Sign In / Sign Up \(/user/login\)](#)

[Submit \(https://susy.mdpi.com/user/manuscripts/upload?journal=jmmp\)](https://susy.mdpi.com/user/manuscripts/upload?journal=jmmp)

Search for Articles:

Title / Keyword

Author / Affiliation / Email

Journal of Manufacturing and Materials Processing (JMMP)

All Article Types

Search

Advanced Search

[Journals \(/about/journals\)](#) / [JMMP \(/journal/jmmp\)](#) / [Editorial Board](#)



Journal of
*Manufacturing and
Materials Processing*

[\(/journal/jmmp\)](#)

JMMP

[Review for JMMP \(/journal/jmmp/review\)](#)



[\(/journal/jmmp/stats\)](#)



<https://www.scopus.com/sourceid/21100977478>

Journal Menu

► Journal Menu

- * [JMMP Home \(/journal/jmmp\)](#)
- * [Aims & Scope \(/journal/jmmp/about\)](#)
- * [Editorial Board \(/journal/jmmp/editors\)](#)
- * [Reviewer Board \(/journal/jmmp/submission_reviewers\)](#)
- * [Topical Advisory Panel \(/journal/jmmp/topical_advisory_panel\)](#)
- * [Instructions for Authors \(/journal/jmmp/instructions\)](#)
- * [Special Issues \(/journal/jmmp/special_issues\)](#)
- * [Topics \(/topics?journal=jmmp\)](#)
- * [Article Processing Charge \(/journal/jmmp/apc\)](#)
- * [Indexing & Archiving \(/journal/jmmp/indexing\)](#)
- * [Editor's Choice Articles \(/journal/jmmp/editors_choice\)](#)
- * [Most Cited & Viewed \(/journal/jmmp/most_cited\)](#)
- * [Journal Statistics \(/journal/jmmp/stats\)](#)
- * [Journal History \(/journal/jmmp/history\)](#)
- * [Journal Awards \(/journal/jmmp/awards\)](#)
- * [Conferences \(/journal/jmmp/events\)](#)
- * [Editorial Office \(/journal/jmmp/editorial_office\)](#)

Journal Browser

► Journal Browser

volume

issue

Go

> [Forthcoming issue \(/2504-4494/8/1\)](#)

> [Current issue \(/2504-4494/7/6\)](#)

[Vol. 8 \(2024\) \(/2504-4494/8\)](#)

[Vol. 7 \(2023\) \(/2504-4494/7\)](#)

[Vol. 6 \(2022\) \(/2504-4494/6\)](#)

[Vol. 5 \(2021\) \(/2504-4494/5\)](#)

[Vol. 4 \(2020\) \(/2504-4494/4\)](#)

[Vol. 3 \(2019\) \(/2504-4494/3\)](#)

[Vol. 2 \(2018\) \(/2504-4494/2\)](#)

[Vol. 1 \(2017\) \(/2504-4494/1\)](#)



[Back to Top](#)

Editorial Board

Please note that the order in which the Editors appear on this page is alphabetical in 2024 follows the structure of the editorial board presented on the MDPI website. For more information for editors: [editorial board responsibilities \(/editors#Editorial Board Responsibilities\)](#).

Members

 **Steven Y. Liang** (https://sciprofiles.com/profile/264728?utm_source=mdpi.com&utm_medium=website&utm_campaign=avatar_name)
Website (<http://www.me.gatech.edu/faculty/liang>)

Editor-in-Chief

George W. Woodruff School of Mechanical Engineering, Georgia Institute of Technology, Atlanta, GA 30332-0405, USA

Interests: precision machining; analysis of manufacturing processes; materials and manufacturing; process mechanics and materials mechanics


Special Issues, Collections and Topics in MDPI journals

 **Zafer Gürdal** (https://sc.edu/study/colleges_schools/engineering_and_computational_sciences/staff/gurdal_zaffer.php)

Advisory Board Member

McNAIR Center for Aerospace Innovation and Research, Department of Mechanical Engineering, University of South Carolina, Columbia, SC 29208, USA


Interests: automated manufacturing of composite material and structures; structural and multidisciplinary optimization

 **Jenny Harding** (https://sciprofiles.com/profile/2213898?utm_source=mdpi.com&utm_medium=website&utm_campaign=avatar_name)
Website (<http://www.lboro.ac.uk/departments/meme/staff/jenny-harding/>)

Advisory Board Member

The Wolfson School of Mechanical, Electrical and Manufacturing Engineering, Loughborough University, Loughborough LE11 3TU, UK


Interests: intelligent manufacturing; knowledge modelling; information modelling; ontologies; Industry 4.0; decision support; data mining for manufacturing; text mining for manufacturing

 **Seán Leen** (https://sciprofiles.com/profile/546786?utm_source=mdpi.com&utm_medium=website&utm_campaign=avatar_name)
Website (<https://www.universityofgalway.ie/engineering-informatics/mechanical-engineering/people/>)

Advisory Board Member

Mechanical Engineering, College of Science and Engineering, National University of Ireland Galway (NUI Galway), H91 HK31 Galway, Ireland


Interests: finite element simulation of manufacturing processes; effects of manufacturing processes on mechanical properties; high temperature materials behaviour (creep, TMF, HTLFCF); additive manufacturing; welding processes; superplasticity and superplastic forming; process-structure-property prediction for plasticity, fatigue, fretting; multi-scale computational mechanics of materials; materials for energy

 **Luis Filipe Menezes** (https://sciprofiles.com/profile/2535870?utm_source=mdpi.com&utm_medium=website&utm_campaign=avatar_name)
Website (<https://apps.uc.pt/mypage/faculty/uc4188/en>)

Advisory Board Member

Department of Mechanical Engineering, University of Coimbra, 3004-531 Coimbra, Portugal


Interests: computational mechanics; sheet metal forming; finite element modelling; experimentation

 **Dirk Mohr** (https://sciprofiles.com/profile/2535865?utm_source=mdpi.com&utm_medium=website&utm_campaign=avatar_name)
Website (<https://imes.ethz.ch/the-institute/people/person-detail.dmoehr.html>)

Advisory Board Member

Department of Mechanical and Process Engineering, ETH Zurich, Rämistrasse 101, 8092 Zurich, Switzerland

Interests: plasticity; ductile fracture; sheet metal forming; additive manufacturing

 **Sung-Hoon Ahn** (https://sciprofiles.com/profile/814547?utm_source=mdpi.com&utm_medium=website&utm_campaign=avatar_name)
Website (<https://me.snu.ac.kr/en/prof/ahnsh>)

Editorial Board Member

Department of Mechanical & Aerospace Engineering, Seoul National University, Building 301, Room 1205, Seoul 151-742, Republic of Korea


Interests: additive manufacturing; soft robotics; appropriate technology

Prof. Dr. Samir Allaoui (https://sciprofiles.com/profile/2257599?utm_source=mdpi.com&utm_medium=website&utm_campaign=avatar_name)
Website (<https://ithemm.univ-reims.fr/spip.php?auteur208>)

Editorial Board Member

Department of Material, Process and Mechanic of EiSiNe Engineering school, University of Reims Champagne Ardennes, 9A rue Claude Chrétien, 08000 Charleville Mézières, France

Interests: process mechanics and materials mechanics; composites forming processes; additive manufacturing; process-structure-property prediction; effects of manufacturing processes on mechanical properties; experimentation; composite materials; fibrous media

 **Markus Bambach** (https://sciprofiles.com/profile/233054?utm_source=mdpi.com&utm_medium=website&utm_campaign=avatar_name)
Website (https://www.iwf.mavt.ethz.ch/people/staff/Bamba_Marku_160287157724192/index)

Editorial Board Member

Advanced Manufacturing Lab, Department of Mechanical and Process Engineering, Institute of Virtual Production, ETH Zurich, Leonhardstrasse 27, Building LEO C1, 8092 Zürich, Switzerland

Interests: metal forming; flexible and hybrid manufacturing processes; lightweight materials; integrated computational materials engineering (ICME)

Special Issues, Collections and Topics in MDPI journals



Search by first name, last name, affiliation, int



MDPI Editor **Salima Bouvier** (https://sciprofiles.com/profile/1643885?utm_source=mdpi.com&utm_medium=website&utm_campaign=avatar_name)
[Website \(https://uteam.fr/consultant/presentation/salima-bouvier\)](https://uteam.fr/consultant/presentation/salima-bouvier)

Editorial Board Member

Department of Mechanical Engineering, University of technology of Compiègne, Centre de recherches de Royallieu, Laboratoire Roberval, BP 20529, Rue Roger Couttolenc, CS 60319, 60203 Compiègne CEDEX, France

Interests: study of the relationships between the behavior at the microstructure scale and the macroscopic response of materials; multi-scale analysis of the behavior of structural materials; characterization, modeling and identification of nonlinear behavior, effects on the simulation of shaping processes; modeling of elasto (visco-) plastic behavior and application in the study of rough contact; modeling of the coupled effects of texture and microstructure



Editor **Marcello Cabibbo**
[Website \(https://www.univpm.it/Entra/Engine/RAServePG.php/P/320710010421/idsel/160/docname/MARCELLO%20CABIBBO\)](https://www.univpm.it/Entra/Engine/RAServePG.php/P/320710010421/idsel/160/docname/MARCELLO%20CABIBBO)

Editorial Board Member

Department of Industrial Engineering and Mathematical Sciences (DIISM), Polytechnic University of Marche, Via Brecce, 60131 Ancona, Italy

Interests: physical metallurgy; mechanical characterization studies of metallic materials



Editor **Shanben Chen** (https://sciprofiles.com/profile/2391350?utm_source=mdpi.com&utm_medium=website&utm_campaign=avatar_name)
[Website \(https://rwlab.sjtu.edu.cn/Article?ID=976\)](https://rwlab.sjtu.edu.cn/Article?ID=976)

Editorial Board Member

Intelligentized Robotic Welding Technology Laboratory, School of Materials Science and Engineering, Shanghai Jiao Tong University (SJTU), Shanghai 200240, China

Interests: intelligentized robot welding; intelligent control of welding dynamical process; intelligent welding manufacturing and systems

[Special Issues, Collections and Topics in MDPI journals](#)



Editor **Michele Chiumenti** (https://sciprofiles.com/profile/2389061?utm_source=mdpi.com&utm_medium=website&utm_campaign=avatar_name)
[Website \(http://chiumenti.rmee.upc.edu/\)](http://chiumenti.rmee.upc.edu/)

Editorial Board Member

Department of Civil and Environmental Engineering, Technical University of Catalonia, UPC BarcelonaTech, 08034 Barcelona, Spain

Interests: computational mechanics; finite element method; computational plasticity; coupled thermomechanical problems

[Special Issues, Collections and Topics in MDPI journals](#)

Prof. Dr. Kevin Chou

[Website \(https://engineering.louisville.edu/faculty/kevin-chou/\)](https://engineering.louisville.edu/faculty/kevin-chou/)

Editorial Board Member

Department of Industrial Engineering, University of Louisville, Louisville, KY 40292, USA

Interests: metal additive manufacturing; laser powder-bed fusion; directed energy deposition; computed tomography; cutting tool wear; diamond coatings



Editor **George Chryssolouris** (https://sciprofiles.com/profile/1458023?utm_source=mdpi.com&utm_medium=website&utm_campaign=avatar_name)
[Website \(http://lms.mech.upatras.gr/lms-key-personnel/professor-george-chryssolouris/\)](http://lms.mech.upatras.gr/lms-key-personnel/professor-george-chryssolouris/)

Editorial Board Member

Laboratory for Manufacturing Systems and Automation (LMS), Department of Mechanical Engineering and Aeronautics, University of Patras, 26504 Patras, Greece

Interests: manufacturing; design; systems; engineering

[Special Issues, Collections and Topics in MDPI journals](#)



Editor **Joao Paulo Davim** (https://sciprofiles.com/profile/92979?utm_source=mdpi.com&utm_medium=website&utm_campaign=avatar_name)
[Website \(http://machining.web.ua.pt/pers-davim.htm\)](http://machining.web.ua.pt/pers-davim.htm)

Editorial Board Member

Department of Mechanical Engineering, University of Aveiro, Campus Santiago, 3810-193 Aveiro, Portugal

Interests: machining; composite materials; tribology; sustainable manufacturing; industrial engineering

[Special Issues, Collections and Topics in MDPI journals](#)



Editor **Luis Norberto López De Lacalle** (https://sciprofiles.com/profile/209036?utm_source=mdpi.com&utm_medium=website&utm_campaign=avatar_name)
[Website \(https://www.ehu.eus/en/web/doktoregoa/doctorate-mechanical-engineering/teaching-staff?p_redirect=fichaPDI&p_idp=4162\)](https://www.ehu.eus/en/web/doktoregoa/doctorate-mechanical-engineering/teaching-staff?p_redirect=fichaPDI&p_idp=4162)

Editorial Board Member

The Aeronautics Advanced Manufacturing Center-CFAA, 48170 Zamudio, Biscay, Spain

Interests: manufacturing process

[Special Issues, Collections and Topics in MDPI journals](#)



Editor **Chad Duty** (https://sciprofiles.com/profile/1486995?utm_source=mdpi.com&utm_medium=website&utm_campaign=avatar_name)
[Website \(https://mabe.utk.edu/people/chad-duty-3/\)](https://mabe.utk.edu/people/chad-duty-3/)

Editorial Board Member

Mechanical, Aerospace, and Biomedical Engineering Department, University of Tennessee-Knoxville, Knoxville, TN 37996, USA

Interests: additive manufacturing; polymer composites; rheology; material extrusion

[Special Issues, Collections and Topics in MDPI journals](#)



Editor **Kornel Ehmann** (https://sciprofiles.com/profile/978220?utm_source=mdpi.com&utm_medium=website&utm_campaign=avatar_name)
[Website \(http://ampl.mech.northwestern.edu/faculty/kornel-ehmann/index.html\)](http://ampl.mech.northwestern.edu/faculty/kornel-ehmann/index.html)

Editorial Board Member

Department of Mechanical Engineering, Northwestern University, Room B224, 2145 Sheridan Road, Evanston, IL 60208, USA

Interests: material removal; machine tool dynamics and control; mechanics of manufacturing processes; micro-manufacturing; surface and precision engineering





Editorial Board Member
Dr. Mohamed El Mansori (https://sciprofiles.com/profile/1320054?utm_source=mdpi.com&utm_medium=website&utm_campaign=avatar_name)
<https://engineering.tamu.edu/industrial/profiles/el-mansori-mohamed.html>)

Editorial Board Member

Arts et Métiers Institute of Technology, MSMP, HESAM Université, F-51006 Châlons-en-Champagne, France

Interests: advanced manufacturing; tribology; functional surfaces; biomimetic engineering

[Special Issues, Collections and Topics in MDPI journals](#)

[\(toggle desktop layout cookie\)](#)



Editorial Board Member
Dr. Mohamed Elbestawi (https://sciprofiles.com/profile/344632?utm_source=mdpi.com&utm_medium=website&utm_campaign=avatar_name)
<https://experts.mcmaster.ca/display/elbestaw>)

Editorial Board Member

Department of Mechanical Engineering, McMaster University, Hamilton, ON L8S 4L7, Canada

Interests: metal additive manufacturing; machining science and technology; machine tools

[Special Issues, Collections and Topics in MDPI journals](#)



Editorial Board Member
Dr. Ming Wang Fu (https://sciprofiles.com/profile/552176?utm_source=mdpi.com&utm_medium=website&utm_campaign=avatar_name)
<https://www.polyu.edu.hk/me/people/academic-teaching-staff/fu-ming-wang-prof/>)

Editorial Board Member

Department of Mechanical Engineering, The Hong Kong Polytechnic University, Hung Hom, Kowloon, Hong Kong, China

Interests: product design and development; numerical modelling and simulation; manufacturing and metal forming; size effect based micro-mechanics; damage and fracture in manufacturing and product service



Editorial Board Member
Dr. Ivan Galvão (https://sciprofiles.com/profile/375042?utm_source=mdpi.com&utm_medium=website&utm_campaign=avatar_name)
<https://www.isel.pt/docentes/ivan-rodolfo-pereira-garcia-de-galvao>)

Editorial Board Member

1. ISEL, Department of Mechanical Engineering, Polytechnic Institute of Lisbon, Rua Conselheiro Emídio Navarro, 1959-007 Lisboa, Portugal

2. CEMMPRE, Department of Mechanical Engineering, University of Coimbra, Rua Luís Reis Santos, 3030-788 Coimbra, Portugal

Interests: solid-state welding; friction stir welding; explosion welding; dissimilar materials welding; solid-state processing

[Special Issues, Collections and Topics in MDPI journals](#)



Editorial Board Member
Dr. Andrea Ghiotti (https://sciprofiles.com/profile/981740?utm_source=mdpi.com&utm_medium=website&utm_campaign=avatar_name)
<http://www.dii.unipd.it/andrea.ghiotti>)

Editorial Board Member

Department of Industrial Engineering, University of Padua, via Venezia 1, 35131 Padova, Italy

Interests: metal forming; bulk metal forming; sheet metal forming; forming machines; numerical simulation; material testing; tribology; machining



Editorial Board Member
Dr. Frank Andrés Giroto Mata (https://sciprofiles.com/profile/808931?utm_source=mdpi.com&utm_medium=website&utm_campaign=avatar_name)
<https://www.ikerbasque.net/en/frank-girot/>)

Editorial Board Member

Department of Mechanical Engineering, University of the Basque Country, Bilbao, Spain

Interests: optimization and simulation of manufacturing processes; sustainable manufacturing processes; application of nanotechnologies to manufacturing processes; process/microstructure/in-service behavior relationships

[Special Issues, Collections and Topics in MDPI journals](#)



Editorial Board Member
Dr. Prashanth Konda Gokuldoss (https://sciprofiles.com/profile/18183?utm_source=mdpi.com&utm_medium=website&utm_campaign=avatar_name)
<https://taltech.ee/en/contacts/prashanth-konda-gokuldoss>)

Editorial Board Member

Department of Mechanical and Industrial Engineering, Tallinn University of Technology, Ehitajate Tee 5, 19086 Tallinn, Estonia

Interests: powder metallurgy; additive manufacturing; selective laser melting; meta-stable materials; amorphous alloys

[Special Issues, Collections and Topics in MDPI journals](#)



Editorial Board Member
Dr. Hitomi Yamaguchi Greenslet (https://sciprofiles.com/profile/2110306?utm_source=mdpi.com&utm_medium=website&utm_campaign=avatar_name)
<https://faculty.eng.ufl.edu/non-traditional-manufacturing-laboratory/dr-greenslet/>)

Editorial Board Member

Department of Mechanical and Aerospace Engineering, University of Florida, Gainesville, FL 32611, USA

Interests: abrasive technology; magnetic field-assisted machining; surface functionalization; medical device development



Editorial Board Member
Dr. Hédi Hamdi (https://sciprofiles.com/profile/1076547?utm_source=mdpi.com&utm_medium=website&utm_campaign=avatar_name)
<https://manutech-sise.universite-lyon.fr/hedi-hamdi--53877.kjsp>)

Editorial Board Member

National Engineering School of Saint-Étienne (ENISE), University of Lyon, Tribology and Systems Dynamics Laboratory LTDS UMR 5513, 58, rue Jean Parot, 42023 Saint-Etienne, France

Interests: finite element modelling and simulations of "cutting, abrasive and mechanical processes"; surface engineering and surface integrity; material characterization; mechanical and material sciences engineering



Editorial Board Member
Dr. Jean-Yves Hascoet (https://sciprofiles.com/profile/1893251?utm_source=mdpi.com&utm_medium=website&utm_campaign=avatar_name)
<https://www.ec-nantes.fr/english-version/directory/jean-yves-hascoet/>)


Editorial Board Member

Institut de Recherche en Génie Civil et Mécanique, UMR 6183, Ecole Centrale de Nantes, 44321 Nantes, France

Interests: additive manufacturing; bioprinting; welding process; high speed machining; open CNC controller; CAD-CAM; parallel kinematic machine; incremental sheet

[Back to TopTop](#)



 **Carsten Heinzel** (https://sciprofiles.com/profile/320320?utm_source=mdpi.com&utm_medium=website&utm_campaign=avatar_name)
<https://www.iwt-bremen.de/de/institut/mitarbeiter/detail/prof-dr-ing-carsten-heinzel>

[Toggle desktop layout cookie](#)  

Editorial Board Member

Leibniz-Institute for Materials Engineering and MAPEX Center for Materials and Processes, University of Bremen, Badgasteiner Str. 3, 28359 Bremen, Germany

Interests: cutting and abrasive machining; optimization of coolant supply; surface integrity aspects; modelling and optimization of manufacturing processes and process chains; precision engineering; monitoring and control of machining processes

[Special Issues, Collections and Topics in MDPI journals](#)

Displaying Editorial board member 1-30 on page 1 of 3.

Go to page [1](#) [2](#) (/journal/jmmp/editors?page_no=2) [3](/journal/jmmp/editors?page_no=3) (/journal/jmmp/editors?page_no=3) [>](/journal/jmmp/editors?page_no=2) (/journal/jmmp/editors?page_no=2)

[J. Manuf. Mater. Process.](#) (</journal/jmmp>), EISSN 2504-4494, Published by MDPI

[RSS](#) (</rss/journal/jmmp>) [Content Alert](#) (</journal/jmmp/toc-alert>)

Further Information

[Article Processing Charges](#) (</apc>)

[Pay an Invoice](#) (</about/payment>)

[Open Access Policy](#) (</openaccess>)

[Contact MDPI](#) (</about/contact>)

[Jobs at MDPI](#) (<https://careers.mdpi.com>)

Guidelines

[For Authors](#) (</authors>)

[For Reviewers](#) (</reviewers>)

[For Editors](#) (</editors>)

[For Librarians](#) (</librarians>)

[For Publishers](#) (/publishing_services)

[For Societies](#) (</societies>)

[For Conference Organizers](#) (/conference_organizers)

MDPI Initiatives

[Sciforum](#) (<https://sciforum.net>)

[MDPI Books](#) (<https://www.mdpi.com/books>)

[Preprints.org](#) (<https://www.preprints.org>)

[Scilit](#) (<https://www.scilit.net>)

[SciProfiles](#) (https://sciprofiles.com?utm_source=mpdi.com&utm_medium=bottom_menu&utm_campaign=initiative)

[Encyclopedia](#) (<https://encyclopedia.pub>)

[JAMS](#) (<https://jams.pub>)

[Proceedings Series](#) (</about/proceedings>)

Follow MDPI

[LinkedIn](#) (<https://www.linkedin.com/company/mdpi>)

[Facebook](#) (<https://www.facebook.com/MDPIOpenAccessPublishing>)

[Twitter](#) (<https://twitter.com/MDPIOpenAccess>)

Subscribe to receive issue release
notifications and newsletters from
MDPI journals

Select options 

Enter your email address...

Subscribe

© 1996-2024 MDPI (Basel, Switzerland) unless otherwise stated

[Disclaimer](#)

[Terms and Conditions](#) (</about/terms-and-conditions>)

[Privacy Policy](#) (</about/privacy>)



Back to Top

[Sign In / Sign Up \(user/login\)](#)[Submit \(https://susy.mdpi.com/user/manuscripts/upload?journal=jmmp\)](https://susy.mdpi.com/user/manuscripts/upload?journal=jmmp)

Search for Articles:

Search

Advanced Search

[Journals \(about/journals\)](#) / [JMMP \(/journal/jmmp\)](#) / [Volume 7 \(/2504-4494/7\)](#) / [Issue 1](#)Journal of
Manufacturing and
Materials Processing[\(/journal/jmmp\)](#)

JMMP

[Review for JMMP \(http://susy.mdpi.com/user/manuscripts/upload?journal=jmmp\)](#)IMPACT
FACTOR

3.2

[\(/journal/jmmp/stats\)](#)

CITESCORE

5.5

<https://www.scopus.com/sourceld/21100977478>

Journal Menu

Journal Menu

- [JMMP Home \(/journal/jmmp\)](#)
- [Aims & Scope \(/journal/jmmp/about\)](#)
- [Editorial Board \(/journal/jmmp/editors\)](#)
- [Reviewer Board \(/journal/jmmp/submission_reviewers\)](#)
- [Topical Advisory Panel \(/journal/jmmp/topical_advisory_panel\)](#)
- [Instructions for Authors \(/journal/jmmp/instructions\)](#)
- [Special Issues \(/journal/jmmp/special_issues\)](#)
- [Topics \(/topics?journal=jmmp\)](#)
- [Article Processing Charge \(/journal/jmmp/apc\)](#)
- [Indexing & Archiving \(/journal/jmmp/indexing\)](#)
- [Editor's Choice Articles \(/journal/jmmp/editors_choice\)](#)
- [Most Cited & Viewed \(/journal/jmmp/most_cited\)](#)
- [Journal Statistics \(/journal/jmmp/stats\)](#)
- [Journal History \(/journal/jmmp/history\)](#)
- [Journal Awards \(/journal/jmmp/awards\)](#)
- [Conferences \(/journal/jmmp/events\)](#)
- [Editorial Office \(/journal/jmmp/editorial_office\)](#)

Journal Browser

Journal Browser

Go

- [Forthcoming issue \(/2504-4494/8/1\)](#)
- [Current issue \(/2504-4494/7/6\)](#)

- [Vol. 8 \(2024\) \(/2504-4494/8\)](#)
- [Vol. 7 \(2023\) \(/2504-4494/7\)](#)
- [Vol. 6 \(2022\) \(/2504-4494/6\)](#)
- [Vol. 5 \(2021\) \(/2504-4494/5\)](#)
- [Vol. 4 \(2020\) \(/2504-4494/4\)](#)
- [Vol. 3 \(2019\) \(/2504-4494/3\)](#)
- [Vol. 2 \(2018\) \(/2504-4494/2\)](#)
- [Vol. 1 \(2017\) \(/2504-4494/1\)](#)

J. Manuf. Mater. Process., Volume 7, Issue 1 (February 2023) – 50 articles



Cover Story ([view full-size image \(/files/uploaded/covers/jmmp/big_cover-jmmp-v7-i1.png\)](#)): The Wire and Arc Additive Manufacturing (WAAM) process has a high potential for industrial applications in aviation. This study presents an approach to determine absolute values of the interlayer temperatures during the process using TI-6AL-4V. The emissivity and transmittance are calibrated to enable a precise thermographic measurement. The methodology is validated by comparing the recorded data with signals from the thermocouples to align the absolute temperature values. Results show that with an interlayer temperature of 200 °C, heat accumulation occurs at the center of the layer due to faster cooling at the free ends. The methodology enables a non-tactile and reproducible measurement of the interlayer temperature during the WAAM process. [View this paper \(https://www.mdpi.com/2504-4494/7/1/10\)](#)

<https://www.mdpi.com/2504-4494/7/1/10>

as officially published after their release is announced to the [table of contents alert mailing list \(/journal/jmmp/toc-alert\)](#).

- You may [sign up for e-mail alerts \(/journal/jmmp/toc-alert\)](#) to receive table of contents of newly released issues.
- PDF is the official format for papers published in both, html and pdf forms. To view the papers in pdf format, click on the "PDF Full-text" link, and use the free [Adobe Reader \(http://www.adobe.com\)](#) to open them.

Order results

Show export options ▼

Open Access Article

12 pages, 5669 KiB [\(/2504-4494/7/1/50/pdf?version=1676455914\)](#)

Real-Time Cutting Temperature Measurement in Turning of AISI 1045 Steel through an Embedded Thermocouple—A Comparative Study with Infrared Thermography ([/2504-4494/7/1/50](#))

by [Bruno Guimarães \(https://sciprofiles.com/profile/2590332?utm_source=mdpi.com&utm_medium=website&utm_campaign=avatar_name\)](#)and [José Rosas \(https://sciprofiles.com/profile/author/WGj2ZhhWXBpc2oxaVY2ZWxIRHFiYyVhZC9ETVJVY2FzY1MvdVJUYTI1MD0=7?utm_source=mdpi.com&utm_medium=website&utm_campaign=avatar_name\)](#), [Cristina M. Fernandes \(https://sciprofiles.com/profile/2106867?utm_source=mdpi.com&utm_medium=website&utm_campaign=avatar_name\)](#), [Daniel Figueiredo \(https://sciprofiles.com/profile/1670750?utm_source=mdpi.com&utm_medium=website&utm_campaign=avatar_name\)](#), [Hernán López \(https://sciprofiles.com/profile/721026?utm_source=mdpi.com&utm_medium=website&utm_campaign=avatar_name\)](#), [Olga C. Paiva \(https://sciprofiles.com/profile/2285494?utm_source=mdpi.com&utm_medium=website&utm_campaign=avatar_name\)](#), [Eliane S. Silva \(https://sciprofiles.com/profile/1492887?utm_source=mdpi.com&utm_medium=website&utm_campaign=avatar_name\)](#) and, [Georgina Miranda \(https://sciprofiles.com/profile/1897112?utm_source=mdpi.com&utm_medium=website&utm_campaign=avatar_name\)](#)*J. Manuf. Mater. Process.* **2023**, *7*(1), 50; <https://doi.org/10.3390/jmmp7010050> (<https://doi.org/10.3390/jmmp7010050>) - 15 Feb 2023Cited by [4 \(/2504-4494/7/1/50/metrics\)](#) | Viewed by 2134

Abstract During machining processes, a high temperature is generated in the cutting zone due to deformation of the material and friction of the chip along the surface of the tool.

This high temperature has a detrimental effect on the cutting tool, and for this [..] [Read more](#).

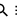

(This article belongs to the Special Issue [Advances in Metal Cutting and Cutting Tools \(/journal/jmmp/special_issues/Metal_Cutting_Tools\)](#))

Show Figures

https://pub.mdpi-res.com/jmmp/jmmp-07-00050/article_deploy/html/images/jmmp-07-00050-g001-550.jpg?1676459433) ([https://pub.mdpi-res.com/jmmp/jmmp-07-00050-g002-550.jpg?1676459431](https://pub.mdpi-res.com/jmmp/jmmp-07-00050/article_deploy/html/images/jmmp-07-00050-g002-550.jpg?1676459431)) ([https://pub.mdpi-res.com/jmmp/jmmp-07-00050-g003-550.jpg?1676459431](https://pub.mdpi-res.com/jmmp/jmmp-07-00050/article_deploy/html/images/jmmp-07-00050-g003-550.jpg?1676459431))


[07-00050-g003-550.jpg?1676459435](https://pub.mdpi-res.com/jmmp/jmmp-07-00050/article_deploy/html/images/jmmp-07-00050-g004-550.jpg?1676459429)) (https://pub.mdpi-res.com/jmmp/jmmp-07-00050/article_deploy/html/images/jmmp-07-00050-g004-550.jpg?1676459429)
(https://pub.mdpi-res.com/jmmp/jmmp-07-00050/article_deploy/html/images/jmmp-07-00050-g005-550.jpg?1676459426) ([https://pub.mdpi-res.com/jmmp/jmmp-07-00050-g006-550.jpg?1676459428](https://pub.mdpi-res.com/jmmp/jmmp-07-00050/article_deploy/html/images/jmmp-07-00050-g006-550.jpg?1676459428)) (<https://pub.mdpi-res.com/jmmp/jmmp-07-00050-g007-550.jpg?1676459427>)
Open Access Article 22 pages, 11634 KIB (Z504-4494/7/1/49/pdf?version=1676432715)
Study on Elucidation of the Roundness Improvement Mechanism of the Internal Magnetic Abrasive Finishing Process Using a Magnetic Machining Tool (Z504-4494/7/1/49)
by
Jianguan Liu (https://sciprofiles.com/profile/author/Rmo5MUtaS202MHFObjU5TKlMekpNdEpiaThSeVhoL0RGNTV2Q09yc2cxYz0=?utm_source=mdpi.com&utm_medium=website&utm_campaign=avatar_name)
and
Yanhua Zou (https://sciprofiles.com/profile/429183?utm_source=mdpi.com&utm_medium=website&utm_campaign=avatar_name)
J. Manuf. Mater. Process. 2023, 7(1), 49; <https://doi.org/10.3390/jmmp7010049> (<https://doi.org/10.3390/jmmp7010049>) - 13 Feb 2023
Viewed by 1438
Abstract The magnetic abrasive finishing process using the magnetic machining tool was proposed to finish the internal surface of the thick tube (the thickness of the tube is 5–30 mm). It has been proved that this process can improve the roundness while improving the [...] [Read more](#).
(This article belongs to the Special Issue [Advances in Metal Cutting and Cutting Tools \(Journal/jmmp/special_issues/Metal_Cutting_Tools\)](#))
[► Show Figures](#)
(https://pub.mdpi-res.com/jmmp/jmmp-07-00049/article_deploy/html/images/jmmp-07-00049-g001a-550.jpg?1676432798) (https://pub.mdpi-res.com/jmmp/jmmp-07-00049/article_deploy/html/images/jmmp-07-00049-g001b-550.jpg?1676432798) (https://pub.mdpi-res.com/jmmp/jmmp-07-00049/article_deploy/html/images/jmmp-07-00049-g002-550.jpg?1676432792) (https://pub.mdpi-res.com/jmmp/jmmp-07-00049/article_deploy/html/images/jmmp-07-00049-g003-550.jpg?1676432812) ([https://pub.mdpi-res.com/jmmp/jmmp-07-00049-g004-550.jpg?1676432780](https://pub.mdpi-res.com/jmmp/jmmp-07-00049/article_deploy/html/images/jmmp-07-00049-g004-550.jpg?1676432780)) ([https://pub.mdpi-res.com/jmmp/jmmp-07-00049-g005-550.jpg?1676432801](https://pub.mdpi-res.com/jmmp/jmmp-07-00049/article_deploy/html/images/jmmp-07-00049-g005-550.jpg?1676432801)) ([https://pub.mdpi-res.com/jmmp/jmmp-07-00049-g006-550.jpg?1676432810](https://pub.mdpi-res.com/jmmp/jmmp-07-00049/article_deploy/html/images/jmmp-07-00049-g006-550.jpg?1676432810)) ([https://pub.mdpi-res.com/jmmp/jmmp-07-00049-g007-550.jpg?1676432781](https://pub.mdpi-res.com/jmmp/jmmp-07-00049/article_deploy/html/images/jmmp-07-00049-g007-550.jpg?1676432781)) (<https://pub.mdpi-res.com/jmmp/jmmp-07-00049-g008-550.jpg?1676432791>) ([https://pub.mdpi-res.com/jmmp/jmmp-07-00049-g009-550.jpg?1676432794](https://pub.mdpi-res.com/jmmp/jmmp-07-00049/article_deploy/html/images/jmmp-07-00049-g009-550.jpg?1676432794)) ([https://pub.mdpi-res.com/jmmp/jmmp-07-00049-g010-550.jpg?1676432802](https://pub.mdpi-res.com/jmmp/jmmp-07-00049/article_deploy/html/images/jmmp-07-00049-g010-550.jpg?1676432802)) ([https://pub.mdpi-res.com/jmmp/jmmp-07-00049-g011-550.jpg?1676432797](https://pub.mdpi-res.com/jmmp/jmmp-07-00049/article_deploy/html/images/jmmp-07-00049-g011-550.jpg?1676432797)) ([https://pub.mdpi-res.com/jmmp/jmmp-07-00049-g012-550.jpg?1676432814](https://pub.mdpi-res.com/jmmp/jmmp-07-00049/article_deploy/html/images/jmmp-07-00049-g012-550.jpg?1676432814)) ([https://pub.mdpi-res.com/jmmp/jmmp-07-00049-g013-550.jpg?1676432787](https://pub.mdpi-res.com/jmmp/jmmp-07-00049/article_deploy/html/images/jmmp-07-00049-g013-550.jpg?1676432787)) (<https://pub.mdpi-res.com/jmmp/jmmp-07-00049-g014-550.jpg?1676432817>) (<https://pub.mdpi-res.com/jmmp/jmmp-07-00049-g015-550.jpg?1676432789>) (<https://pub.mdpi-res.com/jmmp/jmmp-07-00049-g016-550.jpg?1676432800>) (<https://pub.mdpi-res.com/jmmp/jmmp-07-00049-g017a-550.jpg?1676432808>) (<https://pub.mdpi-res.com/jmmp/jmmp-07-00049-g017b-550.jpg?1676432818>) (<https://pub.mdpi-res.com/jmmp/jmmp-07-00049-g018a-550.jpg?1676432783>) (<https://pub.mdpi-res.com/jmmp/jmmp-07-00049-g018b-550.jpg?1676432788>) (<https://pub.mdpi-res.com/jmmp/jmmp-07-00049-g019-550.jpg?1676432805>)
Open Access Article 16 pages, 13639 KIB (Z504-4494/7/1/48/pdf?version=1676343580)
Development of a Computationally Efficient Model of the Heating Phase in Thermoforming Process Based on the Experimental Radiation Pattern of Heaters (Z504-4494/7/1/48)
by
Hadi Hosseinianari (https://sciprofiles.com/profile/2538355?utm_source=mdpi.com&utm_medium=website&utm_campaign=avatar_name),
Milad Ramezankhani (https://sciprofiles.com/profile/2433532?utm_source=mdpi.com&utm_medium=website&utm_campaign=avatar_name),
Rudolf Seethaler (https://sciprofiles.com/profile/2837505?utm_source=mdpi.com&utm_medium=website&utm_campaign=avatar_name) and
Abbas S. Milani (https://sciprofiles.com/profile/316064?utm_source=mdpi.com&utm_medium=website&utm_campaign=avatar_name)
J. Manuf. Mater. Process. 2023, 7(1), 48; <https://doi.org/10.3390/jmmp7010048> (<https://doi.org/10.3390/jmmp7010048>) - 10 Feb 2023
Cited by 1 (Z504-4494/7/1/48#metrics) | Viewed by 1393
Abstract In this study, an accurate and computationally efficient model for the heating process of thin thermoplastic sheets during thermoforming is developed. This model opens the door to efficient training of model-free control approaches in thermoforming applications, which often require extensive training data that [...] [Read more](#).
[► Show Figures](#)
(https://pub.mdpi-res.com/jmmp/jmmp-07-00048/article_deploy/html/images/jmmp-07-00048-g001-550.jpg?1676343667) ([https://pub.mdpi-res.com/jmmp/jmmp-07-00048-g002-550.jpg?1676343665](https://pub.mdpi-res.com/jmmp/jmmp-07-00048/article_deploy/html/images/jmmp-07-00048-g002-550.jpg?1676343665)) (<https://pub.mdpi-res.com/jmmp/jmmp-07-00048-g003-550.jpg?1676343666>) (<https://pub.mdpi-res.com/jmmp/jmmp-07-00048-g004-550.jpg?1676343662>) (<https://pub.mdpi-res.com/jmmp/jmmp-07-00048-g005-550.jpg?1676343673>) (<https://pub.mdpi-res.com/jmmp/jmmp-07-00048-g006-550.jpg?1676343665>) (<https://pub.mdpi-res.com/jmmp/jmmp-07-00048-g007-550.jpg?1676343663>) (<https://pub.mdpi-res.com/jmmp/jmmp-07-00048-g008-550.jpg?1676343661>) (<https://pub.mdpi-res.com/jmmp/jmmp-07-00048-g009-550.jpg?1676343656>) (<https://pub.mdpi-res.com/jmmp/jmmp-07-00048-g010-550.jpg?1676343668>) (<https://pub.mdpi-res.com/jmmp/jmmp-07-00048-g011-550.jpg?1676343659>) (<https://pub.mdpi-res.com/jmmp/jmmp-07-00048-g012-550.jpg?1676343672>) (<https://pub.mdpi-res.com/jmmp/jmmp-07-00048-g013-550.jpg?1676343658>) (<https://pub.mdpi-res.com/jmmp/jmmp-07-00048-g014-550.jpg?1676343669>) (<https://pub.mdpi-res.com/jmmp/jmmp-07-00048-g015-550.jpg?1676343670>)
Open Access Editorial 2 pages, 185 KIB (Z504-4494/7/1/47/pdf?version=1675995716)
Metal Additive Manufacturing and Its Post-Processing Techniques (Z504-4494/7/1/47)
by
Hao Wang (https://sciprofiles.com/profile/358881?utm_source=mdpi.com&utm_medium=website&utm_campaign=avatar_name) and
Jerry Ying Hsi Fuh (https://sciprofiles.com/profile/322670?utm_source=mdpi.com&utm_medium=website&utm_campaign=avatar_name)
J. Manuf. Mater. Process. 2023, 7(1), 47; <https://doi.org/10.3390/jmmp7010047> (<https://doi.org/10.3390/jmmp7010047>) - 10 Feb 2023
Cited by 1 (Z504-4494/7/1/47#metrics) | Viewed by 2002
Abstract Metal additive manufacturing has made substantial progress in the advanced manufacturing sector with competitive advantages for the efficient production of high-quality products [...] [Full article \(Z504-4494/7/1/47\)](#)
(This article belongs to the Special Issue [Metal Additive Manufacturing and Its Post Processing Techniques \(Journal/jmmp/special_issues/metal_additive_manufacturing_post_processing\)](#))
Open Access Editor's Choice Article 19 pages, 16807 KIB (Z504-4494/7/1/46/pdf?version=1675941843)
Using 3D Density-Gradient Vectors in Evolutionary Topology Optimization to Find the Build Direction for Additive Manufacturing (Z504-4494/7/1/46)
by
Dylan Bender (https://sciprofiles.com/profile/author/aDIQaVRwbFhkehZhaGRwDB4RwZrJhY53pkaTIRVIEU1F4MD0=?utm_source=mdpi.com&utm_medium=website&utm_campaign=avatar_name)
and
Ahmad Barari (https://sciprofiles.com/profile/543978?utm_source=mdpi.com&utm_medium=website&utm_campaign=avatar_name)
J. Manuf. Mater. Process. 2023, 7(1), 46; <https://doi.org/10.3390/jmmp7010046> (<https://doi.org/10.3390/jmmp7010046>) - 09 Feb 2023
Cited by 1 (Z504-4494/7/1/46#metrics) | Viewed by 1501
Abstract Given its layer-based nature, additive manufacturing is known as a family of highly capable processes for fabricating complex 3D geometries designed by means of evolutionary topology optimization. However, the required support structures for the overhanging features of these complex geometries can be concerning [...] [Read more](#).
(This article belongs to the Special Issue [Recent Advances in Processes and Design Methods for Additive Manufacturing \(Journal/jmmp/special_issues/AM_Process_Design\)](#))
[► Show Figures](#)
(https://pub.mdpi-res.com/jmmp/jmmp-07-00046/article_deploy/html/images/jmmp-07-00046-g001-550.jpg?1675941913) (<https://pub.mdpi-res.com/jmmp/jmmp-07-00046-g002-550.jpg?1675941919>) (<https://pub.mdpi-res.com/jmmp/jmmp-07-00046-g003-550.jpg?1675941911>) (<https://pub.mdpi-res.com/jmmp/jmmp-07-00046-g004-550.jpg?1675941912>) (<https://pub.mdpi-res.com/jmmp/jmmp-07-00046-g005-550.jpg?1675941918>) ([https://pub.mdpi-res.com/jmmp/jmmp-07-00046-g006-550.jpg?1675941909](https://pub.mdpi-res.com/jmmp/jmmp-07-00046/article_deploy/html/images/jmmp-07-00046-g006-550.jpg?1675941909)) (<https://pub.mdpi-res.com/jmmp/jmmp-07-00046-g007-550.jpg?1675941910>) (<https://pub.mdpi-res.com/jmmp/jmmp-07-00046-g008-550.jpg?1675941917>) (<https://pub.mdpi-res.com/jmmp/jmmp-07-00046-g009-550.jpg?1675941917>) (<https://pub.mdpi-res.com/jmmp/jmmp-07-00046-g010-550.jpg?1675941915>) (<https://pub.mdpi-res.com/jmmp/jmmp-07-00046-g011-550.jpg?1675941908>)
Open Access Editor's Choice Review 24 pages, 2140 KIB (Z504-4494/7/1/45/pdf?version=1676945988)
A Review on Wire-Fed Directed Energy Deposition Based Metal Additive Manufacturing (Z504-4494/7/1/45)
by
Tuğrul Özcel (https://sciprofiles.com/profile/155960?utm_source=mdpi.com&utm_medium=website&utm_campaign=avatar_name),
Hamed Shokri (https://sciprofiles.com/profile/2653599?utm_source=mdpi.com&utm_medium=website&utm_campaign=avatar_name) and
Raphaël Loizeau (https://sciprofiles.com/profile/author/cCt2SIV1UzkweGx0SFBoek3MDRgTkNtMW44Um0wbjJOHdpNnZlaVScz0=?utm_source=mdpi.com&utm_medium=website&utm_campaign=avatar_name)
J. Manuf. Mater. Process. 2023, 7(1), 45; <https://doi.org/10.3390/jmmp7010045> (<https://doi.org/10.3390/jmmp7010045>) - 08 Feb 2023
Cited by 5 (Z504-4494/7/1/45#metrics) | Viewed by 3981

Abstract Metal additive manufacturing has reached a level where products and components can be directly fabricated for applications requiring small batches and customized geometries. From tiny body implants to long pedestrian bridges over rivers. Wire-fed directed energy deposition based additive manufacturing enables fabricating large [...] [Read more](#).

(This article belongs to the Special Issue **Editorial Board Members' Collection Series: Additive Manufacturing** ([/journal/jmmp/special_issues/additive_manufacturing](#)))  

Show Figures

(https://pub.mdpi-res.com/jmmp/jmmp-07-00045/article_deploy/html/images/jmmp-07-00045-g001-550.jpg?1676946080) (https://pub.mdpi-res.com/jmmp/jmmp-07-00045/article_deploy/html/images/jmmp-07-00045-g002-550.jpg?1676946085) (https://pub.mdpi-res.com/jmmp/jmmp-07-00045/article_deploy/html/images/jmmp-07-00045-g003-550.jpg?1676946088) (https://pub.mdpi-res.com/jmmp/jmmp-07-00045/article_deploy/html/images/jmmp-07-00045-g004-550.jpg?1676946089) (https://pub.mdpi-res.com/jmmp/jmmp-07-00045/article_deploy/html/images/jmmp-07-00045-g005-550.jpg?1676946078)

Open Access Article 23 pages, 8556 KIB ([/2504-4494/7/1/44/pdf?version=1676276836](#)) 

Influence of Ambient Temperature and Crystalline Structure on Fracture Toughness and Production of Thermoplastic by Enclosure FDM 3D Printer (2504-4494/7/1/44)

by  Supaphorn Thumsorn (https://sciprofiles.com/profile/1034400?utm_source=mdpi.com&utm_medium=website&utm_campaign=avatar_name),
 Wattanachai Prasong (https://sciprofiles.com/profile/2312928?utm_source=mdpi.com&utm_medium=website&utm_campaign=avatar_name),
 Akira Ishigami (https://sciprofiles.com/profile/1029645?utm_source=mdpi.com&utm_medium=website&utm_campaign=avatar_name),
 Takashi Kurose (https://sciprofiles.com/profile/544835?utm_source=mdpi.com&utm_medium=website&utm_campaign=avatar_name),
 Yutaka Kobayashi (https://sciprofiles.com/profile/1868126?utm_source=mdpi.com&utm_medium=website&utm_campaign=avatar_name) and
 Hiroshi Ito (https://sciprofiles.com/profile/417537?utm_source=mdpi.com&utm_medium=website&utm_campaign=avatar_name)
J. Manuf. Mater. Process. **2023**, *7*(1), 44; <https://doi.org/10.3390/jmmp7010044> (<https://doi.org/10.3390/jmmp7010044>) - 08 Feb 2023

Cited by 6 ([/2504-4494/7/1/44#metrics](#)) | Viewed by 1967

Abstract Fused deposition modeling (FDM) 3D printing has printed thermoplastic materials layer-by-layer to form three dimensional products whereby interlayer adhesion must be well controlled to obtain high mechanical performance and product integrity. This research studied the effects of ambient temperatures and crystalline structure on [...] [Read more](#).

(This article belongs to the Special Issue **Recent Advances in Processes and Design Methods for Additive Manufacturing** ([/journal/jmmp/special_issues/AM_Process_Design](#)))



Show Figures

(https://pub.mdpi-res.com/jmmp/jmmp-07-00044/article_deploy/html/images/jmmp-07-00044-g001-550.jpg?1676276918) (https://pub.mdpi-res.com/jmmp/jmmp-07-00044/article_deploy/html/images/jmmp-07-00044-g002-550.jpg?1676276920) (https://pub.mdpi-res.com/jmmp/jmmp-07-00044/article_deploy/html/images/jmmp-07-00044-g003-550.jpg?1676276935) (https://pub.mdpi-res.com/jmmp/jmmp-07-00044/article_deploy/html/images/jmmp-07-00044-g004-550.jpg?1676276932) (https://pub.mdpi-res.com/jmmp/jmmp-07-00044/article_deploy/html/images/jmmp-07-00044-g005-550.jpg?1676276940) (https://pub.mdpi-res.com/jmmp/jmmp-07-00044/article_deploy/html/images/jmmp-07-00044-g006-550.jpg?1676276937) (https://pub.mdpi-res.com/jmmp/jmmp-07-00044/article_deploy/html/images/jmmp-07-00044-g007-550.jpg?1676276908) (https://pub.mdpi-res.com/jmmp/jmmp-07-00044/article_deploy/html/images/jmmp-07-00044-g008-550.jpg?1676276920) (https://pub.mdpi-res.com/jmmp/jmmp-07-00044/article_deploy/html/images/jmmp-07-00044-g009-550.jpg?1676276910) (https://pub.mdpi-res.com/jmmp/jmmp-07-00044/article_deploy/html/images/jmmp-07-00044-g010-550.jpg?1676276924) (https://pub.mdpi-res.com/jmmp/jmmp-07-00044/article_deploy/html/images/jmmp-07-00044-g011-550.jpg?1676276913) (https://pub.mdpi-res.com/jmmp/jmmp-07-00044/article_deploy/html/images/jmmp-07-00044-g012-550.jpg?1676276931) (https://pub.mdpi-res.com/jmmp/jmmp-07-00044/article_deploy/html/images/jmmp-07-00044-g013-550.jpg?1676276917)

Open Access Editor's Choice Article 16 pages, 2037 KIB ([/2504-4494/7/1/43/pdf?version=1676878772](#))

Building Orientation and Post Processing of Ti6Al4V Produced by Laser Powder Bed Fusion Process (2504-4494/7/1/43)

by  Rosaria Rovetta (https://sciprofiles.com/profile/2673861?utm_source=mdpi.com&utm_medium=website&utm_campaign=avatar_name),
 Paola Ginestra (https://sciprofiles.com/profile/748635?utm_source=mdpi.com&utm_medium=website&utm_campaign=avatar_name),
 Rosalba Monica Ferraro (https://sciprofiles.com/profile/1372913?utm_source=mdpi.com&utm_medium=website&utm_campaign=avatar_name),
 Keren Zohar-Hauber (https://sciprofiles.com/profile/author/Zmx2TDZxb3haL3ZHOUNQSGN0UW1KWERNWnM0bDVozEJoNWlmaHVhbTBCQT0=7?utm_source=mdpi.com&utm_medium=website&utm_campaign=avatar_name)

 Silvia Giliani (https://sciprofiles.com/profile/1285686?utm_source=mdpi.com&utm_medium=website&utm_campaign=avatar_name) and
 Elisabetta Ceretti (https://sciprofiles.com/profile/3273512?utm_source=mdpi.com&utm_medium=website&utm_campaign=avatar_name)
J. Manuf. Mater. Process. **2023**, *7*(1), 43; <https://doi.org/10.3390/jmmp7010043> (<https://doi.org/10.3390/jmmp7010043>) - 07 Feb 2023

Cited by 4 ([/2504-4494/7/1/43#metrics](#)) | Viewed by 1639

Abstract Laser powder bed fusion, particularly the selective laser melting (SLM), is an additive manufacturing (AM) technology used to produce near-net-shaped engineering components for biomedical applications, especially in orthopaedics. Ti6Al4V is commonly used for producing orthopaedic implants using SLM because it has excellent mechanical [...] [Read more](#).

Show Figures

(https://pub.mdpi-res.com/jmmp/jmmp-07-00043/article_deploy/html/images/jmmp-07-00043-g001-550.jpg?1676878853) (https://pub.mdpi-res.com/jmmp/jmmp-07-00043/article_deploy/html/images/jmmp-07-00043-g002-550.jpg?1676878857) (https://pub.mdpi-res.com/jmmp/jmmp-07-00043/article_deploy/html/images/jmmp-07-00043-g003-550.jpg?1676878841) (https://pub.mdpi-res.com/jmmp/jmmp-07-00043/article_deploy/html/images/jmmp-07-00043-g004-550.jpg?1676878848) (https://pub.mdpi-res.com/jmmp/jmmp-07-00043/article_deploy/html/images/jmmp-07-00043-g005-550.jpg?1676878846) ([https://pub.mdpi-res.com/jmmp/jmmp-07-00043-g006-550.jpg?1676878844](https://pub.mdpi-res.com/jmmp/jmmp-07-00043/article_deploy/html/images/jmmp-07-00043-g006-550.jpg?1676878844)) ([https://pub.mdpi-res.com/jmmp/jmmp-07-00043-g007-550.jpg?1676878851](https://pub.mdpi-res.com/jmmp/jmmp-07-00043/article_deploy/html/images/jmmp-07-00043-g007-550.jpg?1676878851))

Open Access Article 14 pages, 8134 KIB ([/2504-4494/7/1/42/pdf?version=1675752042](#))

Investigation of the Pull-Out Behaviour of Metal Threaded Inserts in Thermoplastic Fused-Layer Modelling (FLM) Components (2504-4494/7/1/42)

by  Tobias Kastner (https://sciprofiles.com/profile/2680650?utm_source=mdpi.com&utm_medium=website&utm_campaign=avatar_name),
 Juliane Troschitz (https://sciprofiles.com/profile/1276400?utm_source=mdpi.com&utm_medium=website&utm_campaign=avatar_name),
 Christian Vogel (https://sciprofiles.com/profile/1562064?utm_source=mdpi.com&utm_medium=website&utm_campaign=avatar_name),
 Thomas Behnisch (https://sciprofiles.com/profile/3320092?utm_source=mdpi.com&utm_medium=website&utm_campaign=avatar_name),
 Maik Gude (https://sciprofiles.com/profile/765929?utm_source=mdpi.com&utm_medium=website&utm_campaign=avatar_name) and
 Niels Modler (https://sciprofiles.com/profile/author/Sk9XaUdwWtXotamdivenBKOepYUIN73FMVU1Q1TmxCdnljc3B6RnE2YzdfST0=7?utm_source=mdpi.com&utm_medium=website&utm_campaign=avatar_name)
J. Manuf. Mater. Process. **2023**, *7*(1), 42; <https://doi.org/10.3390/jmmp7010042> (<https://doi.org/10.3390/jmmp7010042>) - 07 Feb 2023

Viewed by 1481

Abstract To provide detachable, secure and long-term stable joints in fused-layer modelling (FLM) components or assemblies, metal threaded inserts are widely used as extrinsic interfaces. However, the load-bearing capacity of such inserts is influenced by the inhomogeneous, anisotropic material structure of the FLM components. [...] [Read more](#).

(This article belongs to the Special Issue **Recent Advances in Processes and Design Methods for Additive Manufacturing** ([/journal/jmmp/special_issues/AM_Process_Design](#)))

Show Figures

(https://pub.mdpi-res.com/jmmp/jmmp-07-00042/article_deploy/html/images/jmmp-07-00042-g001-550.jpg?1675752112) (https://pub.mdpi-res.com/jmmp/jmmp-07-00042/article_deploy/html/images/jmmp-07-00042-g002-550.jpg?1675752111) (https://pub.mdpi-res.com/jmmp/jmmp-07-00042/article_deploy/html/images/jmmp-07-00042-g003-550.jpg?1675752121) (https://pub.mdpi-res.com/jmmp/jmmp-07-00042/article_deploy/html/images/jmmp-07-00042-g004-550.jpg?1675752116) (https://pub.mdpi-res.com/jmmp/jmmp-07-00042/article_deploy/html/images/jmmp-07-00042-g005-550.jpg?1675752127) (https://pub.mdpi-res.com/jmmp/jmmp-07-00042/article_deploy/html/images/jmmp-07-00042-g006-550.jpg?1675752121) (https://pub.mdpi-res.com/jmmp/jmmp-07-00042/article_deploy/html/images/jmmp-07-00042-g007-550.jpg?1675752117) (https://pub.mdpi-res.com/jmmp/jmmp-07-00042/article_deploy/html/images/jmmp-07-00042-g008-550.jpg?1675752126) ([https://pub.mdpi-res.com/jmmp/jmmp-07-00042-g009-550.jpg?1675752133](https://pub.mdpi-res.com/jmmp/jmmp-07-00042/article_deploy/html/images/jmmp-07-00042-g009-550.jpg?1675752133)) (https://pub.mdpi-res.com/jmmp/jmmp-07-00042/article_deploy/html/images/jmmp-07-00042-g010-550.jpg?1675752123) (https://pub.mdpi-res.com/jmmp/jmmp-07-00042/article_deploy/html/images/jmmp-07-00042-g011-550.jpg?1675752132) (https://pub.mdpi-res.com/jmmp/jmmp-07-00042/article_deploy/html/images/jmmp-07-00042-g012-550.jpg?1675752124) (https://pub.mdpi-res.com/jmmp/jmmp-07-00042/article_deploy/html/images/jmmp-07-00042-g013-550.jpg?1675752115) (https://pub.mdpi-res.com/jmmp/jmmp-07-00042/article_deploy/html/images/jmmp-07-00042-g014-550.jpg?1675752119) (https://pub.mdpi-res.com/jmmp/jmmp-07-00042/article_deploy/html/images/jmmp-07-00042-g015-550.jpg?1675752130) (https://pub.mdpi-res.com/jmmp/jmmp-07-00042/article_deploy/html/images/jmmp-07-00042-g016-550.jpg?1675752114) (https://pub.mdpi-res.com/jmmp/jmmp-07-00042/article_deploy/html/images/jmmp-07-00042-g017-550.jpg?1675752128)

Open Access Article 29 pages, 7556 KIB ([/2504-4494/7/1/41/pdf?version=1676618668](#))

Development and Practical Implementation of Digital Observer for Elastic Torque of Rolling Mill Electromechanical System (2504-4494/7/1/41)

by  Vadim R. Gasiyarov (https://sciprofiles.com/profile/1099739?utm_source=mdpi.com&utm_medium=website&utm_campaign=avatar_name),
 Andrey A. Radionov (https://sciprofiles.com/profile/463047?utm_source=mdpi.com&utm_medium=website&utm_campaign=avatar_name),
 Boris M. Logvinov (https://sciprofiles.com/profile/2042009?utm_source=mdpi.com&utm_medium=website&utm_campaign=avatar_name),
 Alexander S. Karandaev (https://sciprofiles.com/profile/463049?utm_source=mdpi.com&utm_medium=website&utm_campaign=avatar_name),
 Olga A. Gasiyarova (https://sciprofiles.com/profile/2778996?utm_source=mdpi.com&utm_medium=website&utm_campaign=avatar_name) and
 Vadim R. Khramshin (https://sciprofiles.com/profile/454741?utm_source=mdpi.com&utm_medium=website&utm_campaign=avatar_name)
J. Manuf. Mater. Process. **2023**, *7*(1), 41; <https://doi.org/10.3390/jmmp7010041> (<https://doi.org/10.3390/jmmp7010041>) - 04 Feb 2023

Cited by 6 ([/2504-4494/7/1/41#metrics](#)) | Viewed by 1315

Abstract The strategic initiative aimed at building "digital metallurgy" implies the introduction of diagnostic monitoring systems to trace the technical condition of critical production units. This problem is relevant for rolling mills, which provide the output and determine the quality of products of metallurgical [...] [Read more](#).

Show Figures

(https://pub.mdpi-res.com/jmmp/jmmp-07-00041/article_deploy/html/images/jmmp-07-00041-g001-550.jpg?1676618773) (https://pub.mdpi-res.com/jmmp/jmmp-07-00041/article_deploy/html/images/jmmp-07-00041-g002-550.jpg?1676618752) (https://pub.mdpi-res.com/jmmp/jmmp-07-00041/article_deploy/html/images/jmmp-07-00041-g003-550.jpg?1676618760) (https://pub.mdpi-res.com/jmmp/jmmp-07-00041/article_deploy/html/images/jmmp-07-00041-g004-550.jpg?1676618759)



Cited by 1 (/2504-4494/7/1/33#metrics) | Viewed by 1722

additive manufacturing of polymers, relying on the absence of a material-specific processing window. To allow for the support-free manufacturing of polymers at [...][Read more.](#)
(This article belongs to the Special Issue [Progress in Powder-Based Additive Manufacturing](#) ([/journal/mmp/special_issues/ER1HXH74Y](#)))

► [Show Figures](#)

(https://pub.mdpi-res.com/jmmp/jmmp-07-00033/article_deploy/html/images/jmmp-07-00033-g001-550.jpg?1675085358) (https://pub.mdpi-res.com/jmmp/jmmp-07-00033/article_deploy/html/images/jmmp-07-00033-g002-550.jpg?1675085359) (https://pub.mdpi-res.com/jmmp/jmmp-07-00033/article_deploy/html/images/jmmp-07-00033-g003-550.jpg?1675085343) (https://pub.mdpi-res.com/jmmp/jmmp-07-00033/article_deploy/html/images/jmmp-07-00033-g004-550.jpg?1675085360) (https://pub.mdpi-res.com/jmmp/jmmp-07-00033/article_deploy/html/images/jmmp-07-00033-g005-550.jpg?1675085339) (https://pub.mdpi-res.com/jmmp/jmmp-07-00033/article_deploy/html/images/jmmp-07-00033-g006-550.jpg?1675085338) (https://pub.mdpi-res.com/jmmp/jmmp-07-00033/article_deploy/html/images/jmmp-07-00033-g007-550.jpg?1675085336) (https://pub.mdpi-res.com/jmmp/jmmp-07-00033/article_deploy/html/images/jmmp-07-00033-g008-550.jpg?1675085342) (https://pub.mdpi-res.com/jmmp/jmmp-07-00033/article_deploy/html/images/jmmp-07-00033-g009-550.jpg?1675085333) (https://pub.mdpi-res.com/jmmp/jmmp-07-00033/article_deploy/html/images/jmmp-07-00033-g010-550.jpg?1675085341) (https://pub.mdpi-res.com/jmmp/jmmp-07-00033/article_deploy/html/images/jmmp-07-00033-g011-550.jpg?1675085355) (https://pub.mdpi-res.com/jmmp/jmmp-07-00033/article_deploy/html/images/jmmp-07-00033-g012-550.jpg?1675085350) ([https://pub.mdpi-res.com/jmmp/jmmp-07-00033-g013-550.jpg?1675085346](https://pub.mdpi-res.com/jmmp/jmmp-07-00033/article_deploy/html/images/jmmp-07-00033-g013-550.jpg?1675085346)) ([https://pub.mdpi-res.com/jmmp/jmmp-07-00033-g014-550.jpg?1675085347](https://pub.mdpi-res.com/jmmp/jmmp-07-00033/article_deploy/html/images/jmmp-07-00033-g014-550.jpg?1675085347)) ([https://pub.mdpi-res.com/jmmp/jmmp-07-00033-g015-550.jpg?1675085357](https://pub.mdpi-res.com/jmmp/jmmp-07-00033/article_deploy/html/images/jmmp-07-00033-g015-550.jpg?1675085357)) ([https://pub.mdpi-res.com/jmmp/jmmp-07-00033-g016-550.jpg?1675085362](https://pub.mdpi-res.com/jmmp/jmmp-07-00033/article_deploy/html/images/jmmp-07-00033-g016-550.jpg?1675085362))

Open Access Article 15 pages, 6944 KiB ([/2504-4494/7/1/32/pdf?version=1674899181](#))

Effect of Heat Treatment on the Mechanical and Tribological Properties of Dual-Reinforced Cold-Sprayed Al Coatings ([/2504-4494/7/1/32](#))

by  [Kia Min Phua](#) (https://sciprofiles.com/profile/2734268?utm_source=mdpi.com&utm_medium=website&utm_campaign=avatar_name),
 [Thomas Stapel](#) (https://sciprofiles.com/profile/author/Z1ZkaGRibzJySlpIRGJ5WGhSZEF5bGVORHhWdWcDgzTE5KUEJ4OTINRT0=?utm_source=mdpi.com&utm_medium=website&utm_campaign=avatar_name) and
 [Troy Y. Ansell](#) (https://sciprofiles.com/profile/809369?utm_source=mdpi.com&utm_medium=website&utm_campaign=avatar_name)
J. Manuf. Mater. Process. **2023**, *7*(1), 32; <https://doi.org/10.3390/jmmp7010032> (<https://doi.org/10.3390/jmmp7010032>) - 28 Jan 2023
Cited by 1 ([/2504-4494/7/1/32#metrics](#)) | Viewed by 1187

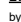




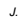
Abstract The aluminum cold spray feedstock powder was single- and dual-reinforced with no greater than 2 vol% boron nitride nanoplatelets (BNNP) and/or nanometric boron carbide (nB₄C). These powders were cold sprayed onto Al-6061 substrates and then heat-treated in an argon environment. In [...][Read more.](#)
(This article belongs to the Special Issue [Advances in Metal Forming and Thermomechanical Processing](#) ([/journal/mmp/special_issues/8804J3WWAQ](#)))

► [Show Figures](#)

(https://pub.mdpi-res.com/jmmp/jmmp-07-00032/article_deploy/html/images/jmmp-07-00032-g001-550.jpg?1674899256) (https://pub.mdpi-res.com/jmmp/jmmp-07-00032/article_deploy/html/images/jmmp-07-00032-g002-550.jpg?1674899270) (https://pub.mdpi-res.com/jmmp/jmmp-07-00032/article_deploy/html/images/jmmp-07-00032-g003-550.jpg?1674899249) (https://pub.mdpi-res.com/jmmp/jmmp-07-00032/article_deploy/html/images/jmmp-07-00032-g004-550.jpg?1674899260) ([https://pub.mdpi-res.com/jmmp/jmmp-07-00032-g005-550.jpg?1674899264](https://pub.mdpi-res.com/jmmp/jmmp-07-00032/article_deploy/html/images/jmmp-07-00032-g005-550.jpg?1674899264)) ([https://pub.mdpi-res.com/jmmp/jmmp-07-00032-g006-550.jpg?1674899255](https://pub.mdpi-res.com/jmmp/jmmp-07-00032/article_deploy/html/images/jmmp-07-00032-g006-550.jpg?1674899255)) (https://pub.mdpi-res.com/jmmp/jmmp-07-00032/article_deploy/html/images/jmmp-07-00032-g007-550.jpg?1674899248) ([https://pub.mdpi-res.com/jmmp/jmmp-07-00032-g0A1-550.jpg?1674899263](https://pub.mdpi-res.com/jmmp/jmmp-07-00032/article_deploy/html/images/jmmp-07-00032-g0A1-550.jpg?1674899263)) ([https://pub.mdpi-res.com/jmmp/jmmp-07-00032-g0A2-550.jpg?1674899252](https://pub.mdpi-res.com/jmmp/jmmp-07-00032/article_deploy/html/images/jmmp-07-00032-g0A2-550.jpg?1674899252)) ([https://pub.mdpi-res.com/jmmp/jmmp-07-00032-g0A3-550.jpg?1674899258](https://pub.mdpi-res.com/jmmp/jmmp-07-00032/article_deploy/html/images/jmmp-07-00032-g0A3-550.jpg?1674899258))

Open Access Article 16 pages, 3245 KiB ([/2504-4494/7/1/31/pdf?version=1674719511](#))

Evaluation of Processing Conditions in the Performance of Purging Compounds for Polypropylene Injection Molding ([/2504-4494/7/1/31](#))

by  [Miguel Carrasco](#) (https://sciprofiles.com/profile/2694493?utm_source=mdpi.com&utm_medium=website&utm_campaign=avatar_name),
 [Jorge Guerrero](#) (https://sciprofiles.com/profile/2738481?utm_source=mdpi.com&utm_medium=website&utm_campaign=avatar_name),
 [Miriam Lazo](#) (https://sciprofiles.com/profile/2246863?utm_source=mdpi.com&utm_medium=website&utm_campaign=avatar_name),
 [Estephany Adrián](#) (https://sciprofiles.com/profile/2729453?utm_source=mdpi.com&utm_medium=website&utm_campaign=avatar_name),
 [Jorge Alberto Medina-Perilla](#) (https://sciprofiles.com/profile/1465218?utm_source=mdpi.com&utm_medium=website&utm_campaign=avatar_name) and
 [Andrés Rigall-Cedeño](#) (https://sciprofiles.com/profile/1947852?utm_source=mdpi.com&utm_medium=website&utm_campaign=avatar_name)
J. Manuf. Mater. Process. **2023**, *7*(1), 31; <https://doi.org/10.3390/jmmp7010031> (<https://doi.org/10.3390/jmmp7010031>) - 26 Jan 2023
Cited by 1 ([/2504-4494/7/1/31#metrics](#)) | Viewed by 2189

Abstract Purging is a fundamental process in the injection molding sector, aiding in color transition, material shifts, and the removal of contaminants. The purging compounds can be classified according to physical or chemical mechanisms and are affected by processing parameters, such as temperature, pressure, [...][Read more.](#)
(This article belongs to the Special Issue [Advances in Injection Molding: Process, Materials and Applications](#) ([/journal/mmp/special_issues/injection_molding_process](#)))

► [Show Figures](#)

(https://pub.mdpi-res.com/jmmp/jmmp-07-00031/article_deploy/html/images/jmmp-07-00031-g001-550.jpg?1674719593) (https://pub.mdpi-res.com/jmmp/jmmp-07-00031/article_deploy/html/images/jmmp-07-00031-g002-550.jpg?1674719582) (https://pub.mdpi-res.com/jmmp/jmmp-07-00031/article_deploy/html/images/jmmp-07-00031-g003-550.jpg?1674719601) (https://pub.mdpi-res.com/jmmp/jmmp-07-00031/article_deploy/html/images/jmmp-07-00031-g004-550.jpg?1674719598) ([https://pub.mdpi-res.com/jmmp/jmmp-07-00031-g005-550.jpg?1674719592](https://pub.mdpi-res.com/jmmp/jmmp-07-00031/article_deploy/html/images/jmmp-07-00031-g005-550.jpg?1674719592)) (https://pub.mdpi-res.com/jmmp/jmmp-07-00031/article_deploy/html/images/jmmp-07-00031-g006-550.jpg?1674719596) (https://pub.mdpi-res.com/jmmp/jmmp-07-00031/article_deploy/html/images/jmmp-07-00031-g007-550.jpg?1674719586) ([https://pub.mdpi-res.com/jmmp/jmmp-07-00031-g008-550.jpg?1674719602](https://pub.mdpi-res.com/jmmp/jmmp-07-00031/article_deploy/html/images/jmmp-07-00031-g008-550.jpg?1674719602))

Open Access Article 19 pages, 6048 KiB ([/2504-4494/7/1/30/pdf?version=1676272833](#))

Design Optimization of Hot Isostatic Pressing Capsules ([/2504-4494/7/1/30](#))

by  [Samaneh Sobhani](#) (https://sciprofiles.com/profile/2620609?utm_source=mdpi.com&utm_medium=website&utm_campaign=avatar_name),
 [Marc Albert](#) (https://sciprofiles.com/profile/2688452?utm_source=mdpi.com&utm_medium=website&utm_campaign=avatar_name),
 [David Gandy](#) (https://sciprofiles.com/profile/author/b0U5cVdnZGFHaDFlSlhZlTCRU5Ga0IKTKFpeDlxTeXPYzDTmMaVM5Yz0=?utm_source=mdpi.com&utm_medium=website&utm_campaign=avatar_name) and
 [Ali Tabei](#) (https://sciprofiles.com/profile/author/M1ReZ0RoMjdxRVB3VUnzeVcySIRBUtVnbHdpM2hySDk1UINFVGjYRXB1az0=?utm_source=mdpi.com&utm_medium=website&utm_campaign=avatar_name)
 [Zhaoyan Fan](#) (https://sciprofiles.com/profile/2785933?utm_source=mdpi.com&utm_medium=website&utm_campaign=avatar_name)
J. Manuf. Mater. Process. **2023**, *7*(1), 30; <https://doi.org/10.3390/jmmp7010030> (<https://doi.org/10.3390/jmmp7010030>) - 25 Jan 2023
Cited by 1 ([/2504-4494/7/1/30#metrics](#)) | Viewed by 1801

Abstract Power metallurgy hot isostatic pressing (PM-HIP) is a manufacturing technique capable of producing net shape or near-net shape components with complicated geometries from materials that are difficult to melt and cast, mechanically deform or weld. However, the process and soundness of the outcome [...][Read more.](#)
(This article belongs to the Topic [Numerical and Experimental Advances in Innovative Manufacturing Processes](#) ([topics/numerical_innovative_manufacturing](#)))

► [Show Figures](#)

(https://pub.mdpi-res.com/jmmp/jmmp-07-00030/article_deploy/html/images/jmmp-07-00030-g001-550.jpg?1676272919) (https://pub.mdpi-res.com/jmmp/jmmp-07-00030/article_deploy/html/images/jmmp-07-00030-g002-550.jpg?1676272905) ([https://pub.mdpi-res.com/jmmp/jmmp-07-00030-g003-550.jpg?1676272905](https://pub.mdpi-res.com/jmmp/jmmp-07-00030/article_deploy/html/images/jmmp-07-00030-g003-550.jpg?1676272905)) (https://pub.mdpi-res.com/jmmp/jmmp-07-00030/article_deploy/html/images/jmmp-07-00030-g004-550.jpg?1676272916) ([https://pub.mdpi-res.com/jmmp/jmmp-07-00030-g005-550.jpg?1676272907](https://pub.mdpi-res.com/jmmp/jmmp-07-00030/article_deploy/html/images/jmmp-07-00030-g005-550.jpg?1676272907)) ([https://pub.mdpi-res.com/jmmp/jmmp-07-00030-g006-550.jpg?1676272906](https://pub.mdpi-res.com/jmmp/jmmp-07-00030/article_deploy/html/images/jmmp-07-00030-g006-550.jpg?1676272906)) ([https://pub.mdpi-res.com/jmmp/jmmp-07-00030-g007-550.jpg?1676272904](https://pub.mdpi-res.com/jmmp/jmmp-07-00030/article_deploy/html/images/jmmp-07-00030-g007-550.jpg?1676272904)) ([https://pub.mdpi-res.com/jmmp/jmmp-07-00030-g008-550.jpg?1676272920](https://pub.mdpi-res.com/jmmp/jmmp-07-00030/article_deploy/html/images/jmmp-07-00030-g008-550.jpg?1676272920)) ([https://pub.mdpi-res.com/jmmp/jmmp-07-00030-g009-550.jpg?1676272921](https://pub.mdpi-res.com/jmmp/jmmp-07-00030/article_deploy/html/images/jmmp-07-00030-g009-550.jpg?1676272921)) ([https://pub.mdpi-res.com/jmmp/jmmp-07-00030-g010-550.jpg?1676272899](https://pub.mdpi-res.com/jmmp/jmmp-07-00030/article_deploy/html/images/jmmp-07-00030-g010-550.jpg?1676272899)) ([https://pub.mdpi-res.com/jmmp/jmmp-07-00030-g011-550.jpg?1676272913](https://pub.mdpi-res.com/jmmp/jmmp-07-00030/article_deploy/html/images/jmmp-07-00030-g011-550.jpg?1676272913)) (<https://pub.mdpi-res.com/jmmp/jmmp-07-00030-g012-550.jpg?1676272901>) (<https://pub.mdpi-res.com/jmmp/jmmp-07-00030-g013-550.jpg?1676272910>) (<https://pub.mdpi-res.com/jmmp/jmmp-07-00030-g014-550.jpg?1676272900>) (<https://pub.mdpi-res.com/jmmp/jmmp-07-00030-g015-550.jpg?1676272912>) ([https://pub.mdpi-res.com/jmmp/jmmp-07-00030-g016-550.jpg?1676272917](https://pub.mdpi-res.com/jmmp/jmmp-07-00030/article_deploy/html/images/jmmp-07-00030-g016-550.jpg?1676272917)) ([https://pub.mdpi-res.com/jmmp/jmmp-07-00030-g017-550.jpg?1676272918](https://pub.mdpi-res.com/jmmp/jmmp-07-00030/article_deploy/html/images/jmmp-07-00030-g017-550.jpg?1676272918))

Open Access Article 18 pages, 6837 KiB ([/2504-4494/7/1/29/pdf?version=1675934304](#))

The Development of an Assembled Truss Core Lightweight Panel and Its Method of Manufacture ([/2504-4494/7/1/29](#))

by  [Zhilei Tian](#) (https://sciprofiles.com/profile/2133565?utm_source=mdpi.com&utm_medium=website&utm_campaign=avatar_name),
 [Chenghai Kong](#) (https://sciprofiles.com/profile/author/UzVGL05JU0NnZENUdWY2OS9mZm9sZmZmcFpsJG9JVFZlXUJyQTQ2dHdnST0=?utm_source=mdpi.com&utm_medium=website&utm_campaign=avatar_name) and
 [Jingchao Guan](#) (https://sciprofiles.com/profile/2445185?utm_source=mdpi.com&utm_medium=website&utm_campaign=avatar_name),
 [Wei Zhao](#) (https://sciprofiles.com/profile/1481103?utm_source=mdpi.com&utm_medium=website&utm_campaign=avatar_name),
 [Apolo B. Fukuchi](#) (https://sciprofiles.com/profile/2053944?utm_source=mdpi.com&utm_medium=website&utm_campaign=avatar_name) and
 [Xilu Zhao](#) (https://sciprofiles.com/profile/1856151?utm_source=mdpi.com&utm_medium=website&utm_campaign=avatar_name)
J. Manuf. Mater. Process. **2023**, *7*(1), 29; <https://doi.org/10.3390/jmmp7010029> (<https://doi.org/10.3390/jmmp7010029>) - 23 Jan 2023
Viewed by 1163

Abstract In this study, a new assembled truss core panel and the method for processing it were proposed in order to improve the performance of the lightweight panel structure. The proposed assembled truss core panel can be easily processed by simple punching and bending. [...][Read more.](#)
(This article belongs to the Special Issue [Design and Additive Manufacturing of Lightweight Composite Structures](#) ([/journal/mmp/special_issues/lightweight_composite_structures](#)))

Show Figures

MDPI https://pub.mdpi-res.com/jmmp/jmmp-07-00029/article_deploy/html/images/jmmp-07-00029-g001-550.jpg?1675934395 https://pub.mdpi-res.com/jmmp/jmmp-07-00029/article_deploy/html/images/jmmp-07-00029-g002-550.jpg?1675934375 https://pub.mdpi-res.com/jmmp/jmmp-07-00029/article_deploy/html/images/jmmp-07-00029-g003-550.jpg?1675934396 https://pub.mdpi-res.com/jmmp/jmmp-07-00029/article_deploy/html/images/jmmp-07-00029-g004-550.jpg?1675934381 https://pub.mdpi-res.com/jmmp/jmmp-07-00029/article_deploy/html/images/jmmp-07-00029-g005-550.jpg?1675934383 https://pub.mdpi-res.com/jmmp/jmmp-07-00029/article_deploy/html/images/jmmp-07-00029-g006-550.jpg?1675934406 https://pub.mdpi-res.com/jmmp/jmmp-07-00029/article_deploy/html/images/jmmp-07-00029-g007-550.jpg?1675934386 https://pub.mdpi-res.com/jmmp/jmmp-07-00029/article_deploy/html/images/jmmp-07-00029-g008-550.jpg?1675934390 https://pub.mdpi-res.com/jmmp/jmmp-07-00029/article_deploy/html/images/jmmp-07-00029-g009-550.jpg?1675934399 https://pub.mdpi-res.com/jmmp/jmmp-07-00029/article_deploy/html/images/jmmp-07-00029-g010-550.jpg?1675934377 https://pub.mdpi-res.com/jmmp/jmmp-07-00029/article_deploy/html/images/jmmp-07-00029-g011-550.jpg?1675934388 https://pub.mdpi-res.com/jmmp/jmmp-07-00029/article_deploy/html/images/jmmp-07-00029-g012-550.jpg?1675934394 [https://pub.mdpi-res.com/jmmp/jmmp-07-00029-g013-550.jpg?1675934379](https://pub.mdpi-res.com/jmmp/jmmp-07-00029/article_deploy/html/images/jmmp-07-00029-g013-550.jpg?1675934379) https://pub.mdpi-res.com/jmmp/jmmp-07-00029/article_deploy/html/images/jmmp-07-00029-g015-550.jpg?1675934397 https://pub.mdpi-res.com/jmmp/jmmp-07-00029/article_deploy/html/images/jmmp-07-00029-g016-550.jpg?1675934384 [https://pub.mdpi-res.com/jmmp/jmmp-07-00029-g017-550.jpg?1675934403](https://pub.mdpi-res.com/jmmp/jmmp-07-00029/article_deploy/html/images/jmmp-07-00029-g017-550.jpg?1675934403) https://pub.mdpi-res.com/jmmp/jmmp-07-00029/article_deploy/html/images/jmmp-07-00029-g018-550.jpg?1675934392 https://pub.mdpi-res.com/jmmp/jmmp-07-00029/article_deploy/html/images/jmmp-07-00029-g019-550.jpg?1675934402

Open Access Article

21 pages, 8614 KiB [\(2504-4494/7/1/28/pdf?version=1674205396\)](#)

Simulated Study of the Machinability of the Nomex Honeycomb Structure [\(2504-4494/7/1/28\)](#)

by [Tarik Zarrouk](#) https://sciprofiles.com/profile/2682414?utm_source=mdpi.com&utm_medium=website&utm_campaign=avatar_name,
[Mohammed Nouari](#) https://sciprofiles.com/profile/77007?utm_source=mdpi.com&utm_medium=website&utm_campaign=avatar_name and
[Hamid Makich](#) https://sciprofiles.com/profile/79321?utm_source=mdpi.com&utm_medium=website&utm_campaign=avatar_name
J. Manuf. Mater. Process. **2023**, *7*(1), 28; <https://doi.org/10.3390/jmmp7010028> <https://doi.org/10.3390/jmmp7010028> - 20 Jan 2023

Cited by 3 [\(2504-4494/7/1/28/metrics\)](#) | Viewed by 1462

Abstract The Nomex honeycomb core has been widely used in many industrial fields, especially the aircraft and aerospace industries, due to its high strength and stiffness to heaviness ratio. Machining of the Nomex honeycomb structure is usually associated with tearing of the walls, deformations [...] [Read more](#).
(This article belongs to the Special Issue [Advances in Machining of Difficult-to-Cut Materials](#) ([Journal/jmmp/special_issues/5FL8T0YQ1L](#)))

Show Figures

https://pub.mdpi-res.com/jmmp/jmmp-07-00028/article_deploy/html/images/jmmp-07-00028-g001-550.jpg?1674205485 https://pub.mdpi-res.com/jmmp/jmmp-07-00028/article_deploy/html/images/jmmp-07-00028-g002-550.jpg?1674205478 https://pub.mdpi-res.com/jmmp/jmmp-07-00028/article_deploy/html/images/jmmp-07-00028-g003-550.jpg?1674205471 https://pub.mdpi-res.com/jmmp/jmmp-07-00028/article_deploy/html/images/jmmp-07-00028-g004-550.jpg?1674205486 https://pub.mdpi-res.com/jmmp/jmmp-07-00028/article_deploy/html/images/jmmp-07-00028-g005-550.jpg?1674205466 https://pub.mdpi-res.com/jmmp/jmmp-07-00028/article_deploy/html/images/jmmp-07-00028-g006-550.jpg?1674205489 https://pub.mdpi-res.com/jmmp/jmmp-07-00028/article_deploy/html/images/jmmp-07-00028-g007-550.jpg?1674205481 https://pub.mdpi-res.com/jmmp/jmmp-07-00028/article_deploy/html/images/jmmp-07-00028-g008-550.jpg?1674205492 https://pub.mdpi-res.com/jmmp/jmmp-07-00028/article_deploy/html/images/jmmp-07-00028-g009-550.jpg?1674205489 https://pub.mdpi-res.com/jmmp/jmmp-07-00028/article_deploy/html/images/jmmp-07-00028-g010-550.jpg?1674205475 https://pub.mdpi-res.com/jmmp/jmmp-07-00028/article_deploy/html/images/jmmp-07-00028-g011-550.jpg?1674205494 https://pub.mdpi-res.com/jmmp/jmmp-07-00028/article_deploy/html/images/jmmp-07-00028-g012-550.jpg?1674205469 [https://pub.mdpi-res.com/jmmp/jmmp-07-00028-g013-550.jpg?1674205479](https://pub.mdpi-res.com/jmmp/jmmp-07-00028/article_deploy/html/images/jmmp-07-00028-g013-550.jpg?1674205479) https://pub.mdpi-res.com/jmmp/jmmp-07-00028/article_deploy/html/images/jmmp-07-00028-g014-550.jpg?1674205472 https://pub.mdpi-res.com/jmmp/jmmp-07-00028/article_deploy/html/images/jmmp-07-00028-g015-550.jpg?1674205487 https://pub.mdpi-res.com/jmmp/jmmp-07-00028/article_deploy/html/images/jmmp-07-00028-g016-550.jpg?1674205495 [https://pub.mdpi-res.com/jmmp/jmmp-07-00028-g017-550.jpg?1674205488](https://pub.mdpi-res.com/jmmp/jmmp-07-00028/article_deploy/html/images/jmmp-07-00028-g017-550.jpg?1674205488) https://pub.mdpi-res.com/jmmp/jmmp-07-00028/article_deploy/html/images/jmmp-07-00028-g018-550.jpg?1674205484 https://pub.mdpi-res.com/jmmp/jmmp-07-00028/article_deploy/html/images/jmmp-07-00028-g019-550.jpg?1674205493 https://pub.mdpi-res.com/jmmp/jmmp-07-00028/article_deploy/html/images/jmmp-07-00028-g020-550.jpg?1674205497 [https://pub.mdpi-res.com/jmmp/jmmp-07-00028-g021-550.jpg?1674205470](https://pub.mdpi-res.com/jmmp/jmmp-07-00028/article_deploy/html/images/jmmp-07-00028-g021-550.jpg?1674205470) https://pub.mdpi-res.com/jmmp/jmmp-07-00028/article_deploy/html/images/jmmp-07-00028-g022-550.jpg?1674205490 https://pub.mdpi-res.com/jmmp/jmmp-07-00028/article_deploy/html/images/jmmp-07-00028-g023-550.jpg?1674205476 https://pub.mdpi-res.com/jmmp/jmmp-07-00028/article_deploy/html/images/jmmp-07-00028-g024-550.jpg?1674205482 [https://pub.mdpi-res.com/jmmp/jmmp-07-00028-g025-550.jpg?1674205474](https://pub.mdpi-res.com/jmmp/jmmp-07-00028/article_deploy/html/images/jmmp-07-00028-g025-550.jpg?1674205474) [https://pub.mdpi-res.com/jmmp/jmmp-07-00028-g026-550.jpg?1674205468](https://pub.mdpi-res.com/jmmp/jmmp-07-00028/article_deploy/html/images/jmmp-07-00028-g026-550.jpg?1674205468)

Open Access Editorial

5 pages, 163 KiB [\(2504-4494/7/1/27/pdf?version=1675852905\)](#)

Acknowledgment to the Reviewers of JMMP in 2022 [\(2504-4494/7/1/27\)](#)

by **JMMP Editorial Office** [\(search?author=JMMP%20Editorial%20Office&orcid=\)](#)
J. Manuf. Mater. Process. **2023**, *7*(1), 27; <https://doi.org/10.3390/jmmp7010027> <https://doi.org/10.3390/jmmp7010027> - 19 Jan 2023
Viewed by 807

Abstract High-quality academic publishing is built on rigorous peer review [...] [Full article](#). [\(2504-4494/7/1/27\)](#)

Open Access Article

15 pages, 5410 KiB [\(2504-4494/7/1/26/pdf?version=1674985815\)](#)

Introduction of a New Test Methodology for Determining the Delayed Cracking Susceptibility [\(2504-4494/7/1/26\)](#)

by [Anton Hopf](#) https://sciprofiles.com/profile/2652665?utm_source=mdpi.com&utm_medium=website&utm_campaign=avatar_name,
[Moritz Klug](#) https://sciprofiles.com/profile/author/Uy8yMGtieJlYmwrSUIPOWswSzMxOXNXTIE5aHJBjY0JRbXlZeSjlZjRRTO?utm_source=mdpi.com&utm_medium=website&utm_campaign=avatar_name,
[Klaus Durmaz](#) https://sciprofiles.com/profile/2719759?utm_source=mdpi.com&utm_medium=website&utm_campaign=avatar_name,
[Xirsa Gorth](#) https://sciprofiles.com/profile/author/SjinSDioTjUQTNoNEVtIm0YRlektCZjNjYk1ld2RzYWZ4dUdaMWp3WT0?utm_source=mdpi.com&utm_medium=website&utm_campaign=avatar_name
and
[Sven Jüttner](#) https://sciprofiles.com/profile/517452?utm_source=mdpi.com&utm_medium=website&utm_campaign=avatar_name
J. Manuf. Mater. Process. **2023**, *7*(1), 26; <https://doi.org/10.3390/jmmp7010026> <https://doi.org/10.3390/jmmp7010026> - 18 Jan 2023
Viewed by 1703

Abstract A missing test methodology that allows for the determination of delayed cracking susceptibility of laser welds of high-strength sheet steel is presented. Unlike other cold crack testing methods, this test is based on a self-restraint testing of specimens welded from thin sheet materials [...] [Read more](#).
(This article belongs to the Special Issue [Advances in Welding Technology](#) ([Journal/jmmp/special_issues/welding_tech](#)))

Show Figures

https://pub.mdpi-res.com/jmmp/jmmp-07-00026/article_deploy/html/images/jmmp-07-00026-g001-550.jpg?1674985884 https://pub.mdpi-res.com/jmmp/jmmp-07-00026/article_deploy/html/images/jmmp-07-00026-g002-550.jpg?1674985892 https://pub.mdpi-res.com/jmmp/jmmp-07-00026/article_deploy/html/images/jmmp-07-00026-g003-550.jpg?1674985889 https://pub.mdpi-res.com/jmmp/jmmp-07-00026/article_deploy/html/images/jmmp-07-00026-g004-550.jpg?1674985882 https://pub.mdpi-res.com/jmmp/jmmp-07-00026/article_deploy/html/images/jmmp-07-00026-g005-550.jpg?1674985880 https://pub.mdpi-res.com/jmmp/jmmp-07-00026/article_deploy/html/images/jmmp-07-00026-g006-550.jpg?1674985891 https://pub.mdpi-res.com/jmmp/jmmp-07-00026/article_deploy/html/images/jmmp-07-00026-g007-550.jpg?1674985890 https://pub.mdpi-res.com/jmmp/jmmp-07-00026/article_deploy/html/images/jmmp-07-00026-g008-550.jpg?1674985881 [https://pub.mdpi-res.com/jmmp/jmmp-07-00026-g009-550.jpg?1674985886](https://pub.mdpi-res.com/jmmp/jmmp-07-00026/article_deploy/html/images/jmmp-07-00026-g009-550.jpg?1674985886) https://pub.mdpi-res.com/jmmp/jmmp-07-00026/article_deploy/html/images/jmmp-07-00026-g010-550.jpg?1674985885 [https://pub.mdpi-res.com/jmmp/jmmp-07-00026-g011-550.jpg?1674985887](https://pub.mdpi-res.com/jmmp/jmmp-07-00026/article_deploy/html/images/jmmp-07-00026-g011-550.jpg?1674985887)

Open Access Article

18 pages, 10358 KiB [\(2504-4494/7/1/25/pdf?version=1674051049\)](#)

Strain-Based Fatigue Experimental Study on Ti–6Al–4V Alloy Manufactured by Electron Beam Melting [\(2504-4494/7/1/25\)](#)

by [Alberto David Pertuz-Comas](#) https://sciprofiles.com/profile/2694313?utm_source=mdpi.com&utm_medium=website&utm_campaign=avatar_name,
[Octavio Andrés González-Estrada](#) https://sciprofiles.com/profile/1197446?utm_source=mdpi.com&utm_medium=website&utm_campaign=avatar_name,
[Elkin Martínez-Díaz](#) https://sciprofiles.com/profile/2709803?utm_source=mdpi.com&utm_medium=website&utm_campaign=avatar_name,
[Diego Fernando Villegas-Bermúdez](#) https://sciprofiles.com/profile/2806758?utm_source=mdpi.com&utm_medium=website&utm_campaign=avatar_name and
[Jorge Guillermo Díaz-Rodríguez](#) https://sciprofiles.com/profile/2301175?utm_source=mdpi.com&utm_medium=website&utm_campaign=avatar_name
J. Manuf. Mater. Process. **2023**, *7*(1), 25; <https://doi.org/10.3390/jmmp7010025> <https://doi.org/10.3390/jmmp7010025> - 18 Jan 2023
Cited by 4 [\(2504-4494/7/1/25/metrics\)](#) | Viewed by 1679

Abstract Additive manufacturing (AM) by electron beam melting (EBM) is a technique used to manufacture parts by melting powder metal layer-by-layer with an electron beam in a high vacuum, thereby generating a 3D topology. This paper studies the low-cycle fatigue of Ti–6Al–4V specimens obtained [...] [Read more](#).
(This article belongs to the Special Issue [Advances in Metal Additive Manufacturing/3D Printing](#) ([Journal/jmmp/special_issues/MetalAM](#)))

Show Figures

https://pub.mdpi-res.com/jmmp/jmmp-07-00025/article_deploy/html/images/jmmp-07-00025-g001-550.jpg?1674051128 https://pub.mdpi-res.com/jmmp/jmmp-07-00025/article_deploy/html/images/jmmp-07-00025-g002-550.jpg?1674051144 <https://pub.mdpi-res.com/jmmp/jmmp-07-00025-g003-550.jpg?1674051142> <https://pub.mdpi-res.com/jmmp/jmmp-07-00025-g004-550.jpg?1674051127> <https://pub.mdpi-res.com/jmmp/jmmp-07-00025-g005-550.jpg?1674051138> <https://pub.mdpi-res.com/jmmp/jmmp-07-00025-g006-550.jpg?1674051146>

https://pub.mdpi-res.com/jmmp/jmmp-07-00025/article_deploy/html/images/jmmp-07-00025-g007-550.jpg?1674051129) (https://pub.mdpi-res.com/jmmp/jmmp-07-00025/article_deploy/html/images/jmmp-07-00025-g009-550.jpg?1674051143) ([https://pub.mdpi-res.com/jmmp/jmmp-07-00025-g010-550.jpg?1674051138](https://pub.mdpi-res.com/jmmp/jmmp-07-00025/article_deploy/html/images/jmmp-07-00025-g010-550.jpg?1674051138)) (https://pub.mdpi-res.com/jmmp/jmmp-07-00025/article_deploy/html/images/jmmp-07-00025-g011-550.jpg?1674051134) (https://pub.mdpi-res.com/jmmp/jmmp-07-00025/article_deploy/html/images/jmmp-07-00025-g012-550.jpg?1674051131) ([https://pub.mdpi-res.com/jmmp/jmmp-07-00025-g013-550.jpg?1674051148](https://pub.mdpi-res.com/jmmp/jmmp-07-00025/article_deploy/html/images/jmmp-07-00025-g013-550.jpg?1674051148)) ([https://pub.mdpi-res.com/jmmp/jmmp-07-00025-g014-550.jpg?1674051136](https://pub.mdpi-res.com/jmmp/jmmp-07-00025/article_deploy/html/images/jmmp-07-00025-g014-550.jpg?1674051136)) ([https://pub.mdpi-res.com/jmmp/jmmp-07-00025-g015-550.jpg?1674051123](https://pub.mdpi-res.com/jmmp/jmmp-07-00025/article_deploy/html/images/jmmp-07-00025-g015-550.jpg?1674051123)) ([https://pub.mdpi-res.com/jmmp/jmmp-07-00025-g016-550.jpg?1674051145](https://pub.mdpi-res.com/jmmp/jmmp-07-00025/article_deploy/html/images/jmmp-07-00025-g016-550.jpg?1674051145)) ([https://pub.mdpi-res.com/jmmp/jmmp-07-00025-g017-550.jpg?1674051140](https://pub.mdpi-res.com/jmmp/jmmp-07-00025/article_deploy/html/images/jmmp-07-00025-g017-550.jpg?1674051140))

Open Access Article 19 pages, 8075 KIB (2504-4494/7/1/24/pdf?version=1673952711)

Fundamental Investigations to Evaluate the Influence of Notching Processes on a Subsequent Cyclic Bending Process for the Production of Wire Cores ((2504-4494/7/1/24)

by  Alina Biallas (https://sciprofiles.com/profile/2229368?utm_source=mdpi.com&utm_medium=website&utm_campaign=avatar_name),
 Sophia Ohmayer (https://sciprofiles.com/profile/author/TVVvKOWNWdzhXNk94ThpCaDJvd1ExncpMQ1NOVEFCdEZOV2JZWDJLS0Iqaz0=?utm_source=mdpi.com&utm_medium=website&utm_campaign=avatar_name) and
 Marion Merklein (https://sciprofiles.com/profile/2214169?utm_source=mdpi.com&utm_medium=website&utm_campaign=avatar_name)

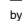


J. Manuf. Mater. Process. **2023**, *7*(1), 24; <https://doi.org/10.3390/jmmp7010024> (<https://doi.org/10.3390/jmmp7010024>) - 17 Jan 2023
Cited by 1 ((2504-4494/7/1/24#metrics)) | Viewed by 1346
Abstract The production of wire cores by notch rolling and cyclic bending promises an ecologically and economically efficient manufacturing option for steel fibers. The paper at hand evaluates the influence of wire strips on cyclic bending by applying rolled wire strips of DP600 sheet [..] [Read more](#).
(This article belongs to the Special Issue [Advances in Metal Forming and Thermomechanical Processing](#) ([/journal/jmmp/special_issues/8804J3WWAQ](#)))

Show Figures

(https://pub.mdpi-res.com/jmmp/jmmp-07-00024/article_deploy/html/images/jmmp-07-00024-g001-550.jpg?1673952793) ([https://pub.mdpi-res.com/jmmp/jmmp-07-00024-g002-550.jpg?1673952791](https://pub.mdpi-res.com/jmmp/jmmp-07-00024/article_deploy/html/images/jmmp-07-00024-g002-550.jpg?1673952791)) ([https://pub.mdpi-res.com/jmmp/jmmp-07-00024-g003-550.jpg?1673952792](https://pub.mdpi-res.com/jmmp/jmmp-07-00024/article_deploy/html/images/jmmp-07-00024-g003-550.jpg?1673952792)) ([https://pub.mdpi-res.com/jmmp/jmmp-07-00024-g004-550.jpg?1673952787](https://pub.mdpi-res.com/jmmp/jmmp-07-00024/article_deploy/html/images/jmmp-07-00024-g004-550.jpg?1673952787)) ([https://pub.mdpi-res.com/jmmp/jmmp-07-00024-g005-550.jpg?1673952775](https://pub.mdpi-res.com/jmmp/jmmp-07-00024/article_deploy/html/images/jmmp-07-00024-g005-550.jpg?1673952775)) ([https://pub.mdpi-res.com/jmmp/jmmp-07-00024-g006-550.jpg?1673952781](https://pub.mdpi-res.com/jmmp/jmmp-07-00024/article_deploy/html/images/jmmp-07-00024-g006-550.jpg?1673952781)) ([https://pub.mdpi-res.com/jmmp/jmmp-07-00024-g007-550.jpg?1673952779](https://pub.mdpi-res.com/jmmp/jmmp-07-00024/article_deploy/html/images/jmmp-07-00024-g007-550.jpg?1673952779)) ([https://pub.mdpi-res.com/jmmp/jmmp-07-00024-g008-550.jpg?1673952777](https://pub.mdpi-res.com/jmmp/jmmp-07-00024/article_deploy/html/images/jmmp-07-00024-g008-550.jpg?1673952777)) ([https://pub.mdpi-res.com/jmmp/jmmp-07-00024-g009-550.jpg?1673952778](https://pub.mdpi-res.com/jmmp/jmmp-07-00024/article_deploy/html/images/jmmp-07-00024-g009-550.jpg?1673952778)) ([https://pub.mdpi-res.com/jmmp/jmmp-07-00024-g010-550.jpg?1673952795](https://pub.mdpi-res.com/jmmp/jmmp-07-00024/article_deploy/html/images/jmmp-07-00024-g010-550.jpg?1673952795)) ([https://pub.mdpi-res.com/jmmp/jmmp-07-00024-g011-550.jpg?1673952793](https://pub.mdpi-res.com/jmmp/jmmp-07-00024/article_deploy/html/images/jmmp-07-00024-g011-550.jpg?1673952793)) ([https://pub.mdpi-res.com/jmmp/jmmp-07-00024-g012-550.jpg?1673952784](https://pub.mdpi-res.com/jmmp/jmmp-07-00024/article_deploy/html/images/jmmp-07-00024-g012-550.jpg?1673952784)) ([https://pub.mdpi-res.com/jmmp/jmmp-07-00024-g013-550.jpg?1673952789](https://pub.mdpi-res.com/jmmp/jmmp-07-00024/article_deploy/html/images/jmmp-07-00024-g013-550.jpg?1673952789)) ([https://pub.mdpi-res.com/jmmp/jmmp-07-00024-g014-550.jpg?1673952790](https://pub.mdpi-res.com/jmmp/jmmp-07-00024/article_deploy/html/images/jmmp-07-00024-g014-550.jpg?1673952790)) ([https://pub.mdpi-res.com/jmmp/jmmp-07-00024-g015-550.jpg?1673952786](https://pub.mdpi-res.com/jmmp/jmmp-07-00024/article_deploy/html/images/jmmp-07-00024-g015-550.jpg?1673952786)) ([https://pub.mdpi-res.com/jmmp/jmmp-07-00024-g016-550.jpg?1673952789](https://pub.mdpi-res.com/jmmp/jmmp-07-00024/article_deploy/html/images/jmmp-07-00024-g016-550.jpg?1673952789)) ([https://pub.mdpi-res.com/jmmp/jmmp-07-00024-g017-550.jpg?1673952783](https://pub.mdpi-res.com/jmmp/jmmp-07-00024/article_deploy/html/images/jmmp-07-00024-g017-550.jpg?1673952783)) ([https://pub.mdpi-res.com/jmmp/jmmp-07-00024-g019-550.jpg?1673952780](https://pub.mdpi-res.com/jmmp/jmmp-07-00024/article_deploy/html/images/jmmp-07-00024-g019-550.jpg?1673952780)) ([https://pub.mdpi-res.com/jmmp/jmmp-07-00024-g020-550.jpg?1673952782](https://pub.mdpi-res.com/jmmp/jmmp-07-00024/article_deploy/html/images/jmmp-07-00024-g020-550.jpg?1673952782))

Open Access Article 16 pages, 10062 KIB (2504-4494/7/1/23/pdf?version=1674983561)

Modelling of Surface Roughness in Honing Processes by Using Fuzzy Artificial Neural Networks ((2504-4494/7/1/23)

by  Irene Buj-Corral (https://sciprofiles.com/profile/448776?utm_source=mdpi.com&utm_medium=website&utm_campaign=avatar_name),
 Piotr Sender (https://sciprofiles.com/profile/1722734?utm_source=mdpi.com&utm_medium=website&utm_campaign=avatar_name) and
 Carmelo J. Luis-Pérez (https://sciprofiles.com/profile/208561?utm_source=mdpi.com&utm_medium=website&utm_campaign=avatar_name)

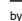



J. Manuf. Mater. Process. **2023**, *7*(1), 23; <https://doi.org/10.3390/jmmp7010023> (<https://doi.org/10.3390/jmmp7010023>) - 15 Jan 2023
Cited by 1 ((2504-4494/7/1/23#metrics)) | Viewed by 1502
Abstract Honing processes are abrasive machining processes which are commonly employed to improve the surface of manufactured parts such as hydraulic or combustion engine cylinders. These processes can be employed to obtain a cross-hatched pattern on the internal surfaces of cylinders. In this present [..] [Read more](#).
(This article belongs to the Special Issue [Advances in Precision Machining Processes](#) ([/journal/jmmp/special_issues/precision_machining_processes](#)))

Show Figures

(https://pub.mdpi-res.com/jmmp/jmmp-07-00023/article_deploy/html/images/jmmp-07-00023-g001-550.jpg?1674983641) ([https://pub.mdpi-res.com/jmmp/jmmp-07-00023-g002-550.jpg?1674983640](https://pub.mdpi-res.com/jmmp/jmmp-07-00023/article_deploy/html/images/jmmp-07-00023-g002-550.jpg?1674983640)) ([https://pub.mdpi-res.com/jmmp/jmmp-07-00023-g003-550.jpg?1674983647](https://pub.mdpi-res.com/jmmp/jmmp-07-00023/article_deploy/html/images/jmmp-07-00023-g003-550.jpg?1674983647)) ([https://pub.mdpi-res.com/jmmp/jmmp-07-00023-g004-550.jpg?1674983644](https://pub.mdpi-res.com/jmmp/jmmp-07-00023/article_deploy/html/images/jmmp-07-00023-g004-550.jpg?1674983644)) ([https://pub.mdpi-res.com/jmmp/jmmp-07-00023-g005-550.jpg?1674983641](https://pub.mdpi-res.com/jmmp/jmmp-07-00023/article_deploy/html/images/jmmp-07-00023-g005-550.jpg?1674983641)) ([https://pub.mdpi-res.com/jmmp/jmmp-07-00023-g006-550.jpg?1674983652](https://pub.mdpi-res.com/jmmp/jmmp-07-00023/article_deploy/html/images/jmmp-07-00023-g006-550.jpg?1674983652)) ([https://pub.mdpi-res.com/jmmp/jmmp-07-00023-g007b-550.jpg?1674983646](https://pub.mdpi-res.com/jmmp/jmmp-07-00023/article_deploy/html/images/jmmp-07-00023-g007b-550.jpg?1674983646)) ([https://pub.mdpi-res.com/jmmp/jmmp-07-00023-g008-550.jpg?1674983642](https://pub.mdpi-res.com/jmmp/jmmp-07-00023/article_deploy/html/images/jmmp-07-00023-g008-550.jpg?1674983642)) ([https://pub.mdpi-res.com/jmmp/jmmp-07-00023-g010-550.jpg?1674983642](https://pub.mdpi-res.com/jmmp/jmmp-07-00023/article_deploy/html/images/jmmp-07-00023-g010-550.jpg?1674983642)) ([https://pub.mdpi-res.com/jmmp/jmmp-07-00023-g011a-550.jpg?1674983650](https://pub.mdpi-res.com/jmmp/jmmp-07-00023/article_deploy/html/images/jmmp-07-00023-g011a-550.jpg?1674983650)) ([https://pub.mdpi-res.com/jmmp/jmmp-07-00023-g011b-550.jpg?1674983658](https://pub.mdpi-res.com/jmmp/jmmp-07-00023/article_deploy/html/images/jmmp-07-00023-g011b-550.jpg?1674983658)) ([https://pub.mdpi-res.com/jmmp/jmmp-07-00023-g012-550.jpg?1674983644](https://pub.mdpi-res.com/jmmp/jmmp-07-00023/article_deploy/html/images/jmmp-07-00023-g012-550.jpg?1674983644)) (<https://pub.mdpi-res.com/jmmp/jmmp-07-00023-g013-550.jpg?1674983643>) (<https://pub.mdpi-res.com/jmmp/jmmp-07-00023-g014-550.jpg?1674983647>) (<https://pub.mdpi-res.com/jmmp/jmmp-07-00023-g015-550.jpg?1674983641>) (<https://pub.mdpi-res.com/jmmp/jmmp-07-00023-g016-550.jpg?1674983653>) ([https://pub.mdpi-res.com/jmmp/jmmp-07-00023-g017-550.jpg?1674983643](https://pub.mdpi-res.com/jmmp/jmmp-07-00023/article_deploy/html/images/jmmp-07-00023-g017-550.jpg?1674983643))

Open Access Article 16 pages, 5192 KIB (2504-4494/7/1/22/pdf?version=1682487887)

Multi-Response Optimization of Ti6Al4V Support Structures for Laser Powder Bed Fusion Systems ((2504-4494/7/1/22)

by  Antonios Dimopoulos (https://sciprofiles.com/profile/2527403?utm_source=mdpi.com&utm_medium=website&utm_campaign=avatar_name),
 Ilias Zournatzis (https://sciprofiles.com/profile/author/T0tVTWJIWEcyM0VmbEc3cG02MDFYWTVseTnk5MmTk80MHVEVTg5bEwrcz0=?utm_source=mdpi.com&utm_medium=website&utm_campaign=avatar_name),
 Tai-Han Gan (https://sciprofiles.com/profile/298628?utm_source=mdpi.com&utm_medium=website&utm_campaign=avatar_name) and
 Panagiotis Chatzarakos (https://sciprofiles.com/profile/author/NGZtR0tH0UkrdTRGOGEmUmkWUWLU1IDNYY5RKFXeYnMrVe0WTh6M1ZvRT0=?utm_source=mdpi.com&utm_medium=website&utm_campaign=avatar_name)

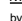


J. Manuf. Mater. Process. **2023**, *7*(1), 22; <https://doi.org/10.3390/jmmp7010022> (<https://doi.org/10.3390/jmmp7010022>) - 13 Jan 2023
Cited by 4 ((2504-4494/7/1/22#metrics)) | Viewed by 2246 | [Correction](#) ((2504-4494/7/3/85))
Abstract Laser Powder Bed Fusion (LPBF) is one of the most commonly used and rapidly developing metal Additive Manufacturing (AM) technologies for producing optimized geometries, complex features, and lightweight components, in contrast to traditional manufacturing, which limits those characteristics. However, this technology faces difficulties [..] [Read more](#).
(This article belongs to the Topic [Additive Manufacturing: Design, Opportunities, and Applications](#) ([Topics/Additive_Manufacturing_2](#)))

Show Figures

(https://pub.mdpi-res.com/jmmp/jmmp-07-00022/article_deploy/html/images/jmmp-07-00022-g001-550.jpg?1682487973) ([https://pub.mdpi-res.com/jmmp/jmmp-07-00022-g002-550.jpg?1682487976](https://pub.mdpi-res.com/jmmp/jmmp-07-00022/article_deploy/html/images/jmmp-07-00022-g002-550.jpg?1682487976)) ([https://pub.mdpi-res.com/jmmp/jmmp-07-00022-g003-550.jpg?1682487975](https://pub.mdpi-res.com/jmmp/jmmp-07-00022/article_deploy/html/images/jmmp-07-00022-g003-550.jpg?1682487975)) ([https://pub.mdpi-res.com/jmmp/jmmp-07-00022-g004-550.jpg?1682487981](https://pub.mdpi-res.com/jmmp/jmmp-07-00022/article_deploy/html/images/jmmp-07-00022-g004-550.jpg?1682487981)) ([https://pub.mdpi-res.com/jmmp/jmmp-07-00022-g005-550.jpg?1682487977](https://pub.mdpi-res.com/jmmp/jmmp-07-00022/article_deploy/html/images/jmmp-07-00022-g005-550.jpg?1682487977)) ([https://pub.mdpi-res.com/jmmp/jmmp-07-00022-g006-550.jpg?1682487987](https://pub.mdpi-res.com/jmmp/jmmp-07-00022/article_deploy/html/images/jmmp-07-00022-g006-550.jpg?1682487987)) ([https://pub.mdpi-res.com/jmmp/jmmp-07-00022-g007-550.jpg?1682487970](https://pub.mdpi-res.com/jmmp/jmmp-07-00022/article_deploy/html/images/jmmp-07-00022-g007-550.jpg?1682487970)) ([https://pub.mdpi-res.com/jmmp/jmmp-07-00022-g008-550.jpg?1682487984](https://pub.mdpi-res.com/jmmp/jmmp-07-00022/article_deploy/html/images/jmmp-07-00022-g008-550.jpg?1682487984)) ([https://pub.mdpi-res.com/jmmp/jmmp-07-00022-g009-550.jpg?1682487982](https://pub.mdpi-res.com/jmmp/jmmp-07-00022/article_deploy/html/images/jmmp-07-00022-g009-550.jpg?1682487982)) (<https://pub.mdpi-res.com/jmmp/jmmp-07-00022-g010-550.jpg?1682487972>) (<https://pub.mdpi-res.com/jmmp/jmmp-07-00022-g011-550.jpg?1682487980>) ([https://pub.mdpi-res.com/jmmp/jmmp-07-00022-g012-550.jpg?1682487986](https://pub.mdpi-res.com/jmmp/jmmp-07-00022/article_deploy/html/images/jmmp-07-00022-g012-550.jpg?1682487986))

Open Access Article 17 pages, 20717 KIB (2504-4494/7/1/21/pdf?version=1673348061)

Three-Body Abrasive Wear-Resistance Characteristics of a 27Cr-Based 3V-3Mo-3W-3Co Multicomponent White Cast Iron with Different Ti Additions ((2504-4494/7/1/21)

by  Riki Hendra Purba (https://sciprofiles.com/profile/2080788?utm_source=mdpi.com&utm_medium=website&utm_campaign=avatar_name),
 Kazumichi Shimizu (https://sciprofiles.com/profile/1681615?utm_source=mdpi.com&utm_medium=website&utm_campaign=avatar_name) and
 Kenta Kusumoto (https://sciprofiles.com/profile/2547952?utm_source=mdpi.com&utm_medium=website&utm_campaign=avatar_name)

J. Manuf. Mater. Process. **2023**, *7*(1), 21; <https://doi.org/10.3390/jmmp7010021> (<https://doi.org/10.3390/jmmp7010021>) - 10 Jan 2023
Viewed by 1425
Abstract A multicomponent white cast iron containing 5 wt.% each of Cr, V, Mo, W, and Co (MWC) is known to have excellent wear-resistance properties due to the precipitation of some very hard carbides, such as MC, M₂C, and M₇C [..] [Read more](#).
[Show Figures](#)

https://pub.mdpi-res.com/jmmp/jmmp-07-00021/article_deploy/html/images/jmmp-07-00021-g001-550.jpg?1673348145) (https://pub.mdpi-res.com/jmmp/jmmp-07-00021/article_deploy/html/images/jmmp-07-00021-g002-550.jpg?1673348151) (https://pub.mdpi-res.com/jmmp/jmmp-07-00021/article_deploy/html/images/jmmp-07-00021-g003-550.jpg?1673348158) (https://pub.mdpi-res.com/jmmp/jmmp-07-00021/article_deploy/html/images/jmmp-07-00021-g004-550.jpg?1673348163) (https://pub.mdpi-res.com/jmmp/jmmp-07-00021/article_deploy/html/images/jmmp-07-00021-g005-550.jpg?1673348164) (https://pub.mdpi-res.com/jmmp/jmmp-07-00021/article_deploy/html/images/jmmp-07-00021-g006-550.jpg?1673348165) (https://pub.mdpi-res.com/jmmp/jmmp-07-00021/article_deploy/html/images/jmmp-07-00021-g007-550.jpg?1673348166) (https://pub.mdpi-res.com/jmmp/jmmp-07-00021/article_deploy/html/images/jmmp-07-00021-g008-550.jpg?1673348145) (https://pub.mdpi-res.com/jmmp/jmmp-07-00021/article_deploy/html/images/jmmp-07-00021-g009-550.jpg?1673348146) (https://pub.mdpi-res.com/jmmp/jmmp-07-00021/article_deploy/html/images/jmmp-07-00021-g010-550.jpg?1673348168) (https://pub.mdpi-res.com/jmmp/jmmp-07-00021/article_deploy/html/images/jmmp-07-00021-g011-550.jpg?1673348142) (https://pub.mdpi-res.com/jmmp/jmmp-07-00021/article_deploy/html/images/jmmp-07-00021-g012-550.jpg?1673348171) ([https://pub.mdpi-res.com/jmmp/jmmp-07-00021-g013-550.jpg?1673348148](https://pub.mdpi-res.com/jmmp/jmmp-07-00021/article_deploy/html/images/jmmp-07-00021-g013-550.jpg?1673348148)) ([https://pub.mdpi-res.com/jmmp/jmmp-07-00021-g014-550.jpg?1673348152](https://pub.mdpi-res.com/jmmp/jmmp-07-00021/article_deploy/html/images/jmmp-07-00021-g014-550.jpg?1673348152))

Open Access Article 15 pages, 8785 KiB (2504-4494/7/1/20/pdf?version=1673327468)

Image Analysis Based Evaluation of Print Quality for Inkjet Printed Structures (2504-4494/7/1/20)

by

- Tim Horter (https://sciprofiles.com/profile/author/MxNdUFMR1p5N2JwUIB5RDBvdGtuaE14RC9gSVRNVGjSVHFUT2R5czdQST0=?utm_source=mdpi.com&utm_medium=website&utm_campaign=avatar_name)
 - Holger Ruehl (https://sciprofiles.com/profile/2639133?utm_source=mdpi.com&utm_medium=website&utm_campaign=avatar_name).
 - Wenqi Yang (https://sciprofiles.com/profile/2653371?utm_source=mdpi.com&utm_medium=website&utm_campaign=avatar_name).
 - Yu-Sheng Chiang (https://sciprofiles.com/profile/author/dEZSbFdWbC9sd01Cc2dwZjNnMVU5MU23V0s2SUjPtbHjUVnITV3V0d0duaz0=?utm_source=mdpi.com&utm_medium=website&utm_campaign=avatar_name)
 - Kerstin Glaeser (https://sciprofiles.com/profile/2615784?utm_source=mdpi.com&utm_medium=website&utm_campaign=avatar_name) and
 - André Zimmermann (https://sciprofiles.com/profile/424415?utm_source=mdpi.com&utm_medium=website&utm_campaign=avatar_name)
- J. Manuf. Mater. Process.* **2023**, *7*(1), 20; <https://doi.org/10.3390/jmmp7010020> (<https://doi.org/10.3390/jmmp7010020>) - 10 Jan 2023
- Cited by 1 (2504-4494/7/1/20#metrics) | Viewed by 2260

Abstract Inkjet printing for printed electronics is a growing market due to its advantages, including scalability, various usable materials and its digital, pixel based layout design. An important quality factor is the wetting of the ink on the substrate. This article proposes a workflow [...] [Read more](#).
(This article belongs to the Topic [Modern Technologies and Manufacturing Systems, 2nd Volume](#) ([/topics/modern_technologies_manufacturing_II](#)))

Show Figures

(https://pub.mdpi-res.com/jmmp/jmmp-07-00020/article_deploy/html/images/jmmp-07-00020-g001-550.jpg?1673327557) (https://pub.mdpi-res.com/jmmp/jmmp-07-00020/article_deploy/html/images/jmmp-07-00020-g002-550.jpg?1673327547) (https://pub.mdpi-res.com/jmmp/jmmp-07-00020/article_deploy/html/images/jmmp-07-00020-g003-550.jpg?1673327546) (https://pub.mdpi-res.com/jmmp/jmmp-07-00020/article_deploy/html/images/jmmp-07-00020-g004-550.jpg?1673327556) (https://pub.mdpi-res.com/jmmp/jmmp-07-00020/article_deploy/html/images/jmmp-07-00020-g005-550.jpg?1673327554) (https://pub.mdpi-res.com/jmmp/jmmp-07-00020/article_deploy/html/images/jmmp-07-00020-g006-550.jpg?1673327544) (https://pub.mdpi-res.com/jmmp/jmmp-07-00020/article_deploy/html/images/jmmp-07-00020-g007-550.jpg?1673327556) (<https://pub.mdpi-res.com/jmmp/jmmp-07-00020-g008-550.jpg?1673327553>) ([https://pub.mdpi-res.com/jmmp/jmmp-07-00020-g009-550.jpg?1673327549](https://pub.mdpi-res.com/jmmp/jmmp-07-00020/article_deploy/html/images/jmmp-07-00020-g009-550.jpg?1673327549)) ([https://pub.mdpi-res.com/jmmp/jmmp-07-00020-g010-550.jpg?1673327551](https://pub.mdpi-res.com/jmmp/jmmp-07-00020/article_deploy/html/images/jmmp-07-00020-g010-550.jpg?1673327551)) ([https://pub.mdpi-res.com/jmmp/jmmp-07-00020-g011-550.jpg?1673327543](https://pub.mdpi-res.com/jmmp/jmmp-07-00020/article_deploy/html/images/jmmp-07-00020-g011-550.jpg?1673327543)) ([https://pub.mdpi-res.com/jmmp/jmmp-07-00020-g012-550.jpg?1673327548](https://pub.mdpi-res.com/jmmp/jmmp-07-00020/article_deploy/html/images/jmmp-07-00020-g012-550.jpg?1673327548)) (https://pub.mdpi-res.com/jmmp/jmmp-07-00020/article_deploy/html/images/jmmp-07-00020-g013-550.jpg?1673327560)

Open Access Article 18 pages, 8529 KiB (2504-4494/7/1/19/pdf?version=1674897946)

Influence of the Process Parameters on the Properties of Cu-Cu Ultrasonic Welds (2504-4494/7/1/19)

- Koen Faes (https://sciprofiles.com/profile/632701?utm_source=mdpi.com&utm_medium=website&utm_campaign=avatar_name).
 - Rafael Nunes (https://sciprofiles.com/profile/1891104?utm_source=mdpi.com&utm_medium=website&utm_campaign=avatar_name).
 - Sylvia De Meester (https://sciprofiles.com/profile/author/bbHGRkxMmdQTQmlQbFvVWE9WQVN4OXNYUiz3pJcGtoZmozanpNUC8zWT0=?utm_source=mdpi.com&utm_medium=website&utm_campaign=avatar_name)
 - Wim De Waele (https://sciprofiles.com/profile/434583?utm_source=mdpi.com&utm_medium=website&utm_campaign=avatar_name).
 - Felice Rubino (https://sciprofiles.com/profile/183277?utm_source=mdpi.com&utm_medium=website&utm_campaign=avatar_name) and
 - Pierpaolo Carlone (https://sciprofiles.com/profile/183020?utm_source=mdpi.com&utm_medium=website&utm_campaign=avatar_name)
- J. Manuf. Mater. Process.* **2023**, *7*(1), 19; <https://doi.org/10.3390/jmmp7010019> (<https://doi.org/10.3390/jmmp7010019>) - 07 Jan 2023
- Cited by 4 (2504-4494/7/1/19#metrics) | Viewed by 1778

Abstract Ultrasonic welding (USW) is a solid-state welding process based on the application of high frequency vibration energy to the workpiece to produce the internal friction between the faying surface and the local heat generation required to promote the joining. The short welding time [...] [Read more](#).
(This article belongs to the Special Issue [Advances in Welding Technology I](#) ([/journal/jmmp/special_issues/welding_tech](#)))

Show Figures

(https://pub.mdpi-res.com/jmmp/jmmp-07-00019/article_deploy/html/images/jmmp-07-00019-g001-550.jpg?1674898043) (https://pub.mdpi-res.com/jmmp/jmmp-07-00019/article_deploy/html/images/jmmp-07-00019-g002-550.jpg?1674898027) (https://pub.mdpi-res.com/jmmp/jmmp-07-00019/article_deploy/html/images/jmmp-07-00019-g003-550.jpg?1674898018) (https://pub.mdpi-res.com/jmmp/jmmp-07-00019/article_deploy/html/images/jmmp-07-00019-g004-550.jpg?1674898025) ([https://pub.mdpi-res.com/jmmp/jmmp-07-00019-g005-550.jpg?1674898040](https://pub.mdpi-res.com/jmmp/jmmp-07-00019/article_deploy/html/images/jmmp-07-00019-g005-550.jpg?1674898040)) ([https://pub.mdpi-res.com/jmmp/jmmp-07-00019-g006-550.jpg?1674898019](https://pub.mdpi-res.com/jmmp/jmmp-07-00019/article_deploy/html/images/jmmp-07-00019-g006-550.jpg?1674898019)) (https://pub.mdpi-res.com/jmmp/jmmp-07-00019/article_deploy/html/images/jmmp-07-00019-g007-550.jpg?1674898021) (https://pub.mdpi-res.com/jmmp/jmmp-07-00019/article_deploy/html/images/jmmp-07-00019-g008-550.jpg?1674898039) ([https://pub.mdpi-res.com/jmmp/jmmp-07-00019-g009-550.jpg?1674898042](https://pub.mdpi-res.com/jmmp/jmmp-07-00019/article_deploy/html/images/jmmp-07-00019-g009-550.jpg?1674898042)) ([https://pub.mdpi-res.com/jmmp/jmmp-07-00019-g010-550.jpg?1674898030](https://pub.mdpi-res.com/jmmp/jmmp-07-00019/article_deploy/html/images/jmmp-07-00019-g010-550.jpg?1674898030)) ([https://pub.mdpi-res.com/jmmp/jmmp-07-00019-g011-550.jpg?1674898045](https://pub.mdpi-res.com/jmmp/jmmp-07-00019/article_deploy/html/images/jmmp-07-00019-g011-550.jpg?1674898045)) ([https://pub.mdpi-res.com/jmmp/jmmp-07-00019-g012-550.jpg?1674898036](https://pub.mdpi-res.com/jmmp/jmmp-07-00019/article_deploy/html/images/jmmp-07-00019-g012-550.jpg?1674898036)) ([https://pub.mdpi-res.com/jmmp/jmmp-07-00019-g013-550.jpg?1674898033](https://pub.mdpi-res.com/jmmp/jmmp-07-00019/article_deploy/html/images/jmmp-07-00019-g013-550.jpg?1674898033)) ([https://pub.mdpi-res.com/jmmp/jmmp-07-00019-g014-550.jpg?1674898032](https://pub.mdpi-res.com/jmmp/jmmp-07-00019/article_deploy/html/images/jmmp-07-00019-g014-550.jpg?1674898032)) ([https://pub.mdpi-res.com/jmmp/jmmp-07-00019-g015-550.jpg?1674898025](https://pub.mdpi-res.com/jmmp/jmmp-07-00019/article_deploy/html/images/jmmp-07-00019-g015-550.jpg?1674898025)) ([https://pub.mdpi-res.com/jmmp/jmmp-07-00019-g016-550.jpg?1674898034](https://pub.mdpi-res.com/jmmp/jmmp-07-00019/article_deploy/html/images/jmmp-07-00019-g016-550.jpg?1674898034)) ([https://pub.mdpi-res.com/jmmp/jmmp-07-00019-g017-550.jpg?1674898022](https://pub.mdpi-res.com/jmmp/jmmp-07-00019/article_deploy/html/images/jmmp-07-00019-g017-550.jpg?1674898022)) ([https://pub.mdpi-res.com/jmmp/jmmp-07-00019-g018-550.jpg?1674898044](https://pub.mdpi-res.com/jmmp/jmmp-07-00019/article_deploy/html/images/jmmp-07-00019-g018-550.jpg?1674898044))

Open Access Article 17 pages, 12468 KiB (2504-4494/7/1/18/pdf?version=1673506600)

Evaluation of the Metallurgical Quality of Nodular Cast Iron in the Production Conditions of a Foundry (2504-4494/7/1/18)

by

- Rafal Dwulat (https://sciprofiles.com/profile/author/RUJJaFkrV09aZkK1ZkcZTRQYzY3VUJwQl9Cc21vVFJrZrZM5cE9TOHJ1TT0=?utm_source=mdpi.com&utm_medium=website&utm_campaign=avatar_name)
 - Krzysztof Janerka (https://sciprofiles.com/profile/2363746?utm_source=mdpi.com&utm_medium=website&utm_campaign=avatar_name)
- J. Manuf. Mater. Process.* **2023**, *7*(1), 18; <https://doi.org/10.3390/jmmp7010018> (<https://doi.org/10.3390/jmmp7010018>) - 04 Jan 2023
- Cited by 2 (2504-4494/7/1/18#metrics) | Viewed by 1904

Abstract The aim of this research was to determine the factors affecting the metallurgical quality of cast iron during serial production of castings using a campaign cupola and a holding furnace. The problem to be solved, which was to obtain cast iron with the [...] [Read more](#).
(This article belongs to the Topic [Advanced Processes in Metallurgical Technologies](#) ([/topics/metallurgical_technologies](#)))

Show Figures

(https://pub.mdpi-res.com/jmmp/jmmp-07-00018/article_deploy/html/images/jmmp-07-00018-g001-550.jpg?1673506691) ([https://pub.mdpi-res.com/jmmp/jmmp-07-00018-g002-550.jpg?1673506691](https://pub.mdpi-res.com/jmmp/jmmp-07-00018/article_deploy/html/images/jmmp-07-00018-g002-550.jpg?1673506691)) ([https://pub.mdpi-res.com/jmmp/jmmp-07-00018-g003-550.jpg?1673506704](https://pub.mdpi-res.com/jmmp/jmmp-07-00018/article_deploy/html/images/jmmp-07-00018-g003-550.jpg?1673506704)) ([https://pub.mdpi-res.com/jmmp/jmmp-07-00018-g004-550.jpg?1673506703](https://pub.mdpi-res.com/jmmp/jmmp-07-00018/article_deploy/html/images/jmmp-07-00018-g004-550.jpg?1673506703)) ([https://pub.mdpi-res.com/jmmp/jmmp-07-00018-g005a-550.jpg?1673506697](https://pub.mdpi-res.com/jmmp/jmmp-07-00018/article_deploy/html/images/jmmp-07-00018-g005a-550.jpg?1673506697)) ([https://pub.mdpi-res.com/jmmp/jmmp-07-00018-g005b-550.jpg?1673506687](https://pub.mdpi-res.com/jmmp/jmmp-07-00018/article_deploy/html/images/jmmp-07-00018-g005b-550.jpg?1673506687)) ([https://pub.mdpi-res.com/jmmp/jmmp-07-00018-g006-550.jpg?1673506682](https://pub.mdpi-res.com/jmmp/jmmp-07-00018/article_deploy/html/images/jmmp-07-00018-g006-550.jpg?1673506682)) ([https://pub.mdpi-res.com/jmmp/jmmp-07-00018-g007-550.jpg?1673506711](https://pub.mdpi-res.com/jmmp/jmmp-07-00018/article_deploy/html/images/jmmp-07-00018-g007-550.jpg?1673506711)) ([https://pub.mdpi-res.com/jmmp/jmmp-07-00018-g008-550.jpg?1673506705](https://pub.mdpi-res.com/jmmp/jmmp-07-00018/article_deploy/html/images/jmmp-07-00018-g008-550.jpg?1673506705)) ([https://pub.mdpi-res.com/jmmp/jmmp-07-00018-g009-550.jpg?1673506694](https://pub.mdpi-res.com/jmmp/jmmp-07-00018/article_deploy/html/images/jmmp-07-00018-g009-550.jpg?1673506694)) ([https://pub.mdpi-res.com/jmmp/jmmp-07-00018-g010-550.jpg?1673506684](https://pub.mdpi-res.com/jmmp/jmmp-07-00018/article_deploy/html/images/jmmp-07-00018-g010-550.jpg?1673506684)) ([https://pub.mdpi-res.com/jmmp/jmmp-07-00018-g011-550.jpg?1673506689](https://pub.mdpi-res.com/jmmp/jmmp-07-00018/article_deploy/html/images/jmmp-07-00018-g011-550.jpg?1673506689)) ([https://pub.mdpi-res.com/jmmp/jmmp-07-00018-g012-550.jpg?1673506690](https://pub.mdpi-res.com/jmmp/jmmp-07-00018/article_deploy/html/images/jmmp-07-00018-g012-550.jpg?1673506690)) ([https://pub.mdpi-res.com/jmmp/jmmp-07-00018-g013-550.jpg?1673506688](https://pub.mdpi-res.com/jmmp/jmmp-07-00018/article_deploy/html/images/jmmp-07-00018-g013-550.jpg?1673506688)) ([https://pub.mdpi-res.com/jmmp/jmmp-07-00018-g014-550.jpg?1673506712](https://pub.mdpi-res.com/jmmp/jmmp-07-00018/article_deploy/html/images/jmmp-07-00018-g014-550.jpg?1673506712)) (<https://pub.mdpi-res.com/jmmp/jmmp-07-00018-g015-550.jpg?1673506692>)

Open Access Article 18 pages, 432 KiB (2504-4494/7/1/17/pdf?version=1672823477)

An Objective Metallographic Analysis Approach Based on Advanced Image Processing Techniques (2504-4494/7/1/17)

- Xabier Sarrionandia (https://sciprofiles.com/profile/2635223?utm_source=mdpi.com&utm_medium=website&utm_campaign=avatar_name).
- Javier Nieves (https://sciprofiles.com/profile/2143128?utm_source=mdpi.com&utm_medium=website&utm_campaign=avatar_name).
- Benat Bravo (https://sciprofiles.com/profile/217520?utm_source=mdpi.com&utm_medium=website&utm_campaign=avatar_name).
- Iker Pastor-López (https://sciprofiles.com/profile/644900?utm_source=mdpi.com&utm_medium=website&utm_campaign=avatar_name) and

MDPI **Pablo G. Bringas** (https://sciprofiles.com/profile/761751?utm_source=mdpi.com&utm_medium=website&utm_campaign=avatar_name)
J. Manuf. Mater. Process. **2023**, *7*(1), 17; <https://doi.org/10.3390/jmmp7010017> (<https://doi.org/10.3390/jmmp7010017>) - 04 Jan 2023
Cited by 3 (2504-4494/7/1/17#metrics) | Viewed by 3136

Abstract Metallographic analyses of nodular iron casting methods are based on visual comparisons according to measuring standards. Specifically, the microstructure is analyzed in a systematic manner by comparing the extracted image from the microscope to pre-defined image templates. The achieved classifications can be confused, [...] [Read more](#).

(This article belongs to the Topic **Artificial Intelligence in Smart Industrial Diagnostics and Manufacturing** (/topics/Smart_Industrial_Diagnostics_and_Analysis))

► **Show Figures**
(https://pub.mdpi-res.com/jmmp/jmmp-07-00017/article_deploy/html/images/jmmp-07-00017-g001-550.jpg?1672823543) ([https://pub.mdpi-res.com/jmmp/jmmp-07-00017-g002-550.jpg?1672823542](https://pub.mdpi-res.com/jmmp/jmmp-07-00017/article_deploy/html/images/jmmp-07-00017-g002-550.jpg?1672823542)) ([https://pub.mdpi-res.com/jmmp/jmmp-07-00017-g003-550.jpg?1672823542](https://pub.mdpi-res.com/jmmp/jmmp-07-00017/article_deploy/html/images/jmmp-07-00017-g003-550.jpg?1672823542)) ([https://pub.mdpi-res.com/jmmp/jmmp-07-00017-g004-550.jpg?1672823541](https://pub.mdpi-res.com/jmmp/jmmp-07-00017/article_deploy/html/images/jmmp-07-00017-g004-550.jpg?1672823541)) ([https://pub.mdpi-res.com/jmmp/jmmp-07-00017-g005-550.jpg?1672823541](https://pub.mdpi-res.com/jmmp/jmmp-07-00017/article_deploy/html/images/jmmp-07-00017-g005-550.jpg?1672823541)) ([https://pub.mdpi-res.com/jmmp/jmmp-07-00017-g006-550.jpg?1672823543](https://pub.mdpi-res.com/jmmp/jmmp-07-00017/article_deploy/html/images/jmmp-07-00017-g006-550.jpg?1672823543)) ([https://pub.mdpi-res.com/jmmp/jmmp-07-00017-g007-550.jpg?1672823540](https://pub.mdpi-res.com/jmmp/jmmp-07-00017/article_deploy/html/images/jmmp-07-00017-g007-550.jpg?1672823540))

Open Access Article 13 pages, 11816 KIB (2504-4494/7/1/16/pdf?version=1672825987)

An Experimental and Numerical Study on Aluminum Alloy Tailor Heat Treated Blanks (/2504-4494/7/1/16)
by **Rui Pereira** (https://sciprofiles.com/profile/2622756?utm_source=mdpi.com&utm_medium=website&utm_campaign=avatar_name),
Nuno Peixinho (https://sciprofiles.com/profile/2752979?utm_source=mdpi.com&utm_medium=website&utm_campaign=avatar_name),
Vitor Carneiro (https://sciprofiles.com/profile/1044778?utm_source=mdpi.com&utm_medium=website&utm_campaign=avatar_name),
Deifim Soares (https://sciprofiles.com/profile/2358962?utm_source=mdpi.com&utm_medium=website&utm_campaign=avatar_name),
Sara Cortez (https://sciprofiles.com/profile/author/ZDBmTUptbmZZZ0FrZmdRN05LVWxKbmVwU1BINTBkQIBHUuRwaUxtcTl3ND0=?utm_source=mdpi.com&utm_medium=website&utm_campaign=avatar_name)
,
Sérgio L. Costa (https://sciprofiles.com/profile/author/aFd1VEdhWTRHU2wvSm9UWmV2kpbHbTZEamhXN2hYNYVMHZydeHtOFZLUt0=?utm_source=mdpi.com&utm_medium=website&utm_campaign=avatar_o)
and
Vitor Branco (https://sciprofiles.com/profile/author/dG2kL0JXK3ZkZINC0t0RjdF3T9OWHZ30WdwjdE3Mk92YUx3dzZZUT0=?utm_source=mdpi.com&utm_medium=website&utm_campaign=avatar_name)
J. Manuf. Mater. Process. **2023**, *7*(1), 16; <https://doi.org/10.3390/jmmp7010016> (<https://doi.org/10.3390/jmmp7010016>) - 04 Jan 2023
Cited by 1 (2504-4494/7/1/16#metrics) | Viewed by 1474

Abstract Information is presented on the conceptualization, experimental study, and numerical process simulation of tailor heat treated aluminum alloy blanks. This concept is intended to improve the forming behavior of aluminum parts in challenging conditions. The implementation requires precise control of laser heat treatment [...] [Read more](#).

(This article belongs to the Special Issue **Advances in Material Forming** (/journal/jmmp/special_issues/material_forming))

► **Show Figures**
(https://pub.mdpi-res.com/jmmp/jmmp-07-00016/article_deploy/html/images/jmmp-07-00016-g001-550.jpg?1672826063) ([https://pub.mdpi-res.com/jmmp/jmmp-07-00016-g002-550.jpg?1672826062](https://pub.mdpi-res.com/jmmp/jmmp-07-00016/article_deploy/html/images/jmmp-07-00016-g002-550.jpg?1672826062)) ([https://pub.mdpi-res.com/jmmp/jmmp-07-00016-g003-550.jpg?1672826062](https://pub.mdpi-res.com/jmmp/jmmp-07-00016/article_deploy/html/images/jmmp-07-00016-g003-550.jpg?1672826062)) ([https://pub.mdpi-res.com/jmmp/jmmp-07-00016-g004-550.jpg?1672826061](https://pub.mdpi-res.com/jmmp/jmmp-07-00016/article_deploy/html/images/jmmp-07-00016-g004-550.jpg?1672826061)) ([https://pub.mdpi-res.com/jmmp/jmmp-07-00016-g005-550.jpg?1672826057](https://pub.mdpi-res.com/jmmp/jmmp-07-00016/article_deploy/html/images/jmmp-07-00016-g005-550.jpg?1672826057)) ([https://pub.mdpi-res.com/jmmp/jmmp-07-00016-g006-550.jpg?1672826068](https://pub.mdpi-res.com/jmmp/jmmp-07-00016/article_deploy/html/images/jmmp-07-00016-g006-550.jpg?1672826068)) ([https://pub.mdpi-res.com/jmmp/jmmp-07-00016-g007-550.jpg?1672826055](https://pub.mdpi-res.com/jmmp/jmmp-07-00016/article_deploy/html/images/jmmp-07-00016-g007-550.jpg?1672826055)) ([https://pub.mdpi-res.com/jmmp/jmmp-07-00016-g008-550.jpg?1672826066](https://pub.mdpi-res.com/jmmp/jmmp-07-00016/article_deploy/html/images/jmmp-07-00016-g008-550.jpg?1672826066)) ([https://pub.mdpi-res.com/jmmp/jmmp-07-00016-g009-550.jpg?1672826059](https://pub.mdpi-res.com/jmmp/jmmp-07-00016/article_deploy/html/images/jmmp-07-00016-g009-550.jpg?1672826059)) ([https://pub.mdpi-res.com/jmmp/jmmp-07-00016-g010-550.jpg?1672826064](https://pub.mdpi-res.com/jmmp/jmmp-07-00016/article_deploy/html/images/jmmp-07-00016-g010-550.jpg?1672826064)) ([https://pub.mdpi-res.com/jmmp/jmmp-07-00016-g011-550.jpg?1672826058](https://pub.mdpi-res.com/jmmp/jmmp-07-00016/article_deploy/html/images/jmmp-07-00016-g011-550.jpg?1672826058)) ([https://pub.mdpi-res.com/jmmp/jmmp-07-00016-g012-550.jpg?1672826065](https://pub.mdpi-res.com/jmmp/jmmp-07-00016/article_deploy/html/images/jmmp-07-00016-g012-550.jpg?1672826065)) ([https://pub.mdpi-res.com/jmmp/jmmp-07-00016-g013-550.jpg?1672826066](https://pub.mdpi-res.com/jmmp/jmmp-07-00016/article_deploy/html/images/jmmp-07-00016-g013-550.jpg?1672826066))

Open Access Review 17 pages, 1104 KIB (2504-4494/7/1/15/pdf?version=1673506283)

Powder Bed Fusion of Multimaterials (/2504-4494/7/1/15)
by **Thywili Cephas Dzoebewu** (https://sciprofiles.com/profile/1448392?utm_source=mdpi.com&utm_medium=website&utm_campaign=avatar_name) and
Deon de Beer (https://sciprofiles.com/profile/2592374?utm_source=mdpi.com&utm_medium=website&utm_campaign=avatar_name)
J. Manuf. Mater. Process. **2023**, *7*(1), 15; <https://doi.org/10.3390/jmmp7010015> (<https://doi.org/10.3390/jmmp7010015>) - 01 Jan 2023
Cited by 9 (2504-4494/7/1/15#metrics) | Viewed by 1974

Abstract Powder bed fusion (PBF) process has been used successfully to produce 3D structures using single material properties. The current industrial demand is to use the technology to produce 3D structures of multimaterial properties. An electron beam melting (EBM) process has been used to [...] [Read more](#).

► **Show Figures**
(https://pub.mdpi-res.com/jmmp/jmmp-07-00015/article_deploy/html/images/jmmp-07-00015-g001-550.jpg?1673506336) (https://pub.mdpi-res.com/jmmp/jmmp-07-00015/article_deploy/html/images/jmmp-07-00015-g002-550.jpg?1673506337)

Open Access Article 0 pages, 6902 KIB (2504-4494/7/1/14/pdf?version=1704869471)

Friction Resistance of Uncured Carbon/Epoxy Prepregs under Thermoforming Process Conditions: Experiments and Modelling (/2504-4494/7/1/14)
by **David Aveiga** (https://sciprofiles.com/profile/2569106?utm_source=mdpi.com&utm_medium=website&utm_campaign=avatar_name),
David GómeZ (https://sciprofiles.com/profile/1119878?utm_source=mdpi.com&utm_medium=website&utm_campaign=avatar_name),
Davide Mocerino (https://sciprofiles.com/profile/2044448?utm_source=mdpi.com&utm_medium=website&utm_campaign=avatar_name),
Bernardo López-Romano (https://sciprofiles.com/profile/author/aUZPaExxRFINRG9gQ2tSiUvJfSxYpKVEVwzjKpMT1U3Qy9yVSINRRt0=?utm_source=mdpi.com&utm_medium=website&utm_campaign=avatar_o)
and
Carlos González (https://sciprofiles.com/profile/413264?utm_source=mdpi.com&utm_medium=website&utm_campaign=avatar_name)
J. Manuf. Mater. Process. **2023**, *7*(1), 14; <https://doi.org/10.3390/jmmp7010014> (<https://doi.org/10.3390/jmmp7010014>) - 01 Jan 2023
Viewed by 1878

Abstract The numerous prepreg characteristics benefit industries like the aerospace and automotive ones, producing a wide range of high-performance components for primary or secondary applications. Parts production is usually assisted by a thermoforming process in which the prepreg is heated and reshaped employing a [...] [Read more](#).

► **Show Figures**
(https://pub.mdpi-res.com/jmmp/jmmp-07-00014/article_deploy/html/images/jmmp-07-00014-g001-550.jpg?1704869505) ([https://pub.mdpi-res.com/jmmp/jmmp-07-00014-g002a-550.jpg?1704869509](https://pub.mdpi-res.com/jmmp/jmmp-07-00014/article_deploy/html/images/jmmp-07-00014-g002a-550.jpg?1704869509)) ([https://pub.mdpi-res.com/jmmp/jmmp-07-00014-g002b-550.jpg?1704869513](https://pub.mdpi-res.com/jmmp/jmmp-07-00014/article_deploy/html/images/jmmp-07-00014-g002b-550.jpg?1704869513)) ([https://pub.mdpi-res.com/jmmp/jmmp-07-00014-g003-550.jpg?1704869516](https://pub.mdpi-res.com/jmmp/jmmp-07-00014/article_deploy/html/images/jmmp-07-00014-g003-550.jpg?1704869516)) ([https://pub.mdpi-res.com/jmmp/jmmp-07-00014-g004-550.jpg?1704869519](https://pub.mdpi-res.com/jmmp/jmmp-07-00014/article_deploy/html/images/jmmp-07-00014-g004-550.jpg?1704869519)) ([https://pub.mdpi-res.com/jmmp/jmmp-07-00014-g005-550.jpg?1704869523](https://pub.mdpi-res.com/jmmp/jmmp-07-00014/article_deploy/html/images/jmmp-07-00014-g005-550.jpg?1704869523)) ([https://pub.mdpi-res.com/jmmp/jmmp-07-00014-g006-550.jpg?1704869527](https://pub.mdpi-res.com/jmmp/jmmp-07-00014/article_deploy/html/images/jmmp-07-00014-g006-550.jpg?1704869527)) ([https://pub.mdpi-res.com/jmmp/jmmp-07-00014-g007-550.jpg?1704869528](https://pub.mdpi-res.com/jmmp/jmmp-07-00014/article_deploy/html/images/jmmp-07-00014-g007-550.jpg?1704869528)) ([https://pub.mdpi-res.com/jmmp/jmmp-07-00014-g008-550.jpg?1704869530](https://pub.mdpi-res.com/jmmp/jmmp-07-00014/article_deploy/html/images/jmmp-07-00014-g008-550.jpg?1704869530)) ([https://pub.mdpi-res.com/jmmp/jmmp-07-00014-g009-550.jpg?1704869533](https://pub.mdpi-res.com/jmmp/jmmp-07-00014/article_deploy/html/images/jmmp-07-00014-g009-550.jpg?1704869533)) ([https://pub.mdpi-res.com/jmmp/jmmp-07-00014-g010-550.jpg?1704869535](https://pub.mdpi-res.com/jmmp/jmmp-07-00014/article_deploy/html/images/jmmp-07-00014-g010-550.jpg?1704869535))

Open Access Article 15 pages, 60449 KIB (2504-4494/7/1/13/pdf?version=1672400192)

Material Behavior around the FSW/FSP Tool Described by Molecular Dynamics (/2504-4494/7/1/13)
by **Bentejui Medina** (https://sciprofiles.com/profile/2664528?utm_source=mdpi.com&utm_medium=website&utm_campaign=avatar_name) and
Ricardo Fernández (https://sciprofiles.com/profile/1044425?utm_source=mdpi.com&utm_medium=website&utm_campaign=avatar_name)
J. Manuf. Mater. Process. **2023**, *7*(1), 13; <https://doi.org/10.3390/jmmp7010013> (<https://doi.org/10.3390/jmmp7010013>) - 30 Dec 2022
Viewed by 1271

Abstract Friction stir welding and processing (FSW/FSP) involves severe plastic deformation of metals or polymers at high temperature around a rotating tool. The material's flow is usually modelled by FEM using a complex combination of thermomechanical and friction models. However, the description of the [...] [Read more](#).

► **Show Figures**
(https://pub.mdpi-res.com/jmmp/jmmp-07-00013/article_deploy/html/images/jmmp-07-00013-g001-550.jpg?1672400265) ([https://pub.mdpi-res.com/jmmp/jmmp-07-00013-g002a-550.jpg?1672400275](https://pub.mdpi-res.com/jmmp/jmmp-07-00013/article_deploy/html/images/jmmp-07-00013-g002a-550.jpg?1672400275)) ([https://pub.mdpi-res.com/jmmp/jmmp-07-00013-g002b-550.jpg?1672400280](https://pub.mdpi-res.com/jmmp/jmmp-07-00013/article_deploy/html/images/jmmp-07-00013-g002b-550.jpg?1672400280)) ([https://pub.mdpi-res.com/jmmp/jmmp-07-00013-g003a-550.jpg?1672400278](https://pub.mdpi-res.com/jmmp/jmmp-07-00013/article_deploy/html/images/jmmp-07-00013-g003a-550.jpg?1672400278)) ([https://pub.mdpi-res.com/jmmp/jmmp-07-00013-g003b-550.jpg?1672400261](https://pub.mdpi-res.com/jmmp/jmmp-07-00013/article_deploy/html/images/jmmp-07-00013-g003b-550.jpg?1672400261)) ([https://pub.mdpi-res.com/jmmp/jmmp-07-00013-g004a-550.jpg?1672400270](https://pub.mdpi-res.com/jmmp/jmmp-07-00013/article_deploy/html/images/jmmp-07-00013-g004a-550.jpg?1672400270)) ([https://pub.mdpi-res.com/jmmp/jmmp-07-00013-g004b-550.jpg?1672400264](https://pub.mdpi-res.com/jmmp/jmmp-07-00013/article_deploy/html/images/jmmp-07-00013-g004b-550.jpg?1672400264)) ([https://pub.mdpi-res.com/jmmp/jmmp-07-00013-g005-550.jpg?1672400267](https://pub.mdpi-res.com/jmmp/jmmp-07-00013/article_deploy/html/images/jmmp-07-00013-g005-550.jpg?1672400267)) ([https://pub.mdpi-res.com/jmmp/jmmp-07-00013-g006-550.jpg?1672400282](https://pub.mdpi-res.com/jmmp/jmmp-07-00013/article_deploy/html/images/jmmp-07-00013-g006-550.jpg?1672400282))

Open Access Article 12 pages, 4350 KIB (2504-4494/7/1/12/pdf?version=1672298954)

Tube Joining by a Sheet Flange Connection (/2504-4494/7/1/12)
by **Rafael M. Afonso** (https://sciprofiles.com/profile/1799741?utm_source=mdpi.com&utm_medium=website&utm_campaign=avatar_name) and
Luis M. Alves (https://sciprofiles.com/profile/902248?utm_source=mdpi.com&utm_medium=website&utm_campaign=avatar_name)
J. Manuf. Mater. Process. **2023**, *7*(1), 12; <https://doi.org/10.3390/jmmp7010012> (<https://doi.org/10.3390/jmmp7010012>) - 29 Dec 2022
Viewed by 1620

Abstract Joining of tubes to tubes by means of plastic deformation at ambient temperature allows one to solve the main limitations produced by the necessity of joining thin-walled tubes of low-to-medium diameter size made from materials that are not suitable to be welded and/or [...] [Read more](#).

(This article belongs to the Special Issue **Joining of Unweldable Materials: Concepts, Techniques and Processes** (/journal/jmmp/special_issues

(joining unweldable materials))

MDPI

Show Figures

(https://pub.mdpi-res.com/jmmp/jmmp-07-00012/article_deploy/html/images/jmmp-07-00012-g001-550.jpg?1672299026) (https://pub.mdpi-res.com/jmmp/jmmp-07-00012/article_deploy/html/images/jmmp-07-00012-g002-550.jpg?1672299028) (https://pub.mdpi-res.com/jmmp/jmmp-07-00012/article_deploy/html/images/jmmp-07-00012-g003-550.jpg?1672299027) (https://pub.mdpi-res.com/jmmp/jmmp-07-00012/article_deploy/html/images/jmmp-07-00012-g004-550.jpg?1672299018) (https://pub.mdpi-res.com/jmmp/jmmp-07-00012/article_deploy/html/images/jmmp-07-00012-g005-550.jpg?1672299031) (https://pub.mdpi-res.com/jmmp/jmmp-07-00012/article_deploy/html/images/jmmp-07-00012-g006-550.jpg?1672299019) (https://pub.mdpi-res.com/jmmp/jmmp-07-00012/article_deploy/html/images/jmmp-07-00012-g007-550.jpg?1672299030) (https://pub.mdpi-res.com/jmmp/jmmp-07-00012/article_deploy/html/images/jmmp-07-00012-g008-550.jpg?1672299023) (https://pub.mdpi-res.com/jmmp/jmmp-07-00012/article_deploy/html/images/jmmp-07-00012-g009-550.jpg?1672299025) (https://pub.mdpi-res.com/jmmp/jmmp-07-00012/article_deploy/html/images/jmmp-07-00012-g010-550.jpg?1672299024) (https://pub.mdpi-res.com/jmmp/jmmp-07-00012/article_deploy/html/images/jmmp-07-00012-g011-550.jpg?1672299032) (https://pub.mdpi-res.com/jmmp/jmmp-07-00012/article_deploy/html/images/jmmp-07-00012-g012-550.jpg?1672299020)

Open Access Article

22 pages, 10323 KIB (/2504-4494/7/1/9/pdf?version=1672222276)

Convexity and Surface Quality Enhanced Curved Slicing for Support-Free Multi-Axis Fabrication (2504-4494/7/1/9)

by

- Don Pubudu Vishwana Joseph Jayakody (https://sciprofiles.com/profile/2609498?utm_source=mdpi.com&utm_medium=website&utm_campaign=avatar_name).
 - Tak Yu Lau (https://sciprofiles.com/profile/author/SD8t1ZPQjISQWpYRG1WTFHaZRCUErhTzcxGxMMEQvWmxVTVVGCmhCWT0e?utm_source=mdpi.com&utm_medium=website&utm_campaign=avatar_name).
 - Ravindra Stephen Goonetilleke (https://sciprofiles.com/profile/2288109?utm_source=mdpi.com&utm_medium=website&utm_campaign=avatar_name) and Kai Tang (https://sciprofiles.com/profile/1308946?utm_source=mdpi.com&utm_medium=website&utm_campaign=avatar_name)
- J. Manuf. Mater. Process. 2023, 7(1), 9; https://doi.org/10.3390/jmmp7010009 (https://doi.org/10.3390/jmmp7010009) - 28 Dec 2022

Cited by 1 (2504-4494/7/1/9#metrics) | Viewed by 1767

Abstract In multi-axis fused deposition modeling (FDM) printing systems, support-free curved layer fabrication is realized by continuous transition of the printer nozzle orientation. However, the ability to print 3D models with complex geometric (e.g., high overhang) and topological (e.g., high genus) features is often [...] [Read more](#). (This article belongs to the Special Issue [Advances in Multi-Axis Machining](#) (./journal/jmmp/special_issues/multi-axis_machining))

Show Figures

(https://pub.mdpi-res.com/jmmp/jmmp-07-00009/article_deploy/html/images/jmmp-07-00009-g001-550.jpg?1672222361) (https://pub.mdpi-res.com/jmmp/jmmp-07-00009/article_deploy/html/images/jmmp-07-00009-g002-550.jpg?1672222356) (https://pub.mdpi-res.com/jmmp/jmmp-07-00009/article_deploy/html/images/jmmp-07-00009-g003-550.jpg?1672222365) (https://pub.mdpi-res.com/jmmp/jmmp-07-00009/article_deploy/html/images/jmmp-07-00009-g004-550.jpg?1672222363) (https://pub.mdpi-res.com/jmmp/jmmp-07-00009/article_deploy/html/images/jmmp-07-00009-g005-550.jpg?1672222354) (https://pub.mdpi-res.com/jmmp/jmmp-07-00009/article_deploy/html/images/jmmp-07-00009-g006-550.jpg?1672222342) (https://pub.mdpi-res.com/jmmp/jmmp-07-00009/article_deploy/html/images/jmmp-07-00009-g007a-550.jpg?1672222363) (https://pub.mdpi-res.com/jmmp/jmmp-07-00009/article_deploy/html/images/jmmp-07-00009-g007b-550.jpg?1672222343) (https://pub.mdpi-res.com/jmmp/jmmp-07-00009/article_deploy/html/images/jmmp-07-00009-g008-550.jpg?1672222353) (https://pub.mdpi-res.com/jmmp/jmmp-07-00009/article_deploy/html/images/jmmp-07-00009-g009-550.jpg?1672222360) (https://pub.mdpi-res.com/jmmp/jmmp-07-00009/article_deploy/html/images/jmmp-07-00009-g010-550.jpg?1672222346) (https://pub.mdpi-res.com/jmmp/jmmp-07-00009/article_deploy/html/images/jmmp-07-00009-g011-550.jpg?1672222365) (https://pub.mdpi-res.com/jmmp/jmmp-07-00009/article_deploy/html/images/jmmp-07-00009-g012-550.jpg?1672222367) (https://pub.mdpi-res.com/jmmp/jmmp-07-00009/article_deploy/html/images/jmmp-07-00009-g013-550.jpg?1672222358) (https://pub.mdpi-res.com/jmmp/jmmp-07-00009/article_deploy/html/images/jmmp-07-00009-g014-550.jpg?1672222347) (https://pub.mdpi-res.com/jmmp/jmmp-07-00009/article_deploy/html/images/jmmp-07-00009-g015-550.jpg?1672222349) (https://pub.mdpi-res.com/jmmp/jmmp-07-00009/article_deploy/html/images/jmmp-07-00009-g016-550.jpg?1672222344) (https://pub.mdpi-res.com/jmmp/jmmp-07-00009/article_deploy/html/images/jmmp-07-00009-g017-550.jpg?1672222343) (https://pub.mdpi-res.com/jmmp/jmmp-07-00009/article_deploy/html/images/jmmp-07-00009-g018-550.jpg?1672222351) (https://pub.mdpi-res.com/jmmp/jmmp-07-00009/article_deploy/html/images/jmmp-07-00009-g019-550.jpg?1672222341) (https://pub.mdpi-res.com/jmmp/jmmp-07-00009/article_deploy/html/images/jmmp-07-00009-g020-550.jpg?1672222350) (https://pub.mdpi-res.com/jmmp/jmmp-07-00009/article_deploy/html/images/jmmp-07-00009-g022-550.jpg?1672222362)

Open Access Article

26 pages, 2773 KIB (/2504-4494/7/1/8/pdf?version=1672278071)

Additive Manufacturing of Slow-Moving Automotive Spare Parts: A Supply Chain Cost Assessment (2504-4494/7/1/8)

by

- Levin Ahlswell (https://sciprofiles.com/profile/author/cmVNU01KMfHkEakg3bm4zbIVSN0eUIIR2hkaUx5ZGN2Y1kxaUSKVHVQOD0e?utm_source=mdpi.com&utm_medium=website&utm_campaign=avatar_name).
 - Didar Jalal (https://sciprofiles.com/profile/2609134?utm_source=mdpi.com&utm_medium=website&utm_campaign=avatar_name).
 - Siavash H. Khajavi (https://sciprofiles.com/profile/1074179?utm_source=mdpi.com&utm_medium=website&utm_campaign=avatar_name).
 - Patrik Jonsson (https://sciprofiles.com/profile/author/eisyT3iUINQci9vdfRzUUNmdH2JUFhKZ2kzU0s5V1E221BMa2dzSlhdST0e?utm_source=mdpi.com&utm_medium=website&utm_campaign=avatar_name)
- and
- Jan Holmström (https://sciprofiles.com/profile/1112302?utm_source=mdpi.com&utm_medium=website&utm_campaign=avatar_name)
- J. Manuf. Mater. Process. 2023, 7(1), 8; https://doi.org/10.3390/jmmp7010008 (https://doi.org/10.3390/jmmp7010008) - 28 Dec 2022

Cited by 2 (2504-4494/7/1/8#metrics) | Viewed by 2460

Abstract This study develops a cost model for the additive manufacturing (AM)-produced spare parts supply chain in the automotive industry. Moreover, we evaluate the economic feasibility of AM for slow-moving automotive spare parts by comparing the costs of the traditional manufacturing (TM) spare parts [...] [Read more](#). (This article belongs to the Special Issue [Frontiers in Digital Manufacturing](#) (./journal/jmmp/special_issues/frontiers_digital_manufacturing))

Show Figures

(https://pub.mdpi-res.com/jmmp/jmmp-07-00008/article_deploy/html/images/jmmp-07-00008-g001-550.jpg?1672278089) (https://pub.mdpi-res.com/jmmp/jmmp-07-00008/article_deploy/html/images/jmmp-07-00008-g002-550.jpg?1672278086) (https://pub.mdpi-res.com/jmmp/jmmp-07-00008/article_deploy/html/images/jmmp-07-00008-g003-550.jpg?1672278085) (https://pub.mdpi-res.com/jmmp/jmmp-07-00008/article_deploy/html/images/jmmp-07-00008-g004-550.jpg?1672278088) (https://pub.mdpi-res.com/jmmp/jmmp-07-00008/article_deploy/html/images/jmmp-07-00008-g005-550.jpg?1672278084) (https://pub.mdpi-res.com/jmmp/jmmp-07-00008/article_deploy/html/images/jmmp-07-00008-g006-550.jpg?1672278089) (https://pub.mdpi-res.com/jmmp/jmmp-07-00008/article_deploy/html/images/jmmp-07-00008-g007-550.jpg?1672278087) (https://pub.mdpi-res.com/jmmp/jmmp-07-00008/article_deploy/html/images/jmmp-07-00008-g008-550.jpg?1672278090) (https://pub.mdpi-res.com/jmmp/jmmp-07-00008/article_deploy/html/images/jmmp-07-00008-g009-550.jpg?1672278091)

Open Access Article

17 pages, 10255 KIB (/2504-4494/7/1/7/pdf?version=1672971867)

Tensile Strength and Microstructure of Rotary Friction-Welded Carbon Steel and Stainless Steel Joints (2504-4494/7/1/7)

by

- Hudiyo Firmanto (https://sciprofiles.com/profile/2583123?utm_source=mdpi.com&utm_medium=website&utm_campaign=avatar_name).
 - Susila Candra (https://sciprofiles.com/profile/author/NHBE13krdk9xZDhdGYvKfTbFCNg1WnBXcFVgbDnScipYcFhJTEjYbz0e?utm_source=mdpi.com&utm_medium=website&utm_campaign=avatar_name).
 - Mohammad Arbi Hadiyat (https://sciprofiles.com/profile/2414447?utm_source=mdpi.com&utm_medium=website&utm_campaign=avatar_name).
 - Yesa Priscilla Triastomo (https://sciprofiles.com/profile/author/NGoxWVhTQ0VsOE1PU1RVMHVZM1dtdBU0STEJxbZhrNWXiZUZxYmxVSXFesYz0e?utm_source=mdpi.com&utm_medium=website&utm_campaign=avatar_name)
- and
- Ivan Wirawan (https://sciprofiles.com/profile/author/LzM3U0Z0G9JM3FIRNFTXMRzB1QmdqSn10RWpaaldVhBDQ2xJeiNIRT0e?utm_source=mdpi.com&utm_medium=website&utm_campaign=avatar_name)
- J. Manuf. Mater. Process. 2023, 7(1), 7; https://doi.org/10.3390/jmmp7010007 (https://doi.org/10.3390/jmmp7010007) - 28 Dec 2022

Cited by 2 (2504-4494/7/1/7#metrics) | Viewed by 1673

Abstract Due to the different properties of the materials, the fusion welding of dissimilar metals may be difficult. Structural irregularities may form as a result of various phase transformations during welding. Solid-state welding, as opposed to fusion welding, occurs below the melting temperature. As [...] [Read more](#).

Show Figures

(https://pub.mdpi-res.com/jmmp/jmmp-07-00007/article_deploy/html/images/jmmp-07-00007-g001-550.jpg?1672971936) (https://pub.mdpi-res.com/jmmp/jmmp-07-00007/article_deploy/html/images/jmmp-07-00007-g002-550.jpg?1672971949) (https://pub.mdpi-res.com/jmmp/jmmp-07-00007/article_deploy/html/images/jmmp-07-00007-g003-550.jpg?1672971934) (https://pub.mdpi-res.com/jmmp/jmmp-07-00007/article_deploy/html/images/jmmp-07-00007-g004-550.jpg?1672971939) (https://pub.mdpi-res.com/jmmp/jmmp-07-00007/article_deploy/html/images/jmmp-07-00007-g005-550.jpg?1672971947) (https://pub.mdpi-res.com/jmmp/jmmp-07-00007/article_deploy/html/images/jmmp-07-00007-g006-550.jpg?1672971936) (https://pub.mdpi-res.com/jmmp/jmmp-07-00007/article_deploy/html/images/jmmp-07-00007-g007-550.jpg?1672971950) (https://pub.mdpi-res.com/jmmp/jmmp-07-00007/article_deploy/html/images/jmmp-07-00007-g008-550.jpg?1672971948) (https://pub.mdpi-res.com/jmmp/jmmp-07-00007/article_deploy/html/images/jmmp-07-00007-g009-550.jpg?1672971941) (https://pub.mdpi-res.com/jmmp/jmmp-07-00007/article_deploy/html/images/jmmp-07-00007-g010-550.jpg?1672971940) (https://pub.mdpi-res.com/jmmp/jmmp-07-00007/article_deploy/html/images/jmmp-07-00007-g011-550.jpg?1672971932)

Open Access Article

13 pages, 2370 KIB (/2504-4494/7/1/6/pdf?version=1672213084)

A New Perspective of Post-Weld Baking Effect on Al-Steel Resistance Spot Weld Properties through Machine Learning and Finite Element Modeling (2504-4494/7/1/6)

by

- Wei Zhang (https://sciprofiles.com/profile/1237831?utm_source=mdpi.com&utm_medium=website&utm_campaign=avatar_name).
- Dali Wang (https://sciprofiles.com/profile/1819397?utm_source=mdpi.com&utm_medium=website&utm_campaign=avatar_name).
- Jian Chen (https://sciprofiles.com/profile/1072587?utm_source=mdpi.com&utm_medium=website&utm_campaign=avatar_name).
- Hassan Ghassemi-Armaki (https://sciprofiles.com/profile/author/TEprOVpaWVM4Kz3L2dKWDBLHVJPaFpPVXYRHRGZEU4azF1dVkvC2FIUT0e?utm_source=mdpi.com&utm_medium=website&utm_campaign=avatar_name).
- Blair Carlson (https://sciprofiles.com/profile/author/dnJ0QzhWeHVXcEdmSmdKWnIBcVFySiXIZcVvXOEZE2bqCWWBnGIPbmXQUIT0e?utm_source=mdpi.com&utm_medium=website&utm_campaign=avatar_name)

Zhili Feng (https://sciprofiles.com/profile/515264?utm_source=mdpi.com&utm_medium=website&utm_campaign=avatar_name)

J. Manuf. Mater. Process. 2023, 7(1), 6; https://doi.org/10.3390/jmmp7010006 (https://doi.org/10.3390/jmmp7010006) - 28 Dec 2022

Viewed by 2038

Abstract The root cause of post-weld baking on the mechanical performance of Al-steel dissimilar resistance spot welds (RSWs) has been determined by machine learning (ML) and finite element modeling (FEM) in this study. A deep neural network (DNN) model was constructed to associate the [..] [Read more](#).
(This article belongs to the Special Issue [Machine Intelligence in Welding and Additive Manufacturing](#) (./journal/jmmp/special_issues/machine_intelligence_welding.))

► [Show Figures](#)

(https://pub.mdpi-res.com/jmmp/jmmp-07-00006/article_deploy/html/images/jmmp-07-00006-g001-550.jpg?1672213160) (https://pub.mdpi-res.com/jmmp/jmmp-07-00006/article_deploy/html/images/jmmp-07-00006-g002-550.jpg?1672213165) (https://pub.mdpi-res.com/jmmp/jmmp-07-00006/article_deploy/html/images/jmmp-07-00006-g003a-550.jpg?1672213159) (https://pub.mdpi-res.com/jmmp/jmmp-07-00006/article_deploy/html/images/jmmp-07-00006-g003b-550.jpg?1672213158) (https://pub.mdpi-res.com/jmmp/jmmp-07-00006/article_deploy/html/images/jmmp-07-00006-g004-550.jpg?1672213163) (https://pub.mdpi-res.com/jmmp/jmmp-07-00006/article_deploy/html/images/jmmp-07-00006-g005-550.jpg?1672213162) (https://pub.mdpi-res.com/jmmp/jmmp-07-00006/article_deploy/html/images/jmmp-07-00006-g006-550.jpg?1672213167)

Open Access Article

18 pages, 11206 KIB

(/2504-4494/7/1/11/pdf?version=1672225181)

Microstructural and Mechanical Characterization of Ledeburitic AISI D2 Cold-Work Tool Steel in Semisolid Zones via Direct Partial Remelting Process (/2504-4494/7/1/11)

by [M. N. Mohammed](#) (https://sciprofiles.com/profile/479126?utm_source=mdpi.com&utm_medium=website&utm_campaign=avatar_name).

[M. Z. Omar](#) (https://sciprofiles.com/profile/author/VkNz4l0SjE0SWlvY1RabFA3ZmVEa08zODVXMk5YODk3RWdQVIRReEdNbz0=7utm_source=mdpi.com&utm_medium=website&utm_campaign=avatar_name)

[Adnan Naji Jameel Al-Tamimi](#) (https://sciprofiles.com/profile/author/dUVxSW1ZY3ozREJyVGEybC9pc0NDNTR5SXpFV1JZU0twNkd1UHRQmRlc0z0=7utm_source=mdpi.com&utm_medium=website&utm_campaign=avatar_name)

.

[Hakim S. Sultan](#) (https://sciprofiles.com/profile/2350247?utm_source=mdpi.com&utm_medium=website&utm_campaign=avatar_name).

[Luay Hashem Abbud](#) (https://sciprofiles.com/profile/2542572?utm_source=mdpi.com&utm_medium=website&utm_campaign=avatar_name).

[Salah Al-Zubaidi](#) (https://sciprofiles.com/profile/402387?utm_source=mdpi.com&utm_medium=website&utm_campaign=avatar_name).

[Oday I. Abdullah](#) (https://sciprofiles.com/profile/562262?utm_source=mdpi.com&utm_medium=website&utm_campaign=avatar_name) and

[M. Abdulrazaq](#) (https://sciprofiles.com/profile/author/ZndaRFIVNmF6d2pjc2hMS2FnWVpubDgGckhrS09RSnRqSkxaN84MIlB2MD0=7utm_source=mdpi.com&utm_medium=website&utm_campaign=avatar_name)

J. Manuf. Mater. Process. 2023, 7(1), 11; https://doi.org/10.3390/jmmp7010011 (https://doi.org/10.3390/jmmp7010011) - 28 Dec 2022

Cited by 1 (/2504-4494/7/1/11#metrics) | Viewed by 1629

Abstract The success of the thixofomming process largely depends on the created microstructure, which must be globular in the liquid phase. The solid-liquid structural changes that occur on as-annealed D2 tool steel when it is subjected to the so-called DPRM are described in this [..] [Read more](#).

► [Show Figures](#)

(https://pub.mdpi-res.com/jmmp/jmmp-07-00011/article_deploy/html/images/jmmp-07-00011-g001-550.jpg?1672225270) (https://pub.mdpi-res.com/jmmp/jmmp-07-00011/article_deploy/html/images/jmmp-07-00011-g002-550.jpg?1672225255) (https://pub.mdpi-res.com/jmmp/jmmp-07-00011/article_deploy/html/images/jmmp-07-00011-g003-550.jpg?1672225277) (https://pub.mdpi-res.com/jmmp/jmmp-07-00011/article_deploy/html/images/jmmp-07-00011-g004-550.jpg?1672225269) (https://pub.mdpi-res.com/jmmp/jmmp-07-00011/article_deploy/html/images/jmmp-07-00011-g005-550.jpg?1672225251) (https://pub.mdpi-res.com/jmmp/jmmp-07-00011/article_deploy/html/images/jmmp-07-00011-g006-550.jpg?1672225272) (https://pub.mdpi-res.com/jmmp/jmmp-07-00011/article_deploy/html/images/jmmp-07-00011-g007-550.jpg?1672225260) (https://pub.mdpi-res.com/jmmp/jmmp-07-00011/article_deploy/html/images/jmmp-07-00011-g008-550.jpg?1672225281) (https://pub.mdpi-res.com/jmmp/jmmp-07-00011/article_deploy/html/images/jmmp-07-00011-g009-550.jpg?1672225278) (https://pub.mdpi-res.com/jmmp/jmmp-07-00011/article_deploy/html/images/jmmp-07-00011-g010-550.jpg?1672225266) (https://pub.mdpi-res.com/jmmp/jmmp-07-00011-g011-550.jpg?1672225263) (https://pub.mdpi-res.com/jmmp/jmmp-07-00011/article_deploy/html/images/jmmp-07-00011-g012-550.jpg?1672225258) (https://pub.mdpi-res.com/jmmp/jmmp-07-00011/article_deploy/html/images/jmmp-07-00011-g013-550.jpg?1672225253) (https://pub.mdpi-res.com/jmmp/jmmp-07-00011/article_deploy/html/images/jmmp-07-00011-g014-550.jpg?1672225274) (https://pub.mdpi-res.com/jmmp/jmmp-07-00011/article_deploy/html/images/jmmp-07-00011-g015-550.jpg?1672225267) (https://pub.mdpi-res.com/jmmp/jmmp-07-00011/article_deploy/html/images/jmmp-07-00011-g016-550.jpg?1672225275) (https://pub.mdpi-res.com/jmmp/jmmp-07-00011/article_deploy/html/images/jmmp-07-00011-g017-550.jpg?1672225266)

Open Access Article

15 pages, 2502 KIB

(/2504-4494/7/1/10/pdf?version=167222150)

Underlying Methodology for a Thermal Process Monitoring System for Wire and Arc Additive Manufacturing (/2504-4494/7/1/10)

by [Daniel Baier](#) (https://sciprofiles.com/profile/2551683?utm_source=mdpi.com&utm_medium=website&utm_campaign=avatar_name).

[Thomas Weckenmann](#) (https://sciprofiles.com/profile/2618501?utm_source=mdpi.com&utm_medium=website&utm_campaign=avatar_name).

[Franz Wolf](#) (https://sciprofiles.com/profile/261785?utm_source=mdpi.com&utm_medium=website&utm_campaign=avatar_name).

[Andreas Wimmer](#) (https://sciprofiles.com/profile/1866724?utm_source=mdpi.com&utm_medium=website&utm_campaign=avatar_name) and

[Michael F. Zaeh](#) (https://sciprofiles.com/profile/1500513?utm_source=mdpi.com&utm_medium=website&utm_campaign=avatar_name)

J. Manuf. Mater. Process. 2023, 7(1), 10; https://doi.org/10.3390/jmmp7010010 (https://doi.org/10.3390/jmmp7010010) - 28 Dec 2022

Viewed by 1725

Abstract The Wire and Arc Additive Manufacturing (WAAM) process has a high potential for industrial applications in aviation. The interlayer temperatures influence the dimensions and geometric deviations of the part. Monitoring the absolute interlayer temperature values is necessary for quantifying these influences. This paper [..] [Read more](#).
(This article belongs to the Topic [Additive Manufacturing: Design, Opportunities, and Applications](#) (topics/Additive_Manufacturing_2))

► [Show Figures](#)

(https://pub.mdpi-res.com/jmmp/jmmp-07-00010/article_deploy/html/images/jmmp-07-00010-g001-550.jpg?1672222234) (https://pub.mdpi-res.com/jmmp/jmmp-07-00010/article_deploy/html/images/jmmp-07-00010-g002-550.jpg?1672222221) (https://pub.mdpi-res.com/jmmp/jmmp-07-00010/article_deploy/html/images/jmmp-07-00010-g003-550.jpg?1672222229) (https://pub.mdpi-res.com/jmmp/jmmp-07-00010/article_deploy/html/images/jmmp-07-00010-g004-550.jpg?1672222222) (https://pub.mdpi-res.com/jmmp/jmmp-07-00010/article_deploy/html/images/jmmp-07-00010-g005-550.jpg?1672222219) (https://pub.mdpi-res.com/jmmp/jmmp-07-00010/article_deploy/html/images/jmmp-07-00010-g006-550.jpg?1672222237) (https://pub.mdpi-res.com/jmmp/jmmp-07-00010/article_deploy/html/images/jmmp-07-00010-g007-550.jpg?1672222216) (https://pub.mdpi-res.com/jmmp/jmmp-07-00010/article_deploy/html/images/jmmp-07-00010-g008-550.jpg?1672222232) (https://pub.mdpi-res.com/jmmp/jmmp-07-00010/article_deploy/html/images/jmmp-07-00010-g009-550.jpg?1672222225)

Open Access Article

17 pages, 5279 KIB

(/2504-4494/7/1/5/pdf?version=1673349099)

Microhardness Distribution of Long Magnesium Block Processed through Powder Metallurgy (/2504-4494/7/1/5)

by [Jiaying Wang](#) (https://sciprofiles.com/profile/2495224?utm_source=mdpi.com&utm_medium=website&utm_campaign=avatar_name) and

[Qizhen Li](#) (https://sciprofiles.com/profile/139838?utm_source=mdpi.com&utm_medium=website&utm_campaign=avatar_name)

J. Manuf. Mater. Process. 2023, 7(1), 5; https://doi.org/10.3390/jmmp7010005 (https://doi.org/10.3390/jmmp7010005) - 27 Dec 2022

Viewed by 1645

Abstract Powder metallurgy is a popular method of making raw powders into specific shaped samples. However, the pressure distribution and the microhardness difference within the sample are nonnegligible and unclear when the sample is large or exceeds a specific size. In this study, the [..] [Read more](#).
(This article belongs to the Topic [Advanced Processes in Metallurgical Technologies](#) (topics/metallurgical_technologies))

► [Show Figures](#)

(https://pub.mdpi-res.com/jmmp/jmmp-07-00005/article_deploy/html/images/jmmp-07-00005-ag-550.jpg?1673349204) (https://pub.mdpi-res.com/jmmp/jmmp-07-00005/article_deploy/html/images/jmmp-07-00005-g001-550.jpg?1673349194) (https://pub.mdpi-res.com/jmmp/jmmp-07-00005/article_deploy/html/images/jmmp-07-00005-g002-550.jpg?1673349188) (https://pub.mdpi-res.com/jmmp/jmmp-07-00005/article_deploy/html/images/jmmp-07-00005-g003-550.jpg?1673349195) (https://pub.mdpi-res.com/jmmp/jmmp-07-00005/article_deploy/html/images/jmmp-07-00005-g004-550.jpg?1673349187) (https://pub.mdpi-res.com/jmmp/jmmp-07-00005/article_deploy/html/images/jmmp-07-00005-g005-550.jpg?1673349183) (https://pub.mdpi-res.com/jmmp/jmmp-07-00005/article_deploy/html/images/jmmp-07-00005-g006-550.jpg?1673349186) (https://pub.mdpi-res.com/jmmp/jmmp-07-00005/article_deploy/html/images/jmmp-07-00005-g007-550.jpg?1673349193) (https://pub.mdpi-res.com/jmmp/jmmp-07-00005/article_deploy/html/images/jmmp-07-00005-g008-550.jpg?1673349191) (https://pub.mdpi-res.com/jmmp/jmmp-07-00005/article_deploy/html/images/jmmp-07-00005-g009-550.jpg?1673349182)

Open Access Article

15 pages, 10984 KIB

(/2504-4494/7/1/4/pdf?version=1676991904)

Binder Jetting Additive Manufacturing: Powder Packing in Shell Printing (/2504-4494/7/1/4)

by [Guanxiong Miao](#) (https://sciprofiles.com/profile/author/U1E3Qkd1OGdpK3JGMWqgEdkaHBKZz09?utm_source=mdpi.com&utm_medium=website&utm_campaign=avatar_name)

.

[Mohammadamin Moghadasi](#) (https://sciprofiles.com/profile/author/UVgzNkZu3lwNWE3SmQxOEIcNiQ1BHL2VGOE5yZXRNMzk4WkNtMU9oMD0=7utm_source=mdpi.com&utm_medium=website&utm_campaign=avatar_name)

.

[Ming Li](#) (https://sciprofiles.com/profile/author/NlnaIagxVzFVN1V0bDRhOTfYbkJmKzUxa8y85SW4S0pWeHNWnFCRT0=7utm_source=mdpi.com&utm_medium=website&utm_campaign=avatar_name)

.

[Zhijian Pei](#) (https://sciprofiles.com/profile/1719426?utm_source=mdpi.com&utm_medium=website&utm_campaign=avatar_name) and

[Chao Ma](#) (https://sciprofiles.com/profile/1595358?utm_source=mdpi.com&utm_medium=website&utm_campaign=avatar_name)

J. Manuf. Mater. Process. 2023, 7(1), 4; https://doi.org/10.3390/jmmp7010004 (https://doi.org/10.3390/jmmp7010004) - 27 Dec 2022

Cited by 1 (/2504-4494/7/1/4#metrics) | Viewed by 1907

Abstract Shell printing is an advanced binder jetting technique that prints only a thin shell of the intended object to enclose the loose powder in the core. In this study, powder packing in the shell and core was investigated for the first time. By [..] [Read more](#).
(This article belongs to the Special Issue [Powder Metallurgy and Additive Manufacturing/3D Printing of Materials](#) (./journal/jmmp/special_issues/AM_3D_jmmp.))

► [Show Figures](#)

(https://pub.mdpi-res.com/jmmp/jmmp-07-00004/article_deploy/html/images/jmmp-07-00004-g001-550.jpg?1676991995) (https://pub.mdpi-res.com/jmmp/jmmp-

https://pub.mdpi-res.com/jmmp/jmmp-07-00004/article_deploy/html/images/jmmp-07-00004-g002-550.jpg?1676991994) (https://pub.mdpi-res.com/jmmp/jmmp-07-00004/article_deploy/html/images/jmmp-07-00004-g003-550.jpg?1676991997) (https://pub.mdpi-res.com/jmmp/jmmp-07-00004/article_deploy/html/images/jmmp-07-00004-g004-550.jpg?1676991993) (https://pub.mdpi-res.com/jmmp/jmmp-07-00004/article_deploy/html/images/jmmp-07-00004-g005-550.jpg?1676991981) (https://pub.mdpi-res.com/jmmp/jmmp-07-00004/article_deploy/html/images/jmmp-07-00004-g006-550.jpg?1676991998) (https://pub.mdpi-res.com/jmmp/jmmp-07-00004/article_deploy/html/images/jmmp-07-00004-g007-550.jpg?1676991989) (https://pub.mdpi-res.com/jmmp/jmmp-07-00004/article_deploy/html/images/jmmp-07-00004-g008-550.jpg?1676991980) (https://pub.mdpi-res.com/jmmp/jmmp-07-00004/article_deploy/html/images/jmmp-07-00004-g009-550.jpg?1676991978) (https://pub.mdpi-res.com/jmmp/jmmp-07-00004/article_deploy/html/images/jmmp-07-00004-g010-550.jpg?1676991983) (https://pub.mdpi-res.com/jmmp/jmmp-07-00004/article_deploy/html/images/jmmp-07-00004-g011-550.jpg?1676991992) (https://pub.mdpi-res.com/jmmp/jmmp-07-00004/article_deploy/html/images/jmmp-07-00004-g012-550.jpg?1676991984) (https://pub.mdpi-res.com/jmmp/jmmp-07-00004/article_deploy/html/images/jmmp-07-00004-g013-550.jpg?1676992004) (https://pub.mdpi-res.com/jmmp/jmmp-07-00004/article_deploy/html/images/jmmp-07-00004-g014-550.jpg?1676992001)

Open Access Article 18 pages, 22677 KiB [.\(/2504-4494/7/1/3/pdf?version=1671884016\)](https://www.mdpi.com/2504-4494/7/1/3/pdf?version=1671884016)

Influence of Wire Arc Additive Manufacturing Beads' Geometry and Building Strategy: Mechanical and Structural Behavior of ER70S-6 Prismatic Blocks *(/2504-4494/7/1/3)*

by  [Ahmed Elsakoty](https://sciprofiles.com/profile/2553348?utm_source=mdpi.com&utm_medium=website&utm_campaign=avatar_name) (https://sciprofiles.com/profile/2553348?utm_source=mdpi.com&utm_medium=website&utm_campaign=avatar_name),  [Omar Oraby](https://sciprofiles.com/profile/2480118?utm_source=mdpi.com&utm_medium=website&utm_campaign=avatar_name) (https://sciprofiles.com/profile/2480118?utm_source=mdpi.com&utm_medium=website&utm_campaign=avatar_name),  [Sameha Sadek](https://sciprofiles.com/profile/2675109?utm_source=mdpi.com&utm_medium=website&utm_campaign=avatar_name) (https://sciprofiles.com/profile/2675109?utm_source=mdpi.com&utm_medium=website&utm_campaign=avatar_name) and  [Hanadi G. Saleh](https://sciprofiles.com/profile/1761189?utm_source=mdpi.com&utm_medium=website&utm_campaign=avatar_name) (https://sciprofiles.com/profile/1761189?utm_source=mdpi.com&utm_medium=website&utm_campaign=avatar_name) and *J. Manuf. Mater. Process.* **2023**, *7*(1), 3; <https://doi.org/10.3390/jmmp7010003> (<https://doi.org/10.3390/jmmp7010003>) - 24 Dec 2022

Cited by [7](#) [\(/2504-4494/7/1/3#metrics\)](#) | Viewed by 2597

Abstract Wire arc additive manufacturing (WAAM) with high deposition rates has attracted industry interest for the demonstrated economic production of medium-to-large-scale metallic components. The structural integrity and mechanical properties of the built parts depend on the selection of the optimum deposition parameters and the [„] [Read more](#). (This article belongs to the Special Issue [Advances in Metal Additive Manufacturing/3D Printing](#) ([/journal/jmmp/special_issues/MetalAM](#)))

Show Figures

(https://pub.mdpi-res.com/jmmp/jmmp-07-00003/article_deploy/html/images/jmmp-07-00003-g001-550.jpg?1671884105) (https://pub.mdpi-res.com/jmmp/jmmp-07-00003/article_deploy/html/images/jmmp-07-00003-g002-550.jpg?1671884097) (https://pub.mdpi-res.com/jmmp/jmmp-07-00003/article_deploy/html/images/jmmp-07-00003-g003-550.jpg?1671884106) (https://pub.mdpi-res.com/jmmp/jmmp-07-00003/article_deploy/html/images/jmmp-07-00003-g004-550.jpg?1671884096) (https://pub.mdpi-res.com/jmmp/jmmp-07-00003/article_deploy/html/images/jmmp-07-00003-g005-550.jpg?1671884105) (https://pub.mdpi-res.com/jmmp/jmmp-07-00003/article_deploy/html/images/jmmp-07-00003-g006-550.jpg?1671884111) (https://pub.mdpi-res.com/jmmp/jmmp-07-00003/article_deploy/html/images/jmmp-07-00003-g007-550.jpg?1671884107) (https://pub.mdpi-res.com/jmmp/jmmp-07-00003/article_deploy/html/images/jmmp-07-00003-g008-550.jpg?1671884101) (https://pub.mdpi-res.com/jmmp/jmmp-07-00003/article_deploy/html/images/jmmp-07-00003-g009-550.jpg?1671884102) (https://pub.mdpi-res.com/jmmp/jmmp-07-00003/article_deploy/html/images/jmmp-07-00003-g010-550.jpg?1671884101) (https://pub.mdpi-res.com/jmmp/jmmp-07-00003/article_deploy/html/images/jmmp-07-00003-g011-550.jpg?1671884093) (https://pub.mdpi-res.com/jmmp/jmmp-07-00003/article_deploy/html/images/jmmp-07-00003-g012-550.jpg?1671884095) (https://pub.mdpi-res.com/jmmp/jmmp-07-00003/article_deploy/html/images/jmmp-07-00003-g013-550.jpg?1671884110) (https://pub.mdpi-res.com/jmmp/jmmp-07-00003/article_deploy/html/images/jmmp-07-00003-g014-550.jpg?1671884091)

Open Access Article 12 pages, 2510 KiB [.\(/2504-4494/7/1/2/pdf?version=1672740628\)](https://www.mdpi.com/2504-4494/7/1/2/pdf?version=1672740628)

Ultrasonic Welding of Additively Manufactured PEEK and Carbon-Fiber-Reinforced PEEK with Integrated Energy Directors *(/2504-4494/7/1/2)*

by  [Bilal Khatri](https://sciprofiles.com/profile/282834?utm_source=mdpi.com&utm_medium=website&utm_campaign=avatar_name) (https://sciprofiles.com/profile/282834?utm_source=mdpi.com&utm_medium=website&utm_campaign=avatar_name),  [Manuel Francis Roth](https://sciprofiles.com/profile/author/UEVnWkHt20wR3oyV25PbINWL0NzZ1FVVVDjOeKFRR2tBUGNlV3RBRE9lQT0=?utm_source=mdpi.com&utm_medium=website&utm_campaign=avatar_name) (https://sciprofiles.com/profile/author/UEVnWkHt20wR3oyV25PbINWL0NzZ1FVVVDjOeKFRR2tBUGNlV3RBRE9lQT0=?utm_source=mdpi.com&utm_medium=website&utm_campaign=avatar_name) and  [Frank Balle](https://sciprofiles.com/profile/1564218?utm_source=mdpi.com&utm_medium=website&utm_campaign=avatar_name) (https://sciprofiles.com/profile/1564218?utm_source=mdpi.com&utm_medium=website&utm_campaign=avatar_name) and *J. Manuf. Mater. Process.* **2023**, *7*(1), 2; <https://doi.org/10.3390/jmmp7010002> (<https://doi.org/10.3390/jmmp7010002>) - 23 Dec 2022

Cited by [6](#) [\(/2504-4494/7/1/2#metrics\)](#) | Viewed by 2210




Abstract The thermoplastic polymer polyether ether ketone (PEEK) offers thermal and mechanical properties comparable to thermosetting polymers, while also being thermally re-processable and recyclable as well as compatible with fused filament fabrication (FFF). In this study, the feasibility of joining additively manufactured PEEK in [„] [Read more](#).

Show Figures

(https://pub.mdpi-res.com/jmmp/jmmp-07-00002/article_deploy/html/images/jmmp-07-00002-g001-550.jpg?1672740723) (https://pub.mdpi-res.com/jmmp/jmmp-07-00002/article_deploy/html/images/jmmp-07-00002-g002-550.jpg?1672740720) (https://pub.mdpi-res.com/jmmp/jmmp-07-00002/article_deploy/html/images/jmmp-07-00002-g003-550.jpg?1672740725) (https://pub.mdpi-res.com/jmmp/jmmp-07-00002/article_deploy/html/images/jmmp-07-00002-g004-550.jpg?1672740712) (https://pub.mdpi-res.com/jmmp/jmmp-07-00002/article_deploy/html/images/jmmp-07-00002-g005-550.jpg?1672740723) (https://pub.mdpi-res.com/jmmp/jmmp-07-00002/article_deploy/html/images/jmmp-07-00002-g006-550.jpg?1672740713) (https://pub.mdpi-res.com/jmmp/jmmp-07-00002/article_deploy/html/images/jmmp-07-00002-g007-550.jpg?1672740718) (https://pub.mdpi-res.com/jmmp/jmmp-07-00002/article_deploy/html/images/jmmp-07-00002-g008-550.jpg?1672740716) (https://pub.mdpi-res.com/jmmp/jmmp-07-00002/article_deploy/html/images/jmmp-07-00002-g009-550.jpg?1672740719) (https://pub.mdpi-res.com/jmmp/jmmp-07-00002/article_deploy/html/images/jmmp-07-00002-g010-550.jpg?1672740715) (https://pub.mdpi-res.com/jmmp/jmmp-07-00002/article_deploy/html/images/jmmp-07-00002-g011-550.jpg?1672740721)

Open Access Article 19 pages, 4492 KiB [.\(/2504-4494/7/1/1/pdf?version=1671706283\)](https://www.mdpi.com/2504-4494/7/1/1/pdf?version=1671706283)

Numerical Modeling of Titanium Alloy Ti10V2Fe3Al Milling Process *(/2504-4494/7/1/1)*

by  [Michael Storchak](https://sciprofiles.com/profile/346648?utm_source=mdpi.com&utm_medium=website&utm_campaign=avatar_name) (https://sciprofiles.com/profile/346648?utm_source=mdpi.com&utm_medium=website&utm_campaign=avatar_name),  [Thomas Stehle](https://sciprofiles.com/profile/author/OGNlBxVN1ZnK0dUMHZlZytmZzdaUjpscZWSmRwTFNBskVrT0tzaUVPD2tJaXpQn1F0VFRnRDNNRHUycytTWQ=?utm_source=mdpi.com&utm_medium=website&utm_campaign=avatar_name) (https://sciprofiles.com/profile/author/OGNlBxVN1ZnK0dUMHZlZytmZzdaUjpscZWSmRwTFNBskVrT0tzaUVPD2tJaXpQn1F0VFRnRDNNRHUycytTWQ=?utm_source=mdpi.com&utm_medium=website&utm_campaign=avatar_name) and  [Hans-Christian Möhring](https://sciprofiles.com/profile/2280420?utm_source=mdpi.com&utm_medium=website&utm_campaign=avatar_name) (https://sciprofiles.com/profile/2280420?utm_source=mdpi.com&utm_medium=website&utm_campaign=avatar_name) and *J. Manuf. Mater. Process.* **2023**, *7*(1), 1; <https://doi.org/10.3390/jmmp7010001> (<https://doi.org/10.3390/jmmp7010001>) - 22 Dec 2022

Cited by [1](#) [\(/2504-4494/7/1/1#metrics\)](#) | Viewed by 1407

Abstract The simulation of material machining using finite element models is a powerful tool for the optimization of simulated processes and tools, as well as for the determination of cutting process characteristics that are difficult or practically impossible to determine by experiment. The paper [„] [Read more](#).

Show Figures

(https://pub.mdpi-res.com/jmmp/jmmp-07-00001/article_deploy/html/images/jmmp-07-00001-g001-550.jpg?1671706361) (https://pub.mdpi-res.com/jmmp/jmmp-07-00001/article_deploy/html/images/jmmp-07-00001-g002-550.jpg?1671706360) (https://pub.mdpi-res.com/jmmp/jmmp-07-00001/article_deploy/html/images/jmmp-07-00001-g003-550.jpg?1671706371) (https://pub.mdpi-res.com/jmmp/jmmp-07-00001/article_deploy/html/images/jmmp-07-00001-g004-550.jpg?1671706370) (https://pub.mdpi-res.com/jmmp/jmmp-07-00001/article_deploy/html/images/jmmp-07-00001-g005-550.jpg?1671706365) (https://pub.mdpi-res.com/jmmp/jmmp-07-00001/article_deploy/html/images/jmmp-07-00001-g006-550.jpg?1671706367) (https://pub.mdpi-res.com/jmmp/jmmp-07-00001/article_deploy/html/images/jmmp-07-00001-g007-550.jpg?1671706380) (https://pub.mdpi-res.com/jmmp/jmmp-07-00001/article_deploy/html/images/jmmp-07-00001-g008a-550.jpg?1671706377) (https://pub.mdpi-res.com/jmmp/jmmp-07-00001/article_deploy/html/images/jmmp-07-00001-g008b-550.jpg?1671706374) (https://pub.mdpi-res.com/jmmp/jmmp-07-00001/article_deploy/html/images/jmmp-07-00001-g009a-550.jpg?1671706368) (https://pub.mdpi-res.com/jmmp/jmmp-07-00001/article_deploy/html/images/jmmp-07-00001-g009b-550.jpg?1671706372)

Show export options ▾

Displaying articles 1-50

Previous Issue

Volume 6, December [\(/2504-4494/6/6\)](#)

Next Issue

Volume 7, April [\(/2504-4494/7/2\)](#)

J. Manuf. Mater. Process. ([/journal/jmmp](#)), EISSN 2504-4494, Published by MDPI

[RSS \(/rss/journal/jmmp\)](#) [Content Alert \(/journal/jmmp/toc-alert\)](#)

Further Information

[Article Processing Charges \(/apc\)](#)

[Pay an Invoice \(/about/payment\)](#)

[Open Access Policy \(/openaccess\)](#)

[Contact MDPI \(/about/contact\)](#)

[Jobs at MDPI \(/careers.mdpi.com\)](#)

Guidelines

[For Authors \(/authors\)](#)

[For Reviewers \(/reviewers\)](#)

[For Editors \(/editors\)](#)

[For Librarians \(/librarians\)](#)



[For Publishers \(/publishing_services\)](#)

[MDPI](#)

[For Societies \(/societies\)](#)

[For Conference Organizers \(/conference_organizers\)](#)

[Toggle desktop layout cookie](#)

[Sciforum \(https://sciforum.net\)](https://sciforum.net)

[MDPI Books \(https://www.mdpi.com/books\)](https://www.mdpi.com/books)

[Preprints.org \(https://www.preprints.org\)](https://www.preprints.org)

[Sciit \(https://www.sciit.net\)](https://www.sciit.net)

[SciProfiles \(https://sciprofiles.com?utm_source=mdpi.com&utm_medium=bottom_menu&utm_campaign=initiative\)](https://sciprofiles.com?utm_source=mdpi.com&utm_medium=bottom_menu&utm_campaign=initiative)

[Encyclopedia \(https://encyclopedia.pub\)](https://encyclopedia.pub)

[JAMS \(https://jams.pub\)](https://jams.pub)

[Proceedings Series \(/about/proceedings\)](#)

Follow MDPI

[LinkedIn \(https://www.linkedin.com/company/mdpi\)](https://www.linkedin.com/company/mdpi)

[Facebook \(https://www.facebook.com/MDPIOpenAccessPublishing\)](https://www.facebook.com/MDPIOpenAccessPublishing)

[Twitter \(https://twitter.com/MDPIOpenAccess\)](https://twitter.com/MDPIOpenAccess)

Subscribe to receive issue release
notifications and newsletters from
MDPI journals

© 1996-2024 MDPI (Basel, Switzerland) unless otherwise stated

[Disclaimer](#) [Terms and Conditions \(/about/terms-and-conditions\)](#) [Privacy Policy \(/about/privacy\)](#)